

Founded 1925

Incorporated
by Royal Charter 1961

*To promote the advancement
of radio electronics and kindred
subjects by the exchange of
information in these branches
of engineering*

Volume 44 No. 9

September 1974

The Radio and Electronic Engineer

The Journal of the Institution of Electronic and Radio Engineers

Environmental Sensors and Applications

THE earliest evidence of man's activities demonstrates that he has always been inquisitive and made measurements to understand and use his surroundings. Today the impact of the communications media is stimulating greater awareness of environmental problems—on land—on and under the sea—and in the air. This interest supports the growing scientific and engineering efforts to measure, understand, and develop resources and to conserve the environment. Pollution is an offshoot of exploitation, and its control is urgent to reduce present undesirable situations and avoid their recurrence in future resource development.

Materials research and the progress of electronics are providing new devices and new approaches to the problem of measuring environmental parameters and transducing the data to interface with data collection systems. At the same time modern technology has provided a vast expansion in communications and the capacity for data collection, signal processing and data analysis which can serve environmental sensing systems. This increases the capability to understand the inter-related effects of the often large scale and dynamic processes being studied.

The sensor is the critical device in the environmental measurement system. However powerful the analytical facilities provided by modern computers, the information can be no better than the ability of the sensing device. The sensor should provide accurate data with precision which implies maintenance of calibration, it must produce minimum disturbance of the parameters under measurement and it must frequently operate for long periods unattended. The interfacing with the data collection system entails the sensor and transducer to be considered as an integral part of the total data acquisition system.

During the past 10 years several of the Institution's conferences have discussed the design of sensors but nearly always in the context of their integration into a measurement system for a particular purpose. We may recall for instance, the conferences on oceanography and ocean technology in particular. However, the applications of the basic sensors can be related to a number of general principles and types of system and it is therefore considered timely for a conference to be organized which will explore the present problems existing in the instrumentation of sensors and transducers, note special requirements and examine future trends. It will provide an opportunity for those who are engaged in diverse fields of investigation to discuss common problems which arise in measurement of environmental parameters.

The conference which is to be held in the Wellcome Lecture Theatre of the Royal Society, London, on 18th–19th November next, will include twenty papers grouped in a number of sessions having the broad titles of Air Pollution, Meteorological Sensors, Remote Environmental Sensing, Monitoring Systems and Computer Analysis. The provisional programme published in the August issue of the Journal shows that the authorship of the papers has been drawn in similar proportions from universities, government research establishments and industry; this balance must surely augur well for comprehensive coverage at the conference and emphasize that there is an awareness throughout the scientific community of the important role that electronic techniques can play in enabling man to investigate and overcome the abuses of the environment.

J. B. LOCK

Contributors to this issue



Mr. J. Hywel Williams who obtained his H.N.C. in Electrical Engineering following studies at the Glamorgan Technical College, Treforest, has held posts as a Development Engineer with BSA, Hoover Ltd., and Teddington Aircraft Controls. In 1972 he graduated in mathematics at the University of Wales Institute of Science and Technology, Cardiff, and he was then appointed as Industrial Research Associate in

the Dynamic Analysis Group of the Department of Mechanical Engineering and Engineering Production. His main research interests are in quality assurance and fault identification.



Mr. Walter Funk spent the first eight years of his professional life with the optical company of I. D. Möller, where he worked in the department concerned with microphotographic precision divisions. He joined the Philips Research Laboratories in Hamburg in 1964 and is now head of the Process Technology Group in the Advanced Materials Research Department.



Dr. Wolfram M. Schilz received the Diploma in Physics from the University of Göttingen in 1959 and the Dr. rer. nat. from the same University in 1960. From 1960 to 1966 he was a Research Assistant at the Physikalische Institut in Göttingen. In 1966 he joined the Philips Research Laboratories in Hamburg, and during the next four years he worked on electronic processes in narrow gap semiconductors.

Since 1970 Dr. Schilz has led the research group on microwave applications and is engaged in microwave integration techniques and microwave measuring systems.



Mr. D. A. James (Member 1969) served in the Royal Artillery from the outbreak of war in 1939 until he retired in 1958 in the rank of Lieutenant Colonel. During his service he specialized in electronics, communications and radar. He attended the Technical Staff Course at the Royal Military College of Science and also graduated with first class honours from London University. Afterwards he did a tour of duty at the

Royal Armament Research and Development Establishment as a technical staff officer. For the past 16 years, apart from a short attachment to the Royal College, Nairobi, he has been employed on the lecturing staff of the Royal Military College of Science in the Electronics Branch. His specialities are radar, missile guidance, microwave ferrites and surface acoustic wave devices.



A graduate of the University of Wales, **Dr. John Dunlop** gained his B.Sc. at Swansea University College in 1966 and in 1970 was awarded the Ph.D. for his thesis on 'Signal regeneration from non-regular samples.' He was appointed to a Lectureship in Telecommunications in the Department of Electronic Science and Telecommunications of the University of Strathclyde in 1969.

His present research activities are concerned with signal processing and time-varying networks in communications systems.



Dr. V. J. Phillips graduated with first class honours in electrical engineering in 1955 from Imperial College, London. Following a period of research work at the College, he was awarded the degree of Ph.D. in 1959. From 1958 to 1960 he worked at the GEC Research Laboratories (now Hirst Research Centre) at Wembley, Middlesex, and he took up his present lecturing post at the University College of

Swansea in 1960; he is now a Senior Lecturer. He received, jointly with two of his research students, the Dr. Norman Partridge Memorial Premium in 1971 for a paper on speech scrambling.

A biographical note about Mr. V. G. Devereux was published in the July issue.

Application of p.c.m. to broadcast quality video signals*

Part 2: Subjective Study of Digit Errors and Timing Jitter

V. G. DEVEREUX, M.A.†

SUMMARY

This part of the paper concerning p.c.m. video signals describes two series of subjective tests performed to examine picture impairments caused by unwanted components which may be introduced into System I (PAL, 625-line) video signals while they are encoded in p.c.m. form.

The first series of tests examined the subjective effect of digital transmission errors. Both random single-digit errors and burst errors were examined. The tests included an investigation of a system for concealing errors based on the use of parity bits. For random errors, it was found that error concealment reduced the maximum tolerable error rate from 1 in 10^7 to 1 in 10^4 .

The second series of tests examined the subjective effect of timing jitter in the analogue samples of video signals obtained from a p.c.m. digital-to-analogue converter. Certain alignment errors in the PAL decoder used in conjunction with the display monitor can considerably increase the impairment caused by timing jitter. One of the most critical adjustments in the PAL decoder is the alignment of the static phase of the reference colour subcarrier. The results of the tests indicate that the amplitude of random jitter should not exceed about 0.3 ns r.m.s. assuming that PAL decoders are aligned to within specified tolerances which allow for long term drifts.

* The first part of this paper, 'Subjective study of the coding parameters' was published in Vol. 44, No. 7, July 1974, (pp. 373-381).

† British Broadcasting Corporation, Research Department, Kingswood Warren, Tadworth, Surrey.

1 Introduction

There are two possible forms of instrumental imperfection in a pulse code modulation (p.c.m.) system (excluding the coder and decoder) which can introduce unwanted components into the decoded analogue signal. Firstly, some digits may be incorrectly detected at the receiving terminal. Incorrectly detected digits will be referred to as transmission or digit errors. Secondly, assuming that all timing information is derived from the p.c.m. pulse train, variations in the delay of the p.c.m. circuit can cause pulse-position modulation of the decoded analogue signal samples. This pulse-position modulation will be referred to as timing jitter (or jitter).

This paper (Part 2) describes subjective tests which were performed to examine the picture impairments caused by varying error rates and varying amounts of timing jitter in a p.c.m. link handling System I (PAL, 625-line) video signals.

2 Examination of Transmission Errors

Tests were carried out to examine the impairment caused by both random single-digit errors (i.e. errors which are randomly distributed in time, each error affecting only one digit), and errors which affect many successive digits, often referred to as 'burst' errors. Since very little is known concerning the most likely duration and time distribution of burst errors on a video p.c.m. link, it was not thought worthwhile to carry out extensive tests on their subjective effect at the present time. However, an indication of the effects of burst errors was obtained using randomly distributed groups of errors lasting for 120 digits, i.e. about 1 μ s. Also, the effect of errors with a duration of 3-12 μ s can be deduced from the results of subjective tests on the impairment caused by drop-outs on video tape recordings,¹ and an analysis of these results is included.

The investigations included tests in which the effect of errors was concealed by a technique based on the addition of a single parity digit per sample. As in computer systems, this digit was made zero or one depending on whether the number of ones in the original number (or any selected part of it) was even or odd. By checking the state of this parity digit, it was possible to detect an odd number of errors in the protected digits in a given sample. Following detection, the effect of errors was concealed by replacing samples in error by a sample corresponding to an adjacent picture element.

An alternative approach to reducing the picture impairment caused by errors is to employ a more complex parity code which indicates the individual digits rather than the samples which are in error.² With these complex codes, errors can be corrected, as well as detected, so that no sample replacement is required. The relative merits of error correction and error concealment are currently being investigated by the BBC.

2.1 Equipment Used for Inserting and Concealing Errors

A block diagram of the equipment used to insert and conceal errors in the p.c.m. signal is shown in Fig. 1.

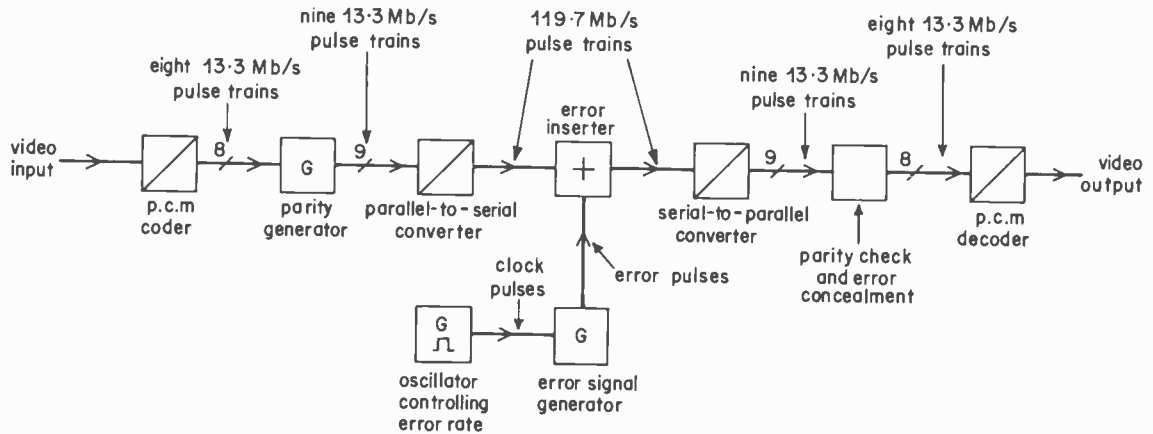


Fig. 1. Block diagram of equipment used in subjective tests on errors.

The p.c.m. coder operated at a sampling rate of 13.3 MHz and provided 8 bits per sample in parallel form; this form of signal was also required at the input of the p.c.m. decoder. Errors could have been inserted in the parallel data stream, but parallel-to-serial and serial-to-parallel converters³ were already available and it was decided to be more realistic by inserting errors in a serial data stream. The generator which provided a pseudo-random sequence of error pulses is described in Section 2.1.1.

In the parity generator, a single parity digit was derived for each sample, giving a total of nine digits per sample. This unit was provided with 8 on/off switches which enabled the parity sum to be applied to any combination of the 8 digits in a sample. The parity checking unit was provided with corresponding switches which had to be set to the same positions as those used in the parity generator. The parity checking unit also contained the circuits for concealing the effect of errors detected by means of parity violation. Further details of the error concealment system are given in Section 2.1.3.

2.1.1 Error signal generator

In order to introduce known error rates and known error durations into the p.c.m. signal, it was found to be more convenient to use a pseudo-random error generator rather than to generate errors from a truly random source.

In the pseudo-random error generator, clock pulses which controlled the error rate were applied to a 25-stage shift register with feedback which provided a 'maximal-length' pseudo-random sequence of 0's and 1's, the sequence being repeated after every $2^{25}-1$ (i.e. 33.5×10^6) clock pulses. If the pseudo-random sequence were used directly as the error signal, the mean time between error pulses, as indicated by the presence of 1's, would be two clock pulse periods and the minimum time would be one clock pulse period. To increase the randomness of the errors, the outputs from 7 different stages of the shift register were fed to an AND gate, the output of which was used as the error signal. The mean time between the error pulses thus obtained is

equal to 128 (i.e. 2^7) clock pulse periods and the minimum time remains at one clock pulse period. Using this system, the maximum clock frequency at which the shift register would operate, which was about 5 MHz, limited the maximum obtainable error rate to about 1 error pulse for every 2000 digits of the 120 Mb/s p.c.m. signal. To obtain higher error rates, the number of inputs to the AND gate was reduced to 6 or 3 thus increasing the maximum error rate by a factor of 2 or 16 respectively.

One difference between the pseudo-random error signal described above and a truly random signal was that the pseudo-random signal never caused two or more separate errors in the protected bits of one sample. (The minimum possible time between error pulses was 200 ns and the interval between video samples was 75 ns.) Such multiple errors should be considered since if the protected bits in one sample contain an even number of errors, the parity rule is not violated and the errors are not detected. This difference is only significant, however, at high error rates and the additional impairment which would be obtained with a truly random signal as a result of these undetected errors can be allowed for in the manner described in Section 2.3.2.

2.1.2 Error inserter unit

On receipt of an error pulse, this unit caused an error whose duration could be varied so that it affected any number of digits between one and about 200. The type of error could be altered so that the affected digits were either (a) complemented (i.e. 0's changed to 1's and vice-versa) or (b) all set to '1' or (c) all set to '0'.

In the subjective tests, condition (a) was used for single-digit errors, and conditions (b) and (c) for burst errors. The reasons for this choice of conditions are as follows:

In practice, single-digit errors are most likely to be caused by the addition of random noise to the p.c.m. signal and this effect would cause digits to be complemented. On the other hand, burst errors are most likely to be caused by impulsive interference which would set all digits during a single impulse to the same state. This assumes that a simple on-off binary code is used

to transmit the p.c.m. signal; in practice, a more complex transmission code would almost certainly be employed but it was outside the scope of the present tests to investigate the effect of such codes on the final error pattern.

2.1.3 Error concealment

Two methods of concealing errors were developed. In the first method, samples in error were replaced by the last good sample received before the commencement of the error. This technique gave a marked reduction in the impairment caused by single-digit errors on monochrome pictures. With colour pictures, however, less satisfactory results were obtained since the presence of large-amplitude colour subcarrier causes significant differences in the analogue signal level between successive samples. To overcome this difficulty, a second concealment system was developed⁴ which made use of the fact that the sampling rate used in the tests was close or equal to three times colour subcarrier frequency. By replacing an incorrect sample by the sample which occurs three sampling periods earlier, information is taken from the correct part of the subcarrier cycle: this system will be referred to as the 'third-previous sample' method of concealment.

During burst errors, the three samples obtained prior to the error were repeated in succession, thus maintaining the phase and amplitude of any subcarrier present in the video signal before the error commenced. In order to overcome the difficulty that there was about a 50% probability that a burst error would affect an even number of digits in the samples at the beginning and end of the error, the error concealment process was extended to cover the samples which immediately preceded and followed a succession of samples in which errors had been detected. The presence of a burst error was indicated when two or more successive samples were found to be in error.

Only the third-previous sample method of concealment was used in the subjective tests because it gave much better concealment of errors than the previous sample system in areas of a picture containing saturated colours and was only very slightly inferior in unsaturated areas.

If the sampling rate is not exactly equal to three times subcarrier frequency, the substitute samples obtained with the third-previous sample method will not be precisely correct in plain coloured areas of a picture. If the sampling frequency is 2.8% different from three times subcarrier frequency, then the maximum difference between every third sample in a plain field of 100% saturated cyan will be equal to an error in the fourth most significant bit. Initial tests indicated that digital errors in the fourth and subsequent bits caused negligible impairment on a 100% colour bar picture with error rates as high as 1 in 1000. It was therefore concluded that the results obtained from the tests will apply for any sampling frequency which is within about 2.8% of three times subcarrier frequency, but further tests would be required for sampling frequencies outside this range.

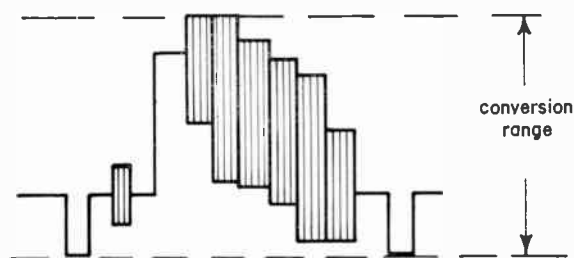


Fig. 2. Adjustment of video levels relative to the conversion range of the coder, shown for 100% colour bar signal.

2.2 Subjective Tests: Method

2.2.1 Experimental arrangement

The video signals obtained from the output of the p.c.m. decoder shown in Fig. 1 were displayed on a high quality 48 cm (19 in) colour monitor having a peak brightness of 55 candela/metre² (16 ft-L); with zero beam current, the brightness of the screen resulting from ambient illumination was 0.1 candela/metre² (0.03 ft-L). In the coder, the video signal was clamped with the tips of synchronizing pulses at the bottom of the conversion range and its amplitude adjusted so that a 100%† colour bar signal would just reach the top of the conversion range (see Fig. 2). The video level corresponding to the tips of synchronizing pulses was converted into the binary code 0000 0000 while 1111 1111 represented the highest level reached by the video signal. With such a code, if a '0' is incorrectly received as a '1', a 'white-going' error pulse is introduced into the decoded video signal; alternatively, if a '1' is received as a '0', a 'black-going' pulse is obtained.

For the purpose of the present tests, arrangements were made to introduce error-free synchronizing pulses and colour bursts into the decoded video signal thus avoiding timing or clamping errors caused by digital errors in the line and field blanking intervals. In normal circumstances when no error-free signal would be available, such errors could always be substantially removed by relatively simple video processing techniques.

2.2.2 Signal sources

Both monochrome and colour pictures were used in the tests, the signal sources being:

- A 35 mm colour slide scanner containing a slide of which a monochrome version was illustrated in Part I of the paper (Fig. 6). Both monochrome and colour versions were shown in the tests.
- A video tape recorder replaying a recording of musical variety programme called 'Music, Music, Music'. The pictures were typical of those used for good-quality, highly-coloured light entertainment.
- A high-quality receiver providing off-air colour pictures obtained from a good picture-quality demonstration film used for 'trade tests'.

† For this form of colour bar signal, the R, G and B signals fed to the PAL coder switch between 0% and 100% of the maximum allowable values for both coloured and uncoloured bars.

These were selected as being fairly typical sources of both moving and stationary pictures provided by a high-quality broadcasting service.

2.2.3 Test procedure

Each test condition was shown to two separate groups of six observers seated at a mean distance of six times picture height from the monitor. At any one sitting, judgements were obtained on 15 different test conditions, each being shown twice with other conditions in between. The observers were all engineers having previous experience of assessing picture quality.

The degradation in picture quality caused by digital errors was graded using the 6-point impairment scale, with additional descriptions in parentheses, as shown below in Table 1.

Table 1. 6-point impairment scale

Grade	Degree of impairment
1	Imperceptible (No impairment)
2	Just perceptible (Negligible impairment)
3	Definitely perceptible but not disturbing (Slight impairment)
4	Somewhat objectionable (Marked impairment)
5	Definitely objectionable (Severe impairment)
6	Unusable (Complete impairment)

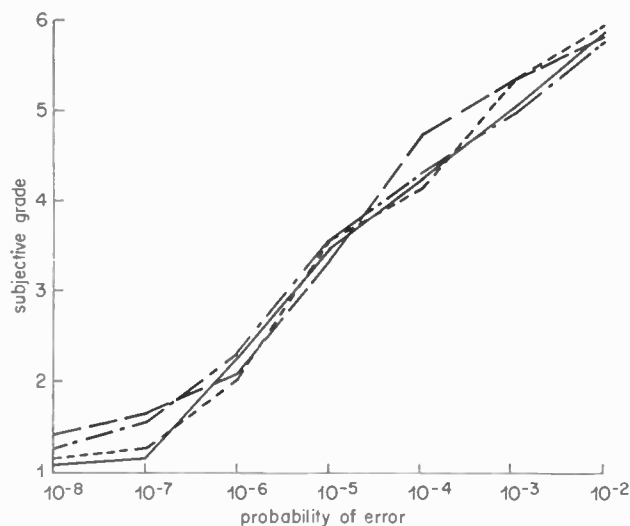


Fig. 3. Impairment produced by random single-digit errors; no error concealment.

- slide; colour
- - - slide; monochrome
- · - colour film
- · · video-tape recording

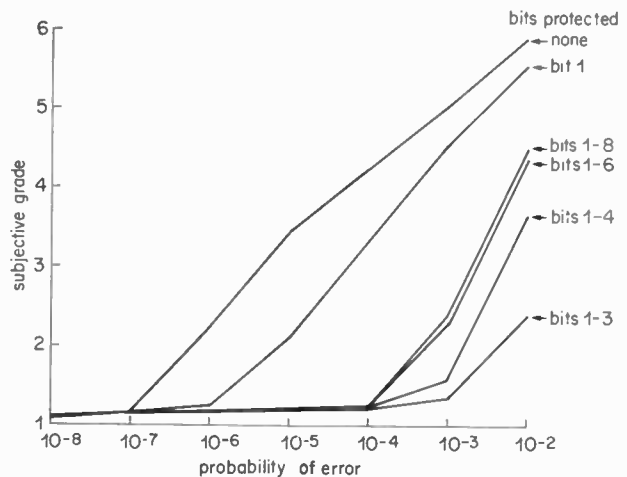


Fig. 4. Impairment produced by single-digit errors using error concealment. Picture: colour slide. bit 1 = m.s.b.; bit 8 = l.s.b.

The additional comments in parentheses were added to avoid a slightly confusing aspect of the normal scale with the type of impairment caused by errors. For example, single errors separated by long intervals might be 'definitely perceptible' at their moments of occurrence, yet, because of their infrequency, they constitute too trivial an impairment to merit the comparatively adverse assessment implied by grade 3. These comments were originally used in subjective tests on the impairment caused by drop-outs in video tape recordings,¹ for which a similar confusion can arise.

2.3 Results of Subjective Tests

The results of the tests are shown in Figs. 3 to 8. The horizontal axes in all these figures are calibrated in terms of the probability of an error in any one digit; thus, if there were on average N burst errors per second and each burst affected D digits in a p.c.m. signal having a bit-rate of B bits per second, the error probability would be ND/B .

In the figures concerned with error concealment systems, 'bit 1' refers to the most significant bit (m.s.b.) in a word describing a sample and 'bit 8' refers to the least significant bit (l.s.b.).

In assessing allowable error rates, acceptable picture quality has been assumed to correspond to impairment grades equal to or lower than 1.5.

2.3.1 Random single-digit errors without concealment

The results obtained for this type of error are shown in Fig. 3. It will be seen that the impairment corresponding to a given probability of error was very similar for both monochrome and colour pictures and also for still and moving pictures. These results indicate that for acceptable picture quality, the probability of an error should not be greater than about 10^{-7} with no error concealment in use. This figure of 10^{-7} was also obtained in similar work in Japan.⁵

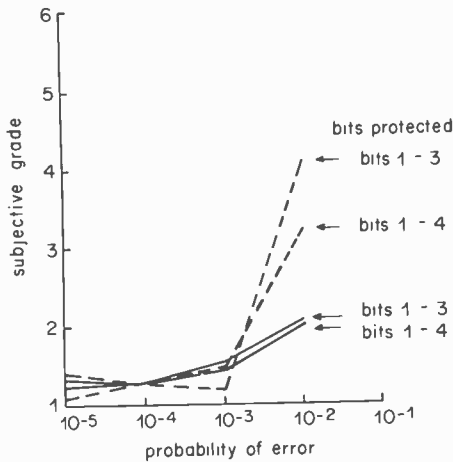


Fig. 5. Impairment produced by single-digit errors using error concealment—moving pictures.

— — — video tape pictures
 ————— colour film

2.3.2 Random single-digit errors with concealment

Tests were carried out with error concealment based on parity protection of various numbers of bits in each sample. The results obtained are shown in Figs. 4 and 5. It can be seen from Fig. 4 that, on a colour picture from a slide scanner, the impairment for a given error probability was a minimum with parity protection on only the three most significant digits. With moving pictures, initial tests indicated that least impairment was obtained with either 3 or 4 bits protected and only these two types of protection were shown to the panel of observers; the results obtained are given in Fig. 5. Subsidiary tests showed that similar results are obtained with monochrome pictures.

The reason for the higher grading obtained with parity protection on more than 3 or 4 bits is that the impairment produced by replacing samples containing errors in bits of low significance is more noticeable than the impairment produced if such errors are left unconcealed. Using protection on only a few bits also has the advantage that it reduces the probability of two errors occurring in the protected bits of any one sample; such double errors would not violate the parity rule and would therefore not be detected. This latter effect was not noticed in the tests however, since the minimum interval between errors was always greater than the interval between successive samples (see Sect. 2.1.1). To make an allowance for the additional impairment that would be obtained with truly random errors, the probability of double errors for a given error rate was calculated and the corresponding impairment was estimated from the results obtained for unconcealed errors. The effect of this additional impairment was calculated using an impairment summing technique similar to that given in Ref. 6. The corrected mean grades for all picture sources are shown in Fig. 6. This figure indicates that, with error concealment in use, acceptable picture quality will be obtained if the probability of random single-digit errors is no greater than 10^{-4} .

2.3.3 Random 'burst' errors; no concealment

To obtain an indication of the impairment caused by 'burst' errors, i.e. errors affecting many successive digits, subjective tests were performed in which each error pulse set all the following 120 digits either to the '1' state or to the '0' state, only one of these two different types of error being used in a given test; since the video p.c.m. bit-rate was 120 Mb/s, 120 bits corresponds to a duration of 1 μ s. The effect of setting digits to '1' was to produce white horizontal dashes on the picture; setting to '0' produced black dashes. The impairments produced by 'burst' errors were found to be very similar for both stationary and moving pictures. The mean grades obtained for both types of picture are shown in Fig. 7 together with the mean grades obtained for single-digit errors. The figure also includes results deduced from tests to determine the impairments caused by 3, 6 and 12 μ s drop-outs in conventional video tape recordings of monochrome pictures;¹ these results only covered impairment grades in the range 1.5 to 2.5. In these tests, the signal level during a drop-out excused to a voltage level 10% above white level, thus producing an almost identical effect to setting all digits in the p.c.m. system to the '1' state for the same duration.

The results given in Fig. 7 indicate that, with no error concealment, acceptable picture quality will be obtained if not more than 1 in 10^7 bits are in error; this result applies to both single-digit and 'burst' errors. The degree of impairment appears to decrease slightly as the duration of the errors is increased, although more comprehensive tests would be needed to confirm this conclusion. Further, it would appear that black errors must occur about 5 to 10 times as frequently as white errors for a given degree of impairment; in the work concerning drop-outs,¹ the value of this ratio was found to be 'about 3 times'.

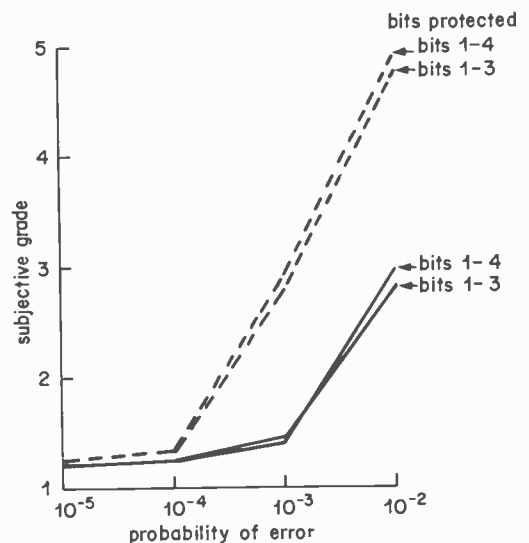


Fig. 6. Corrected results for single-digit errors with concealment to allow for effect of double errors: mean grades for all picture sources.

———— uncorrected results
 - - - - - results corrected for effect of double errors

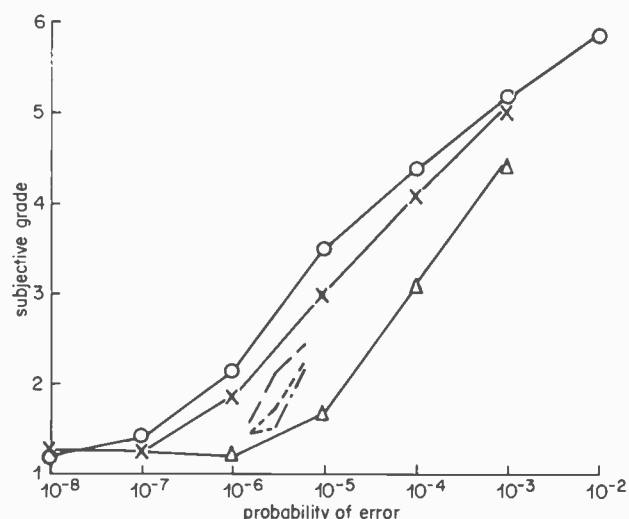


Fig. 7. Impairment produced by errors of different durations; no error concealment.

- single digit errors—mean grade from Fig. 3
- × white 1 μs errors } mean grade for still and
- △ black 1 μs errors } moving colour pictures
- white 3 μs errors } results of tests on drop-outs
- - - white 6 μs errors } in video tape recordings
- - - white 12 μs errors }

In calculating the error probability for 'burst' errors, it was assumed that all bits occurring during the error were incorrect. An alternative assumption would be that only half these bits were in error since, on average, half of them would already be in the state to which they were set by the error; the effect of a 2 to 1 change in error rate is quite small, however, and would not affect the conclusions given above.

In order that the results obtained should not be too critical, the pictures used for the drop-out tests were deliberately chosen to have 'some measure of interest to the observer and the tests were therefore carried out using moving pictures, with sound'. These represent less critical conditions than those used in the tests described in this paper.

2.3.4 Random 'burst' errors; with concealment

The results of tests on the impairment caused by 1 μs 'burst' errors concealed by the technique described in Section 2.1.3 are shown in Fig. 8. This figure shows an appreciable difference between the impairments observed on stationary and moving pictures. With the most critical picture (i.e. the coloured slide), acceptable picture quality was obtained provided that the error probability was no greater than about 10⁻⁵.

Subsidiary tests indicated that the method used for concealing 'burst' errors, i.e. the maintenance of constant luminance and chrominance levels during the errors, gave less effective concealment as the duration of the errors increased. More effective concealment of 'burst' errors might well be achieved by other techniques such as the use of information occurring on the previous line; such a technique is already employed for concealing drop-outs in video tape recordings.

3 Acceptable Limits for Timing Jitter in the Analogue Samples Obtained from a P.C.M. Video Signal

In most pulse code modulation systems, it is important that the pulses should arrive at regular intervals at the digital-to-analogue converter. Assuming that all timing information is derived from the p.c.m. pulse train, any timing jitter in these pulses causes pulse-position modulation of the samples forming the decoded analogue signals, thus introducing unwanted components.^{7,8} A large amount of timing jitter will also cause errors in the p.c.m. decoding process, i.e. 0's may be decoded as 1's and vice-versa, but this extreme condition will not be considered in this paper.

One of the most common sources of jitter in a digital system is the regenerative repeaters used in long transmission links. In such repeaters, the pulses are re-timed using clock pulses derived from the p.c.m. pulse trains; jitter is then introduced by the addition of noise and because the timing of the derived clock pulses is affected by the pattern density, i.e. the relative proportions of ones and zeros, in the pulse train.

If necessary, the jitter in a p.c.m. pulse train may be reduced prior to digital-to-analogue conversion by a re-timing process which is more efficient than that used in the repeaters.^{9,10} The reduction in the amount of jitter resulting from this final re-timing process is obtained at the cost of instrumental complications and it is therefore desirable to know the amount of jitter which can be tolerated in the decoded signal. For this reason, subjective tests have been performed to examine the effect, on a television display, of varying amounts of jitter in the analogue samples obtained from a p.c.m. system handling PAL, 625-line video signals. The results of these tests are given in Section 3.4.3.

The characteristics of the unwanted noise introduced by jitter depend to a certain extent on the method of

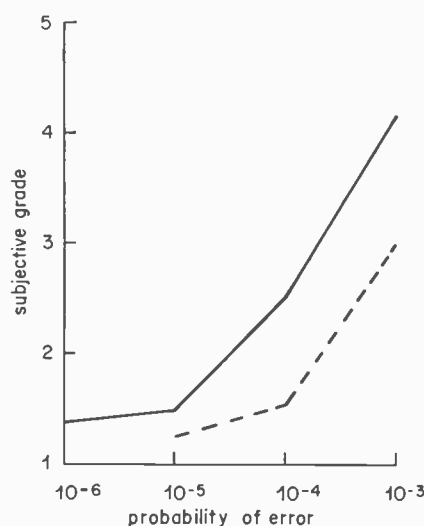


Fig. 8. Impairment produced by 1 μs burst errors with concealment.

- colour slide
- - - pictures from off-air colour film

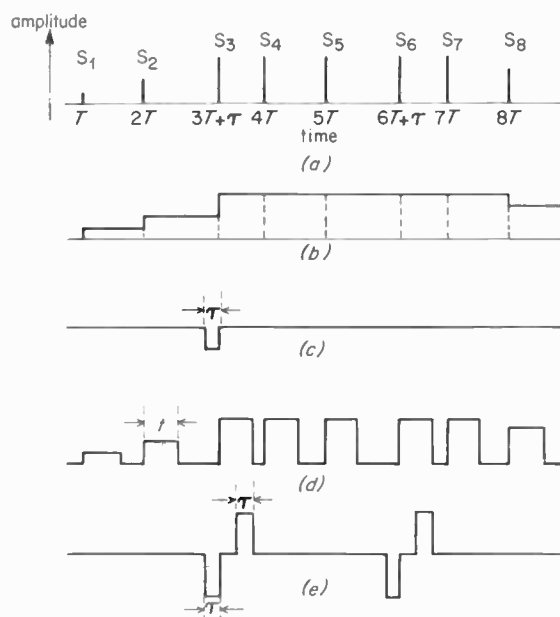


Fig. 9. Effect of mistiming of analogue samples.

- (a) Relative amplitudes and time of start of samples.
 (b) Waveform obtained with sample held constant until arrival of following sample—boxcar method.
 (c) Error in waveform (b) caused by mistiming of S_3 and S_6 .
 (d) Waveform obtained with samples of constant duration.
 (e) Error in waveform (d) caused by mistiming of S_3 and S_6 .

determining the duration of the analogue samples obtained from the digital-to-analogue converter. Figure 9 illustrates the effect of two different methods with a series of analogue samples whose relative magnitude and starting times are given by S_1 , S_2 , etc., in Fig. 9(a); in this figure S_3 and S_6 are incorrectly timed each being delayed by time τ . Figure 9(b) illustrates the case in which the magnitude of each sample is held constant until the following sample is decoded; this will be referred to as the boxcar method and was used in the equipment described in this paper. Figure 9(d) illustrates the alternative case in which all the samples have the same duration t which is less than the sampling period; this will be referred to as the constant-duration method. Figure 9(c) and 9(e) corresponding to Figs. 9(b) and 9(d) respectively, show the extent of the errors in the decoded analogue signal produced by the mistiming of samples S_3 and S_6 .

It will be seen that the boxcar method has the advantage that the mistiming of a sample such as S_6 , which is preceded by another of the same magnitude, produces no overall error (see Fig. 9(c)) whereas, in the constant duration method errors are produced by the mistiming of both S_3 and S_6 (see Fig. 9(e)). On the other hand, when there is a large difference between the magnitudes of a mistimed sample and the preceding sample, the errors resulting from the constant duration method may have such a spectrum as to be less visible than those produced by the boxcar method. The spectrum of any error produced by the boxcar method has maximum

amplitude at d.c. whereas the spectrum of an error from the constant duration method has zero amplitude at d.c. and a maximum amplitude at about $1/2T$, which is above the cut-off frequency of the low-pass filter following the decoder. It is thus very difficult to predict which is the better method for the majority of pictures. For the subjective tests described in this report, the only available type of digital-to-analogue converter used the boxcar method, and all further discussion relates to this type of equipment.

3.1 Picture Impairment Produced by Jitter

The impairment caused by jitter is far more noticeable in coloured areas than in monochrome areas of a picture.

Assuming that its magnitude is insufficient to cause digital errors, the most noticeable effect of any jitter in the samples of a composite colour video signal is that it causes unwanted variations in the colour hue and saturation. With random forms of jitter, these variations look similar to those caused by additional noise in the chrominance channel; on the other hand, sinusoidal jitter produces regular patterns similar to those caused by co-channel interference. The magnitude of the unwanted components in the colour difference signals is directly proportional to the amplitude of the colour subcarrier and therefore the resulting picture degradation is most noticeable with 100% saturated colours. Other factors affecting the magnitude and form of these unwanted components are discussed in Section 3.2 and 3.3.

The maximum amount of jitter which could be introduced in the tests to be described was insufficient to produce any noticeable impairment on monochrome signals. However, tests on the effects of timing instability in analogue video signals¹¹ indicate that the threshold of perceptibility of sinusoidal jitter on monochrome pictures is between 10 and 20 ns peak-to-peak for the most critical jitter frequencies. It will be seen from the results given in this paper that this threshold is about 10 times greater than the threshold for colour pictures.

3.2 Effect of PAL Decoder Alignment

It has been discovered in connexion with video tape recorder problems that certain alignment errors in PAL decoders can considerably increase the picture impairment caused by timing jitter although these same errors cause no significant degradation of jitter-free video signals.¹²

The most important error likely to occur in practice in the alignment of delay-line PAL decoders is an incorrect adjustment of the static phase of the reference subcarrier applied to the colour difference demodulators. With jitter-free video signals the only effect of such an error is to cause a reduction in the output level of the demodulators according to a cosine law as shown in Fig. 10; this can easily be compensated for by an increase in the chrominance gain. However, if the chrominance signals fed to the demodulators are jittering in phase

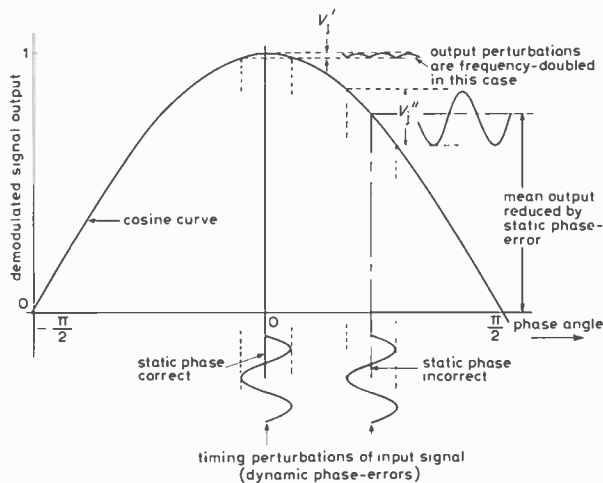


Fig. 10. Synchronous demodulation: the combined effects of static and dynamic phase errors.

with respect to the reference subcarrier, the magnitude of the resulting variations in the demodulated colour-difference signals (V'_j and V''_j in Fig. 10) are increased in the presence of a static phase error. Moreover, re-adjustment of the chrominance gain to compensate for the static phase error causes a further increase in the magnitude of these variations. It can be seen from Fig. 10 that when the static phase adjustment is correct, the output variations caused by jitter are at a minimum and, also, that a frequency doubling effect occurs which reduces the coarseness of the resulting impairment pattern on a television display, thereby further reducing its visibility.

With a delay-line PAL decoder, the situation is further complicated since timing jitter in the colour subcarrier at the input of the delay line can cause both amplitude and phase perturbations of the (R-Y) and (B-Y) components of the subcarrier obtained by adding and subtracting the input and output signals of the delay-line. The relative proportions of these phase and amplitude perturbations depend on the repetition frequency of the jitter.¹³ If the jitter repetition frequency is close to nf_L where f_L is the line frequency of the video signal and $n = 0, 1, 2, \text{etc.}$, the overall effect of jitter is to cause variations only in the saturation of the colour as discussed in relation to Fig. 10, no hue variations being obtained. On the other hand, if the repetition frequency is close to $(n + \frac{1}{2})f_L$, the jitter then causes variations in hue but no variations in saturation; in this case, the magnitude of the hue variations is nearly independent of the setting of the static phase of the reference subcarrier.

Other decoding errors which increase the impairment resulting from jitter include:

- (i) Decoding axes at the two colour difference demodulators not in quadrature.
- (ii) Error in chrominance delay-line length.
- (iii) Gain error in delay-line adder/subtractor.

These three types of error are generally less important than an error in the static phase of reference subcarrier

and were not examined in the subjective tests; details of their effects are discussed elsewhere.¹²

3.3 Factors Affecting Permissible Amount of Very Low Frequency Jitter

Assuming that the reference colour subcarrier used to demodulate the chrominance signal in a PAL decoder is locked to the colour burst in the jittered video signal, the colour hue and saturation errors caused by jitter progressively decrease at jitter frequencies below about 50 Hz because the burst-locked oscillator is able to follow slow variations in the phase of the burst. However, when considering the permissible jitter on video signals within broadcasting networks, the most critical conditions for very low frequency jitter arise when it is necessary to maintain separate video signals in synchronism to enable operations such as mixing to be carried out satisfactorily. With the slowest-acting synchronizing system now in use within the BBC (NATLOCK¹⁴), any variation in link transmission time should not change the phase of the colour subcarrier by more than 1.5° in 40 ms. This leads to a specification that the peak-to-peak amplitude of sinusoidal jitter should not exceed $7.5/f$ ns where f is the jitter frequency in Hz; this specification applies only if f is less than about 25 Hz.

3.4 Subjective Tests

A block diagram of the equipment is shown in Fig. 11. In the p.c.m. coder the video signal was sampled at approximately 13.3 MHz and each sample was coded into an 8-digit binary number in parallel form.

The jitter on the analogue samples was produced by retiming the digital signals in a store controlled by jittered clock pulses. All eight digits described by a given sample were jittered by the same amount. The same effect could have been obtained by means of two sample-and-hold circuits in tandem operating on an analogue video signal but it was instrumentally convenient to convert the signal into p.c.m. form and back to analogue as described above.

Both random Gaussian and sinusoidal forms of jitter were used in the tests. The source of the random jitter was a white noise generator having a wide band output which was filtered as appropriate by low-pass filters. The sinusoidal control voltage was obtained from a frequency synthesizer giving a very stable frequency and the frequencies chosen were such as to give maximum visibility patterns on the display.

In the jitter generator, the signal from the white-noise or sine-wave generator was added to a clock frequency sawtooth waveform. The resulting signal was applied to a Schmitt trigger followed by a monostable producing pulses with a duration of half a clock period. These pulses formed the jittered clock pulse signal.

For a constant amplitude of sinusoidal jitter signal, the amount of jitter produced was sensibly constant over the range of frequencies used in the subjective tests. Also, the amount of jitter was linearly related to the amplitude of a sinusoidal jitter signal up to at least 12.5 ns peak-to-peak.

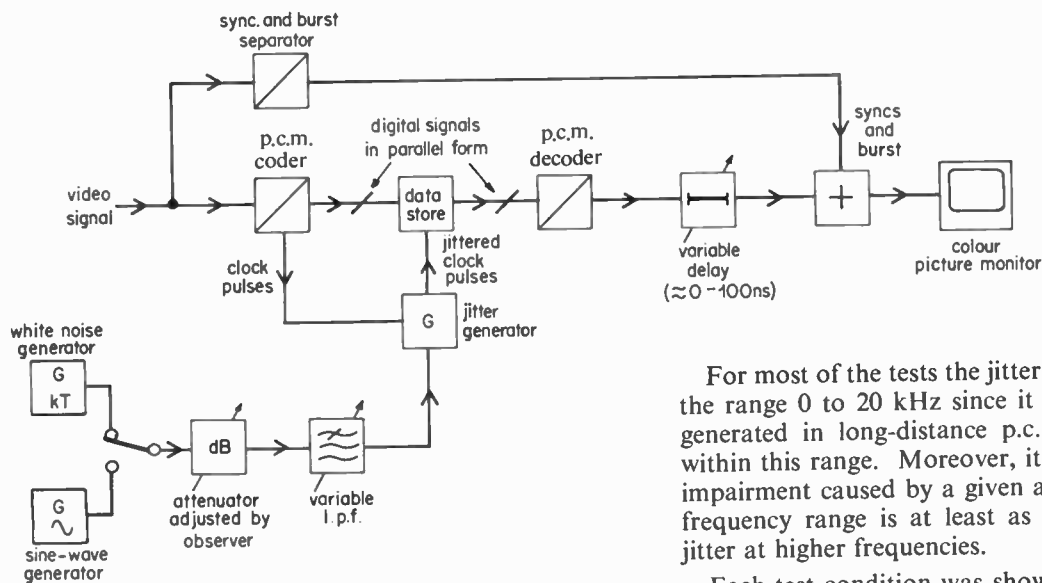


Fig. 11. Block diagram of test equipment.

Variation of the static phase of the reference subcarrier in the PAL decoder was obtained by adjusting the signal path delay, as shown in Fig. 11, at a point before adding unjittered syncs and bursts to the reconstituted analogue signal. Subsidiary tests had shown that the absence of jitter on the syncs and burst in the signal fed to the PAL decoder had no noticeable effect on the degree of impairment caused by the forms of jitter used in the tests.

The video signals were displayed on a high-quality 53 cm monitor having a peak brightness of 70 candela/metre²; with zero beam current the brightness of the monitor resulting from ambient illumination was 0.1 candela/metre².

3.4.1 Test procedure

The video signal used in all the tests was 100% colour bars, this signal being the most critical for showing the effects of jitter. The amplitude of this signal relative to the conversion range of the p.c.m. coder was adjusted to just fill the conversion range as described in Section 2.2.

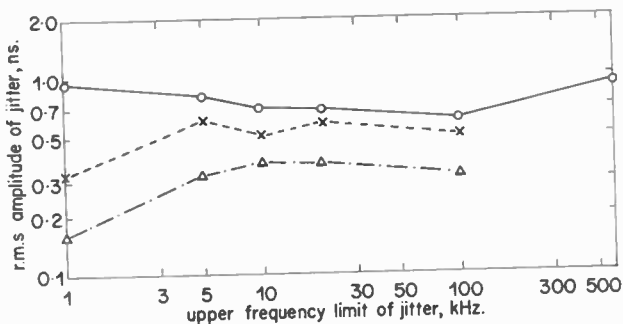


Fig. 12. Amplitude of random jitter causing just perceptible picture impairment for different errors in the phase of the reference subcarrier.

- phase error = 0°
- ×--- phase error = 16°
- △— phase error = 32°

For most of the tests the jitter frequencies used were in the range 0 to 20 kHz since it is understood that jitter generated in long-distance p.c.m. links is likely to lie within this range. Moreover, it has been found that the impairment caused by a given amplitude of jitter in this frequency range is at least as great as that caused by jitter at higher frequencies.

Each test condition was shown to eight skilled observers seated in turn at a distance of about six times picture height from the display. Each observer was asked to adjust the variable attenuator controlling the amplitude of jitter until the picture impairment was judged to be at the threshold between grades 1 and 2 on the 6 point impairment scale given in Table 1, without the words in parenthesis. This procedure has been found previously¹⁵ to give a reliable indication of an impairment grade of 1.5 as determined from a curve of mean grade versus jitter amplitude when subjects are asked to grade various fixed amounts of jitter.

3.4.2 Results

The results of the tests for three different settings of the static phase of reference subcarrier are shown in Figs. 12 and 13. Figure 12 shows the r.m.s. magnitude of random jitter giving grade 1.5 impairment plotted

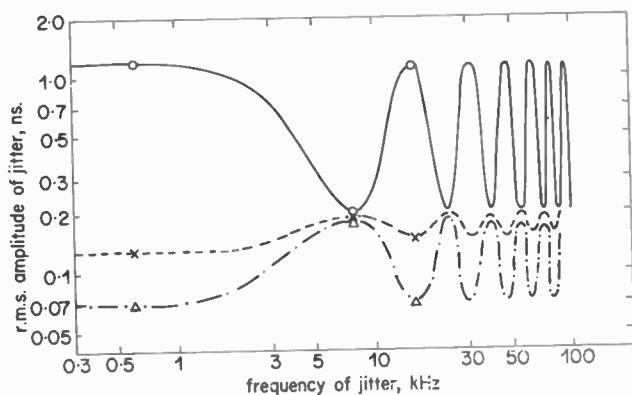


Fig. 13. Amplitude of sinusoidal jitter causing just perceptible picture impairment for different errors in the phase of the reference subcarrier.

- phase error = 0°
- ×--- phase error = 16°
- △— phase error = 32°

Points ○ × △ are results from tests using 8 observers; lines show general form of variations obtained by one observer.

as a function of the cut-off frequency of the low-pass filter limiting the bandwidth of the random noise jitter signal. Figure 13 shows the r.m.s. magnitude of sinusoidal jitter which causes grade 1.5 impairment plotted as a function of jitter frequency.

It will be seen that irrespective of the bandwidth of random jitter, with zero offset of the static phase of the reference subcarrier in the PAL decoder, a jitter amplitude of less than 0.6 ns r.m.s. will result in a grading of 1.5 or less. However, from discussions with manufacturers, it would seem that the long-term drift of the static phase in commercial receivers could not be guaranteed to be better than about $\pm 15^\circ$ even if special precautions were taken in this direction; until very recently, the alignment of the static phase was not thought to be a critical adjustment and in an examination of 20 present-day receivers, errors of up to $\pm 50^\circ$ were encountered.

Assuming that errors in the static phase will not be greater than $\pm 15^\circ$, the results of the tests show that the impairment caused by random jitter will be within acceptable limits for r.m.s. amplitudes less than 0.3 ns. For sinusoidal jitter, the r.m.s. amplitude should not be greater than 0.15 ns at the most critical jitter frequencies.

4 Conclusions

The picture impairments caused by both digital transmission errors and by timing jitter in a p.c.m. system handling PAL, 625-line video signals have been investigated by way of subjective tests.

The results of the tests on transmission errors indicate that for a high-quality television broadcasting system, the error probability should not be greater than:

- (a) 10^{-7} for unconcealed errors; this figure applies to both single-digit and 'burst' errors of any duration up to at least 1 μ s.
- (b) 10^{-4} for concealed single-digit errors.
- (c) 10^{-5} for concealed 'burst' errors of any duration up to 1 μ s.

The error concealment technique used in the tests consisted of replacing erroneous samples by previous samples in the same line of the picture. (See Sect. 2.1.3).

Errors longer than 1 μ s were not examined but previous tests on drop-outs in video tape recording indicate that the conclusions given above for unconcealed errors still apply to errors on monochrome pictures having burst durations up to 12 μ s.

In the tests on timing jitter, controlled amounts of jitter were introduced into the analogue samples of a video signal obtained by decoding a p.c.m. video signal.

These tests showed that the picture impairment caused by jitter is significantly affected by errors in the adjustment of the static phase of the reference colour subcarrier in the PAL decoder used in displaying these signals. For static phase errors no greater than $\pm 15^\circ$, it was found that the impairment caused by random jitter was within acceptable limits for broadcast quality pictures if the r.m.s. amplitude of the jitter was no greater than 0.3 ns.

More specific limits for random jitter of a given bandwidth or for sinusoidal jitter of a given frequency are shown in Figs. 12 and 13.

It should be noted that the jitter frequencies used in the tests were sufficiently high as to have little effect on the timing stability of the reference colour subcarrier derived in the PAL decoder. Factors affecting the maximum permissible jitter at low frequencies are discussed in Sect. 3.3.

Although investigations into the problems of long distance transmission of video p.c.m. signals are still at an early stage, the work so far carried out indicates that the acceptable limits for error rates and jitter given in this report can be achieved without imposing undue practical difficulties or incurring undue expense.

5 References

1. Geddes, W. K. E., 'The subjective impairment produced by drop-outs in video tape recordings'. BBC Research Department Report No. T-143, Serial No. 1965/1, 1965.
2. Peterson, W. W. and Weldon, E. J., 'Error Correcting Codes', 2nd edition (MIT Press, Cambridge, Mass., 1972).
3. Meares, D. J., 'Pulse code modulation of video signals: parallel-to-serial and serial-to-parallel conversion'. BBC Research Department Report No. 1971/14, 1971.
4. British Patent No. 1,313,832. 'Reduction of errors in television signals'.
5. Ashida, J., 'Subjective impairment by bit error in pcm tv transmission', *NHK Tech. J.*, 23, No. 4, pp. 245-51, 1971 (in Japanese).
6. Lewis, N. W. and Allnatt, J. W., 'Subjective quality of television pictures with multiple impairments', *Electronics Letters*, 1, No. 7, pp. 187-8, 1965.
7. Manley, J. M., 'The generation and accumulation of timing noise in p.c.m. systems—an experimental and theoretical study', *Bell Syst. Tech. J.*, 48, No. 3, pp. 541-615, 1969.
8. Byrne, C. J., Karafin, B. J. and Robinson, D. B., 'Systematic jitter in a chain of digital regenerators', *Bell Syst. Tech. J.*, 42, No. 6, pp. 2679-2714, 1963.
9. Witt, F. J., 'An experimental 224 Mb/s digital multiplexer-demultiplexer using pulse stuffing synchronization', *Bell Syst. Tech. J.*, 64, No. 9, pp. 1852-6, 1965.
10. Mayo, J. S., 'Experimental 224 Mb/s pcm terminals', *Bell Syst. Tech. J.*, 64, No. 9, pp. 1827-30, 1965.
11. Chew, J. R. and Edwardson, S. M., 'Specification of the timing stability of 625/50 monochrome and PAL colour broadcast television signals'. International Broadcasting Conference, IEE Conference Publication No. 88, September 1972, pp. 257-61.
12. 'Specification of the timing stability of broadcast monochrome and PAL colour television signals'. BBC Research Department Report (in course of preparation).
13. Devereux, V. G., 'Digital video: effect of PAL decoder alignment on the acceptable limits for timing jitter'. BBC Research Department Report No. 1973/1, 1973.
14. Gregory, D. N., Bliss, J. L., Millar, I. D. B. and Allen, C. J., 'Colour picture source synchronization by the Natlock system', *J. Soc. Mot. Pict. Telev. Engrs*, 78, No. 8, pp. 611-4, 1969.
15. Devereux, V. G., 'Pulse code modulation of video signals: subjective tests on acceptable limits for timing jitter in the decoded analogue samples'. BBC Research Department Report No. 1971/42, 1971.

Manuscript received by the Institution on 26th February 1974.
(Paper No. 1601/Com. 97).

© The Institution of Electronic and Radio Engineers, 1974

Principal component analysis of production data

J. HYWEL WILLIAMS,
B.Sc.(Tech.), M.Inst. M.C.*

SUMMARY

This paper develops the use of principal component analysis as an aid to quality assurance. The sensitivity of the analysis to changes in the statistical characteristics of the measurements is examined. The analysis can reduce the number of time series that have to be monitored for quality assurance. The technique is to linearly combine groups of the measurements. This grouping of measurements excludes the use of the cusum as a quality assurance aid. A new quality monitoring process is proposed; the cumoderror, which enables the detection of mean level and variance changes in single or combined measurements.

* *Dynamic Analysis Group, Department of Mechanical Engineering and Engineering Production, University of Wales Institute of Science and Technology, King Edward VII Avenue, Cardiff CF1 3NU.*

List of Symbols

x	measurement vector
x_i	i th measurement
A_1	covariance matrix of measurements
A	correlation matrix of measurements
λ_j	j th eigenvalue of A
u^j	j th eigenvector of A
z	principal component vector
x_m	m th measurement whose statistical characteristics have changed
δa^{mc}	resulting change in m th column of A
$\delta \lambda_j$	resulting change in j th eigenvalue of A
δu_k^j	resulting change in k th element of j th eigenvector of A
$S(\delta \lambda_j)_m$	sensitivity coefficient of j th eigenvalue with respect to m th measurement
$S(e_{jk})_m$	sensitivity coefficient associated with j th eigenvector
$\langle a, b \rangle$	inner product of vectors a and b
\hat{a}	estimated value of a parameter a
$E(x)$	expected value of a parameter x
C_k	cusum after k readings
T	'target' for cusum
K_k	cumoderror after k readings
T^1	'target' for cumoderror
ε_{ik}	error between T and mean level for i th measurement at k th reading

1 Introduction

The quality control manager concerned with the manufacture of electronic assemblies will be provided with visual and mathematical aids based on test data made available at various stages of manufacture. In addition to monitoring present values of physical variables, he is concerned with detecting changes in the various production processes which cause the quality to deteriorate in time to take effective corrective action.

It is usual in a pre-production run or at full production start-up of a new product to monitor a large number of parameters such as component values, performance levels, etc. To maximize the amount of information these parameters should be recorded as actual values rather than go/no-go. As production throughput increases, the test schedule is (or should be) adjusted in the light of the data processing results. Of course, some measurements will be retained regardless of any data analysis, for example, those monitoring specific customer requirements. However, many measurements are carried out to check production processes and design quality and so the test schedule and subsequent data processing should be capable of adjusting to changes in these factors.

2 The Use of Principal Components

If the test schedule is optimum, in that each measurement is absolutely necessary and contributes positive information which cannot be obtained from any other source, then little more can be done. If, however, there is redundant information, then the exclusion of unneces-

sary measurements will result in a reduction of costs. It is likely that experienced engineers are ultimately able to anticipate redundant measurements, i.e. those which are effectively linear combinations of others. Measurements which contribute little to the overall variability of the product are 'redundant' as far as efficient and cost effective quality monitoring are concerned. This does not imply that the test is necessarily discontinued, rather the quality control effort is concentrated on those production processes or components where the greatest benefit is to be gained.

This paper describes how the principal component (of variance not hardware) method¹ of analysis may be used to indicate the areas where quality control effort may be most effective. The method does not rely on the engineer's skill or experience in interpreting the measurements undertaken. It is a special case of a multiple regression analysis and it specifically grades groups of measurements by their contribution to overall variability. Jolliffe² has shown that the principal component analysis is much more efficient in data processing time than standard multiple regression methods.

This paper also indicates how the measurement correlation matrix, which is crucial to the method, can be up-dated iteratively, thus saving storage requirements and develops a sensitivity analysis of the results to statistical changes in the measurements. It also suggests a data processing scheme for single or grouped data that monitors changes in level and variance with only one graphical display.

3 Measurement Correlation Matrix

Suppose that n measurements are made on a unit under test at a particular stage in manufacture. The test can then be defined by an $(n \times 1)$ measurement vector

$$x \triangleq [x_i], \quad i = 1, 2, \dots, n. \quad (1)$$

For any particular measurement, repeated on a succession of units, a time series may be formed, and the variance a_{ii} estimated, where

$$\hat{a}_{ii} = E[x_i^2] - (E[x_i])^2 \quad (2)$$

(where E denotes the 'expected value').

If the time series for the i th and j th measurements are compared, then the covariance a_{ij} is estimated by

$$\hat{a}_{ij} = E[x_i x_j] - E[x_i]E[x_j] \quad (3)$$

and the covariance matrix A_1 ,

$$A_1 = E[xx^T] = [a_{ij}] \quad (4)$$

is symmetrical, i.e.

$$a_{ij} = a_{ji}.$$

As the measurement vector x may have elements which are measures of different physical quantities, correlations rather than covariances will be considered. The elements a_{ij} are replaced by $a_{ij}/\sqrt{(a_{ii}a_{jj})}$, resulting in the correlation matrix A . If the measurements made on the unit under test are independent, then each measurement contributes useful knowledge regarding the quality of the unit, and this knowledge cannot be inferred from the other measurements made. In statistical terms, independence corresponds to the correlation matrix A being

the unit matrix I . In general, the correlation matrix A will have non-zero off-diagonal terms, suggesting sufficient correlation may exist between certain measurements. The correlation matrix is a measure of the total variability of the measurement vector. To implement a principal component analysis, which transforms the correlation matrix into a diagonal matrix, a method of updating the correlation matrix is required. One such method is given in Appendix 3.

4 Principal Components

If a set of different measurements is uncorrelated then the total variance is the sum of the variances of the individual measurements.

A principal component analysis breaks down a correlation matrix into a set of orthogonal components equal in number to the number of measurements. It is a linear transformation which produces a set of uncorrelated variables, as outlined in Appendix 1. Although all the components are required to reproduce the total variance of the measurement vector a few of them may contribute a significantly large percentage of the total variance.

The basic equations are

$$x_i = \sum_{t=1}^n w_{it} z_t, \quad i = 1, 2, \dots, n \quad (5)$$

where

z_t = t th principal component

w_{it} = weight of the t th component in the i th measurement.

Some criterion is required to select the principal components to be retained.⁴ The variances of the principal components are proportional to the eigenvalues of the correlation matrix (Appendix 1). As the principal components are uncorrelated it is possible to find the proportion of the total variance contributed by each component. It is customary^{2,4} to retain those components that represent approximately 75% of the total variance.

The selected principal components are then written in terms of weighted sums of the measurements, the weights correspond to the elements of the eigenvectors. There is the same number of eigenvector elements as measurements, but it is the usual practice to normalize the eigenvector (by dividing through by the largest element) and to retain only those elements greater than 0.7. Thus the application of principal component analysis produces a reduced number of uncorrelated variables, each of which are weighted sums of a restricted number of original measurements.

5 Sensitivity Analysis

Having obtained the principal components and initiated further data processing on them for quality monitoring, the up-dated correlation matrix is examined for significant changes. One would not initiate a fresh principal component analysis if the up-dated correlation matrix showed no significant changes. Appendix 2 develops a sensitivity analysis of the eigenvalues and

eigenvectors of the correlation matrix to changes in the off-diagonal terms. These terms will change as the statistical characteristics of a measurement alter.

If

- x_m = the measurement that has altered
- δa^{mc} = resulting change in the m th column of A
- λ_j = j th eigenvalue prior to change
- $\delta \lambda_j$ = resulting change in the j th eigenvalue
- u_k^j = k th element of j th eigenvector prior to change
- δu_k^j = resulting change in k th element of j th eigenvector.

Then from Appendix 2:

$$|\delta \lambda_j| \leq 2 \|\delta a^{mc}\| |u_m^j|, \quad j = 1, 2, \dots, n \quad (6)$$

$$|\delta u_k^j| \leq 2 \|\delta a^{mc}\| \sum_{t=1}^n \frac{|u_m^t| |u_k^t|}{|\lambda_j - \lambda_t|}, \quad j = 1, 2, \dots, n, \quad k = 1, 2, \dots, n, \quad j \neq k \quad (7)$$

where the Euclidean norm

$$\|\delta a^{mc}\| \triangleq [(\delta a_1^{mc})^2 + (\delta a_2^{mc})^2 + \dots + (\delta a_n^{mc})^2]^{\frac{1}{2}}$$

$(\delta a_i^{mc} \triangleq i$ th element of δa^{mc}).

Sensitivity coefficients can be defined as follows:

$$S(\delta \lambda_j)_m \triangleq 2 |u_m^j|, \quad j = 1, 2, \dots, n \quad (8)$$

$$S(e_{jk})_m \triangleq 2 \frac{|u_m^k|}{|\lambda_j - \lambda_k|}, \quad j = 1, 2, \dots, n, \quad k = 1, 2, \dots, n, \quad j \neq k \quad (9)$$

where

$$|\delta u_k^j| \leq \sum_{k=1}^n |e_{jk}| |u_m^k|, \quad j \neq k. \quad (10)$$

The sensitivity coefficients given by (8) and (9) can be calculated when the principal component analysis is initiated. Then at each correlation matrix up-date the upper bounds of the changes in the principal components due to changes in the m th measurement can be estimated by calculating $\|\delta a^{mc}\|$, and using the sensitivity coefficients given in equations (8) and (9).

6 An Example

Test data for a servo system which has been in production for many years were made available to the

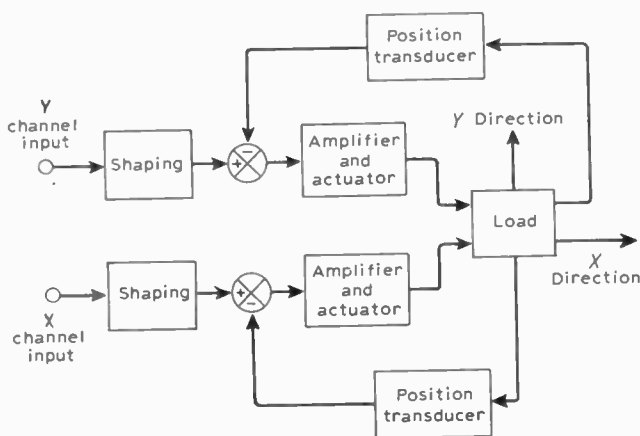


Fig. 1. Simplified block schematic of sub-assembly under test
Note. X and Y directions are orthogonal.

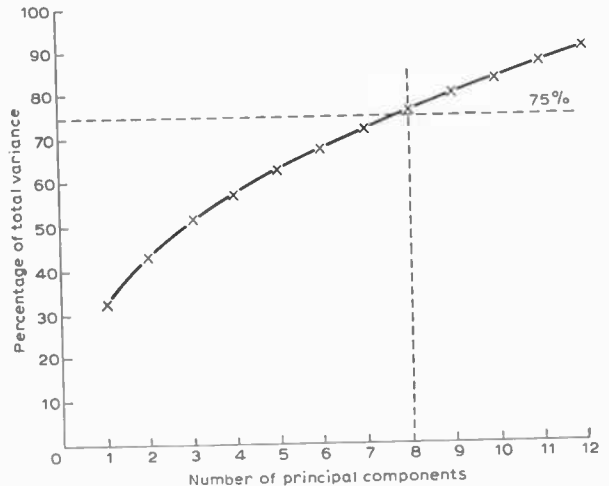


Fig. 2. Percentage of total variance against number of principal components.

author. Whilst the greatest gain is to be obtained at production start-up, the manufacturers have encouraged the analysis in order to illustrate the principles involved.

Figure 1 illustrates the sub-assembly examined. It is basically a load positioning device with two orthogonal channels (X and Y). Each channel consists of an input demand shaping network feeding an amplifier which in turn controls a pneumatic actuator. Position feedback is obtained from position transducers in each channel. The tests carried out on the sub-assembly are listed in Table 1. The first six measurements check the mechanical backlash and maximum excursions in both directions while measurements seven to eighteen consist of a frequency response check at 4, 8 and 16 Hz for both channels. Measurements 19 and 20 check the electrical zero of the position feedback transducers and the last two measurements are a repeat of the backlash checks.

Test results on a batch of 131 sub-assemblies which had successfully passed the test specification were processed. The correlation matrix was set-up non-iteratively and the eigenvalues and eigenvectors calculated and normalized. Figure 2 summarizes the results

Table 1. Tests carried out on sub-assembly

Measurement No.	Test details	
1	Backlash in Y direction	Mechanical checks
2	Backlash in X direction	
3	Max. excursion in Y positive direction	
4	Max. excursion in Y negative direction	
5	Max. excursion in X positive direction	
6	Max. excursion in X negative direction	
7, 8	In-phase and quad volts at 4 Hz Y direction	Frequency response
9, 10	In-phase and quad volts at 8 Hz Y direction	
11, 12	In-phase and quad volts at 16 Hz Y direction	
13, 14	In-phase and quad volts at 4 Hz X direction	
15, 16	In-phase and quad volts at 8 Hz X direction	
17, 18	In-phase and quad volts at 16 Hz X direction	
19	Electrical zeroing in Y direction	Elec. check
20	Electrical zeroing in X direction	
21	Repeat of measurement No. 1	
22	Repeat of measurement No. 2	

Table 2. Measurements contributing to principal components Nos. 1-8

Principal component No.	Measurement No.																					
	1	2	3	4	5	6	7	8	9	10	11	12	13	14	15	16	17	18	19	20	21	22
1											x	x	x	x	x	x						
2			x	x	x	x					x											
3														x	x	x	x					
4		x					x															x
5														x								x
6		x									x											
7							x															
8		x																				

of the principal component analysis. It is seen that eight principal components account for 75% of the total variance exhibited by the set of measurements. Table 2 gives the decomposition of these eight components into the original measurements. The measurements shown are those which have a weighting factor greater than 0.7 in the normalized eigenvectors.

6.1 Measurement Grouping

The first principal component, which accounts for 33% of the total variance is made up of the quadrature voltage measurements at 16 Hz in the Y-direction and 4, 8 and 16 Hz in the X-direction together with backlash and electrical zeroing measurements in the Y-direction. The second principal component groups the maximum excursions of the load together with the quadrature volts in the Y-direction at 16 Hz, while the third is made up of the quadrature voltage in the X-direction with the X-direction electrical zeroing of the feedback transducer. This measurement grouping is unlikely to be haphazard. One would expect the in-phase voltage to form one component with the quadrature voltage forming another. Of interest are measurements of the mechanical characteristics which are associated with the frequency response measurements in the principal components. It is always dangerous to relate cause and effect in any statistical analysis without using engineering knowledge of the unit under test. However, groupings indicated by the principal component analysis can, at an early stage of production, furnish useful information on the statistical interdependence of certain measurements.

6.2 Redundant Measurements

It is seen from Table 2 that measurements 7 and 10 do not appear in the first eight principal components. In fact the frequency measurements at 4 and 8 Hz in the Y-direction are of lesser importance than the other frequency response measurements so far as overall variability is concerned. So whilst the measurements have to be carried out due to test specification requirements and convenience it is suggested by the analysis that they need not be further processed in any quality assurance scheme.

By monitoring the eight principal components instead of the original 22 measurements, quality assurance effort is reduced by 63%. The reduced number of variables to be processed still retains 75% of the total variability of the measurements.

6.3.1 Data processing the principal components

A well-known and useful method of processing measurements in a quality control scheme is the cusum.⁷ Briefly, it entails plotting the cumulative error between the measurement and the expected mean value of the measurement. Changes in the mean level are indicated by slopes in the cusum plot. The scheme is given by

$$C_{k+1} = \sum_{t=1}^{k+1} [a_t - T] \tag{11}$$

a_t = t th reading of measurement being monitored

where

C_{k+1} = cusum after $k+1$ readings

T = target (usually expected mean).

Equation (11) can be written in the form

$$C_{k+1} = C_k + (x_{k+1} - T) \tag{12}$$

or

$$C_{k+1} = C_k + \epsilon_{k+1}$$

where ϵ_{k+1} is the error between the $(k+1)$ th reading and the target, T .

A principal component, z_j say, can be written as a weighted sum of some of the original measurements, as discussed in Section 5. The cusum of z_j is effective as a quality assurance aid if the mean value of only one of the measurements in the sum changes. If more than one measurement changes, which is likely for the measurements forming the principal component, then their changes in mean could cancel. So the cusum in its present form is unsuitable as a scheme for processing principal components.

6.3.2 Cumulative modulus error

The suggested modification to the cusum is to sum the modulus error for each measurement in the principal component.

$$K_{k+1, j} = K_{k, j} + \sum_{i=1}^m |x_{i, k+1} - T_i| - T_j^1 \tag{13}$$

where

$K_{k, j}$ = 'cumoderror' for j th component after k readings

T_i = target for i th measurement

T_j^1 = target for cumoderror

$x_{i, k+1}$ = $(k+1)$ reading of the i th measurement

m = number of measurements used in j th component.

The measurements used in the j th component are those having a normalized weight greater than 0.7 in the j th eigenvector of the correlation matrix, as discussed in Section 4.

There seems little to be gained in retaining the actual values of the weights in forming the cumoderror.

Let

$$\epsilon_{ik} = x_{i, k} - T_i. \tag{14}$$

Then

$$E[|\epsilon_{ik}|] = \sqrt{\frac{2}{\pi}} \sigma_i \tag{15}$$

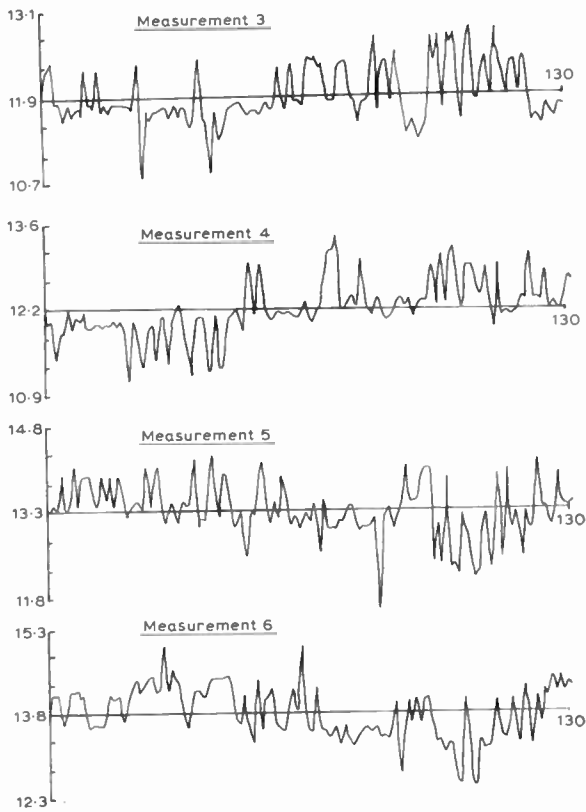


Fig. 3. Time series of measurements 3, 4, 5 and 6.

example given, the second principal component consists of measurements 3, 4, 5 and 6, which are measures of similar mechanical properties, together with the quadrature voltage at 16 Hz in the Y direction, measurement 12. It would be expedient in this case to form the sum of measurements 3, 4, 5 and 6 and to include measurement 12 in the third sum, for the third principal component is made up of quadrature voltage measurements.

6.3.4 Application of cumoderror to example

As an illustration of the use of the cumoderror as an aid for quality assurance, measurements 3, 4, 5 and 6 were processed individually, using the standard cusum and collectively using the cumoderror. Time series of the four measurements are given in Fig. 3 with their cusums illustrated in Fig. 4. The time series formed by summing the four measurements is shown in Fig. 5 with the resulting cusum. Figure 6 shows the corresponding cumoderror.

As the measurements processed were of sub-assemblies that had successfully met the test requirements any interpretation of the cusum and cumoderror plots is restricted to estimating the within tolerance variability of the measurements, although Figs. 5 and 6 show how the cumoderror overcomes the inadequacies of the cusum of the summed measurements.

To illustrate more fully the use of the cumoderror three time series were simulated from normal distributions. Step change in mean level and variance were imposed after ten readings.

where

$$\sigma_i^2 = \text{var of } i\text{th measurement.}$$

Thus

$$E \left[\sum_{i=1}^m |e_{ik}| \right] = \sqrt{\frac{2}{\pi}} \sum_{i=1}^m \sigma_i. \quad (16)$$

This is the target for the cumoderror.

Thus equation (13) can be written as

$$K_{k+1, j} = K_{k, j} + \sum_{i=1}^m |e_{i, k+1}| - \sqrt{\frac{2}{\pi}} \sum_{i=1}^m \sigma_i. \quad (17)$$

By plotting successive values of $K_{k, j}$ the mean levels and variances of all the measurements in the j th principal component can be monitored. If one or any number of the mean levels change the value of $K_{k, j}$ will always increase. If one or any number of the variances increase or decrease then $K_{k, j}$ will increase or decrease respectively. The cumoderror is not restricted to monitoring sums of measurements but can also be implemented for single measurements. The cumoderror requires two target values and it is suggested that a run-in period is used to establish good estimates of mean levels and variances. (This run-in period would be required if a cusum was used.)

6.3.3 Modified measurement selection

It is not necessary to adhere strictly to the measurement grouping given by the measurements with weights greater than 0.7 in the normalized eigenvector. In the

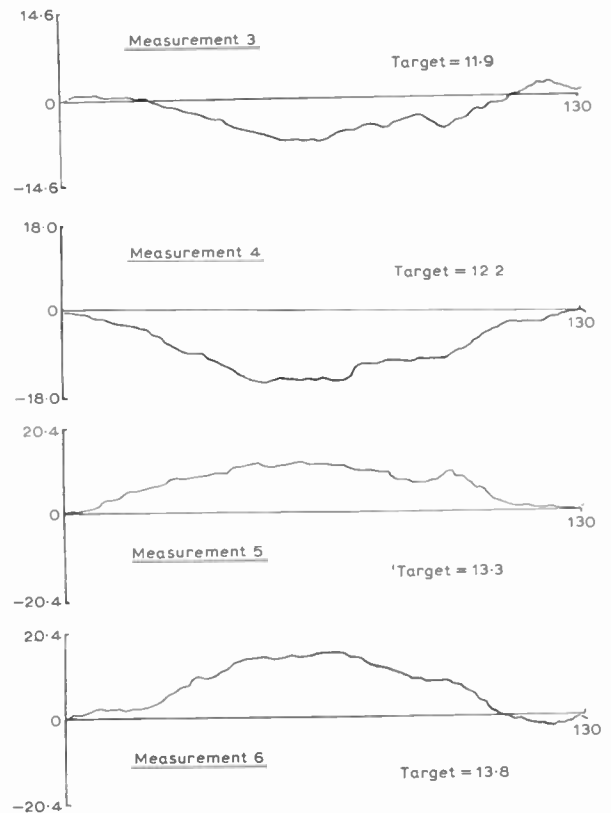


Fig. 4. Cusums of measurements 3, 4, 5 and 6.

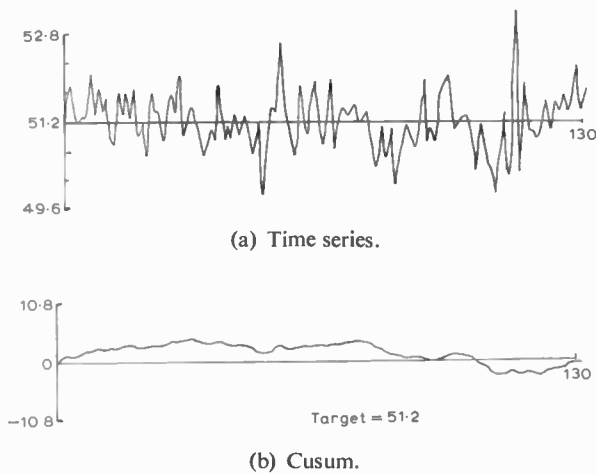


Fig. 5. Time series and cusum of the sum of measurements 3, 4, 5 and 6.

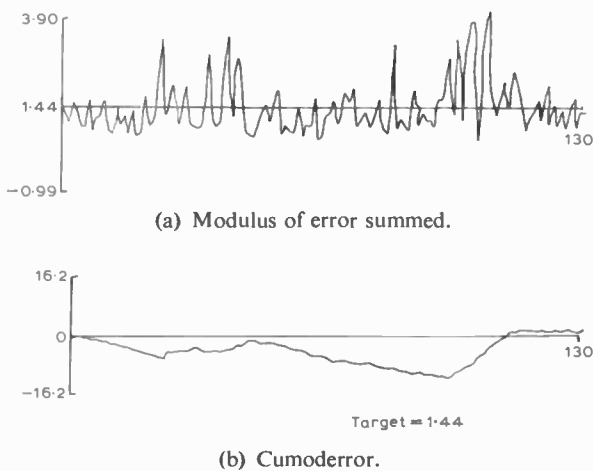


Fig. 6. Sum of modulus of errors for measurements 3, 4, 5 and 6 with corresponding cumoderror.

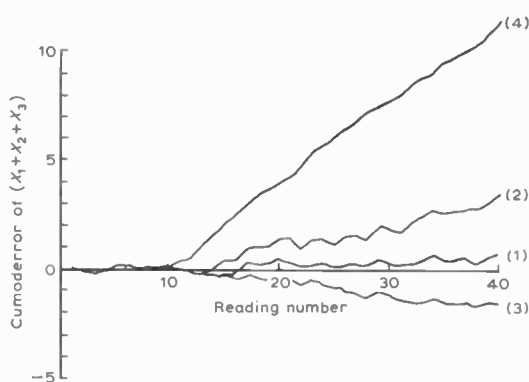


Fig. 7. Illustrating use of cumoderror.

$X_1 = N(3, 0.1)$ Normal distribution mean = 3
 Standard deviation = 0.1
 $X_2 = N(4, 0.2)$
 $X_3 = N(4, 0.2)$
 Y monitored where $Y = X_1 + X_2 + X_3$ (X s independent)
 Case (1) No change
 Case (2) At 11th reading $X_3 = N(4, 0.3)$
 Case (3) At 11th reading $X_3 = N(4, 0.1)$
 Case (4) At 11th reading $X_3 = N(4.5, 0.2)$

Figure 7 clearly shows the change in slope in the cumoderror, thus illustrating the theoretical slope changes in the cumoderror discussed in Section 6.3.2.

7 Conclusions

The method of principal components has been shown to be a useful aid in reducing the amount of data to be monitored for quality assurance. It also highlights those areas where quality assurance effort may be best utilized.

The cusum technique applied to summed data is insensitive to changes in the individual measurements making up the sum. The cumoderror overcomes this problem and its use has been illustrated using actual and simulated data.

8 Acknowledgments

The author wishes to thank the British Aircraft Corporation for supplying the data and the Electrical Quality Assurance Directorate for their continued financial support and encouragement.

9 References

1. Jeffers, J. N. R., 'Two case studies in the application of principal component analysis', *Applied Statistics*, 16, pp. 225-36, 1967.
2. Jolliffe, I. T., 'Discarding variables in a principal component analysis, 1: Artificial data', *Applied Statistics*, 21, pp. 160-73, 1972.
3. Brown, R. G., 'Smoothing, Forecasting and Prediction' (Prentice-Hall, Englewood Cliffs, N.J., 1967).
4. Lawley, D. N. and Maxwell, A. E., 'Factor Analysis as a Statistical Method' (Butterworth, London, 1963).
5. Bellman, R., 'Introduction to Matrix Analysis' (McGraw-Hill, New York, 1960).
6. Franklin, J. N., 'Matrix Theory' (Prentice-Hall, Englewood Cliffs, N.J., 1968).
7. de Bruyn, C. S. Van D., 'Cumulative Sum Tests: Theory and Practice' (Griffin, London, 1968).

10 Appendix 1: Principal Component Analysis

A linear transformation is applied to the n observed measurements $x_i, i = 1, 2, \dots, n$, to produce a new set of n normalized uncorrelated variates, $z_i, i = 1, 2, \dots, n$ which are known as principal components.⁴ A description of the method follows.

An $(n \times 1)$ measurement vector, x , is defined as

$$x \triangleq [x_i]$$

and an $(n \times n)$ covariance matrix A_1 is defined by

$$A_1 = E[xx^T] \tag{18}$$

where E denotes 'expected value'.

Since A_1 is symmetric it is well known⁵ that an orthogonal matrix U can be found whose columns are the normalized eigenvectors of A_1 and such that

$$U^T A_1 U = \text{diag} [\lambda_1, \lambda_2, \dots, \lambda_N] \tag{19}$$

where $\lambda_1, \lambda_2, \dots, \lambda_N$ are the eigen values of A_1 and

$$\lambda_1 > \lambda_2 > \lambda_3 > \dots > \lambda_N. \tag{20}$$

If y is an $(n \times 1)$ vector formed by performing a linear transformation on x given by

$$y = U^T x. \tag{21}$$

Then from (18) and (21)

$$E[yy^T]_I = U^T A_I U. \tag{22}$$

Hence from (19)

$$\text{var}(y_i) = \lambda_i$$

and

$$\text{covar}(y_i y_j) = 0 \quad \text{if } i \neq j$$

that is, the y_i are uncorrelated and

$$\text{var}(y_1) > \text{var}(y_2) \dots > \text{var}(y_n).$$

The principal components vector z is related to y by the expression

$$z = \Lambda^{-\frac{1}{2}} y \tag{23}$$

where

$$\Lambda = \text{diag}[\lambda_1, \lambda_2, \lambda_3, \dots, \lambda_n] = U^T A_I U \tag{24}$$

so the variance of each z_i is unity.

Equation (23) can be written as

$$y = \Lambda^{\frac{1}{2}} z$$

or

$$U^T x = \Lambda^{\frac{1}{2}} z$$

Therefore

$$x = U \Lambda^{\frac{1}{2}} z \tag{25}$$

which gives the x_i in terms of the z_j .

11 Appendix 2

The relationships between the eigenvalues λ_j and the corresponding eigenvectors u^j of a matrix A are given by

$$A u^j = \lambda_j u^j. \tag{26}$$

Let

δA = changes in A

$\delta \lambda_j$ = corresponding change in λ_j

δu^j = corresponding changes in u^j .

Then

$$(A + \delta A)(u^j + \delta u^j) = (\lambda_j + \delta \lambda_j)(u^j + \delta u^j). \tag{27}$$

It is assumed that A , δA , u^j and λ_j are known and $\delta \lambda_j$ and δu^j are required. Franklin⁶ has shown that, neglecting second-order terms in (27),

$$\delta \lambda_j = \frac{\langle \delta A u^j, u^j \rangle}{\langle u^j, u^j \rangle} \tag{28}$$

$$\delta u^j = \sum_{k=1}^n e_{jk} u^k e_{kk} = 0 \tag{29}$$

where

$$e_{jk} = \frac{\langle \delta A u^j, u^k \rangle}{(\lambda_j - \lambda_k) \langle u^k, u^k \rangle}. \tag{30}$$

$\langle a, b \rangle$ is the inner product of vectors a and b and is defined as

$$\langle a, b \rangle \triangleq a_1 b_1 + a_2 b_2 + \dots + a_n b_n.$$

As A is a symmetric matrix

$$\langle u^j, u^k \rangle = 0. \tag{31}$$

Further, if the u^j are normalized then

$$\langle u^j, u^j \rangle = 1. \tag{32}$$

Then equations (28) and (30) reduce to

$$\delta \lambda_j = \langle \delta A u^j, u^j \rangle \tag{33}$$

$$e_{jk} = \frac{\langle \delta A u^j, u^k \rangle}{(\lambda_j - \lambda_k)}. \tag{34}$$

11.1 Upper Bounds of $|\delta \lambda_j|$ and $|e_{jk}|$

Equations (33) and (34) do not enable estimates of $\delta \lambda_j$ and δu^j for given δA to be easily obtained. It is desirable that $|\delta \lambda_j|$ and $|e_{jk}|$ can be related to changes in a particular measurement. If the statistical characteristics of a measurement alter then the correlations between it and the other measurements are likely to change. This will result in changes in the corresponding row and column of A . While the development that follows is not restricted to single row and column changes, the general results are given in terms of individual row and column changes.

11.1.1 $|\delta \lambda_j|$

Now

$$\delta \lambda_j = \langle \delta A u^j, u^j \rangle$$

where

$$\delta A u^j = \begin{bmatrix} \sum_{i=1}^n \delta a_{1i} u_i^j \\ \sum_{i=1}^n \delta a_{2i} u_i^j \\ \vdots \\ \sum_{i=1}^n \delta a_{ni} u_i^j \end{bmatrix}. \tag{35}$$

Then

$$\begin{aligned} \langle \delta A u^j, u^j \rangle &= \left[u_1^j \sum_{i=1}^n \delta a_{1i} u_i^j + \dots + u_n^j \sum_{i=1}^n \delta a_{ni} u_i^j \right] \\ &= \sum_{k=1}^n \left[u_k^j \sum_{i=1}^n \delta a_{ki} u_i^j \right]. \end{aligned}$$

Thus

$$\begin{aligned} \langle \delta A u^j, u^j \rangle &= \sum_{k=1}^n [u_k^j \langle \delta a^k, u^j \rangle] \\ |\langle \delta A u^j, u^j \rangle| &= \left| \sum_{k=1}^n [u_k^j \langle \delta a^k, u^j \rangle] \right| \\ |\langle \delta A u^j, u^j \rangle| &\leq \sum_{k=1}^n |u_k^j \langle \delta a^k, u^j \rangle|. \end{aligned}$$

By the Cauchy-Swartz theorem

$$|\langle b, c \rangle| \leq \|b\| \|c\|$$

where the Euclidean norm

$$\|b\| \triangleq [b_1^2 + b_2^2 + \dots + b_n^2]^{\frac{1}{2}}.$$

Therefore

$$|\delta \lambda_j| \leq \sum_{k=1}^n |u_k^j| \|\delta a^k\| \|u^j\|.$$

If the eigenvectors are normalized,

$$\|u^j\| = 1$$

and

$$|\delta \lambda_j| \leq \sum_{k=1}^n |u_k^j| \|\delta a^k\|. \tag{36}$$

Note— δa^k is the k th row of δA .

If only the m th measurement has changed or the m th measurement is the cause of the principal change in A , then the right-hand side of equation (36) does not reduce to $|u^m| \|\delta a^m\|$, for δA is symmetric and an element δa^m will appear in the i th row. To overcome this $\|\delta a^k\|$ can be redefined.

Let

$$\delta^c a^k = k\text{th column of } \delta A.$$

Then equation (35) when only the m th measurement has changed reduces to

$$|\delta \lambda_j|_m \leq 2|u_m^j| \|\delta^c a^m\|. \tag{37}$$

Hence in order to estimate the effect of the m th measurement change on $|\delta \lambda_j|$ only the m th element of u^j and the m th column norm of δa is required.

11.1.2 $|e_{jk}|$

Now

$$\langle \delta A u^j, u^k \rangle = u_1^k \langle \delta a^1, u^j \rangle + \dots + u_n^k \langle \delta a^n, u^j \rangle$$

where

$$\delta a^j = j\text{th row of } \delta A.$$

Therefore

$$\langle \delta A u^j, u^k \rangle = \sum_{i=1}^n u_i^k \langle \delta a^i, u^j \rangle$$

and

$$\begin{aligned} |\langle \delta A u^j, u^k \rangle| &\leq \sum_{i=1}^n |u_i^k| |\langle \delta a^i, u^j \rangle| \\ &\leq \sum_{i=1}^n |u_i^k| \|\delta a^i\| \|u^j\| \\ |\langle \delta A u^j, u^k \rangle| &\leq \sum_{i=1}^n |u_i^k| \|\delta a^i\| \end{aligned} \tag{38}$$

Hence

$$|e_{jk}| \leq \sum_{i=1}^n \frac{|u_i^k| \|\delta a^i\|}{|\lambda_j - \lambda_k|}. \tag{39}$$

If only the m th measurement has changed, then by defining

$$\delta^c a^i = i\text{th column of } \delta A$$

then

$$|e_{jk}|_m \leq \frac{2|u_m^k| \|\delta^c a^m\|}{|\lambda_j - \lambda_k|}. \tag{40}$$

From equation (29)

$$|\delta u_p^j|_m \leq \sum_{k=1}^n |e_{jk}| |u_p^k|.$$

Therefore

$$|\delta u_p^j|_m \leq 2 \|\delta^c a^m\| \sum_{k=1}^n \frac{|u_m^k| |u_p^k|}{|\lambda_j - \lambda_k|}. \tag{41}$$

12 Appendix 3: Up-dating the Correlation Matrix

Let

x_i = i th measurement of the measurement vector x

μ_i = population mean of the i th measurement

\bar{x}_i = estimate of μ_i

where after k readings

$$\bar{x}_{ik} = \frac{1}{k} \sum_{i=1}^k x_{ii} \tag{42}$$

σ_{ij} = covariance of the i th and j th measurements

σ_{ii} = variance of the i th measurement

s_{ijk} = estimate of σ_{ij} after k readings

s_{iik} = estimate of σ_{ii} after k readings

where

$$s_{ijk} = \frac{1}{k-1} \sum_{i=1}^k (x_{ii} - \mu_i)(x_{ji} - \mu_j) \tag{43}$$

and

$$s_{iik} = \frac{1}{k-1} \sum_{i=1}^k (x_{ii} - \mu_i)^2. \tag{44}$$

Equations (42)–(44) can be written in an iterative manner

$$\bar{x}_{i,k+1} = \frac{1}{k+1} x_{i,k+1} + \frac{k}{k+1} \bar{x}_{i,k} \tag{45}$$

$$\begin{aligned} s_{i,j,k+1} &= \frac{k+1}{k^2} (x_{i,k+1} - \bar{x}_{i,k+1})(x_{j,k+1} - \bar{x}_{j,k+1}) + \\ &\quad + \frac{k-1}{k} s_{i,j,k} \end{aligned} \tag{46}$$

$$s_{i,i,k+1} = \frac{k+1}{k^2} (x_{i,k+1} - \bar{x}_{i,k+1})^2 + \frac{k-1}{k} s_{i,i,k}. \tag{47}$$

So to update the correlation matrix A only the previous estimates of the means, covariances and variances of the measurement vector need to be stored together with the current measurement vector.

From equations (45)–(47) it will be seen that as $k \rightarrow \infty$ we have

$$\bar{x}_{i,k+1} - \bar{x}_{i,k} \rightarrow 0$$

$$s_{i,j,k+1} - s_{i,j,k} \rightarrow 0$$

$$s_{i,i,k+1} - s_{i,i,k} \rightarrow 0$$

which means that no updating takes place and information from the current measurement vector is discounted. If the data warrant a more dynamic updating it is better to put more emphasis on the current readings and to discount those in the past. A convenient method is to use exponential smoothing³ so that

$$\bar{x}_{i,k+1} = \alpha x_{i,k+1} + (1-\alpha)\bar{x}_{i,k} \tag{48}$$

$$\begin{aligned} s_{i,j,k+1} &= \alpha(x_{i,k+1} - \bar{x}_{i,k+1})(x_{j,k+1} - \bar{x}_{j,k+1}) + \\ &\quad + (1-\alpha)s_{i,j,k} \end{aligned} \tag{49}$$

$$s_{i,i,k+1} = \alpha(x_{i,k+1} - \bar{x}_{i,k+1})^2 + (1-\alpha)s_{i,i,k} \tag{50}$$

where typically α is of the order 0.2.

Manuscript first received by the Institution 28th November 1972 and in revised form on 19th November 1973. (Paper No. 1602/MST4.)

© The Institution of Electronic and Radio Engineers, 1974

Reflexion coefficient of a magnetized ferrite sphere in a rectangular waveguide

D. A. JAMES,

B.Sc., M.Inst.P., C.Eng., M.I.E.R.E.*

SUMMARY

Work on small narrow resonance line-width ferrite spheres in waveguide leads to a need for theoretical quantitative understanding of the interaction between the ferrite and the waveguide fields. Analysis in the literature has previously relied on equivalent circuits with voltage and current, but belief that the concept of electromagnetic fields comes more naturally to waveguides led to the analysis in this paper. The main contribution is the derivation of an expression for the reflexion coefficient presented by a small transversely magnetized ferrite sphere in a hollow rectangular metal waveguide propagating an H_{01} mode. The expression is valid for any location of the ferrite in the H-plane transverse dimension (a dimension) of the waveguide. From this general expression are derived subsidiary expressions for the impedance presented by the ferrite at four principal locations, at the centre, at the edge and in the two planes of circular polarization.

The derivation of expressions for the H_{01} mode excited in a rectangular waveguide by a magnetic dipole is of interest outside the field of ferrite technology. Expressions are derived separately for transverse and longitudinal orientations and hold good for all locations in the a dimension.

* Department of Electrical and Electronic Engineering, Royal Military College of Science, Shrivenham, Swindon, Wiltshire SN6 8LA.

List of Symbols

a	the broad, H plane internal cross-sectional dimension of the waveguide
A, B, C, S	symbols defined in equations (13) and (15)
b	the narrow, E plane internal cross-sectional dimension of the waveguide
d	distance of the ferrite from one of the b walls of the waveguide
G	conductance of a series resonant circuit
H	magnetic field strength
ΔH	ferrite resonance line width
k	$2\pi/\lambda$
K	waveguide field parameter defined in equation (29)
l, m, n	direction cosines of \mathbf{I}_ϕ with respect to the x, y, z axes respectively
m	alternating component of the magnetic moment of the dipole
n	an integer
M	magnetization of the ferrite
M_s	saturation magnetization of the ferrite
Q_u	unloaded Q factor of a resonant circuit
\mathbf{R}	tensor connecting \mathbf{H} and \mathbf{M}
R_D	resonant resistance of a parallel resonant circuit
T	Bloch-Blombergen ferrite damping parameter
v	volume of ferrite
x, y, z	waveguide Cartesian coordinates
y	frequency parameter
Y	waveguide admittance
Y_0	waveguide characteristic admittance
Z	waveguide impedance
Z_0	waveguide characteristic impedance
α	Landau-Lifshitz ferrite damping parameter
β	$2\pi/\lambda_g$
Γ_H	magnetic field reflexion coefficient
γ	gyromagnetic ratio for electron spin
ϵ_0	permittivity of free space
θ	an angle defined in Fig. 4
κ	off-diagonal component of the susceptibility tensor
λ	wavelength in unbounded medium
λ_g	wavelength of the H_{01} mode pattern
μ_0	permeability of free space
ϕ	an angle defined in Fig. 4
χ	($= \chi' - j\chi''$), relative susceptibility of the ferrite
χ_r	value of χ at resonance
ω	$2\pi \times$ frequency
ω_m	M_s/γ
ω_r	value of ω at resonance
\mathbf{I}_ϕ	unit vector in the ϕ direction

Directional suffixes:

$x, -x, y, z, -z$ indicating directions parallel to these Cartesian axes

i incident

r reflected

Vectors are indicated by bold type, e.g. \mathbf{H}

Tensors are indicated by square faced bold type, e.g. \mathbf{X}

1 Introduction

This investigation arose out of work on electronically tunable microwave band pass filters using a magnetized single crystal of yttrium iron garnet (YIG) of narrow resonant linewidth (about 0.5 oersted) as the resonant element. This work was supported by the widely used theory developed by Carter *et al.*,¹ based on reducing the waveguide to an equivalent two-conductor transmission line carrying voltage and current, and on reducing the ferrite resonator to an equivalent resonant circuit and voltage generator. Since waveguides are more easily understood by reference to the electromagnetic fields within, this approach seemed far-fetched. A more natural theory would be based on the interaction between the magnetic field components of the H_{01} mode and the ferrite.

The broad aim of this paper is to show that this approach is feasible. This aim is narrowed down to deriving expressions for the reflexion coefficient and impedance presented by such a ferrite in a single length of waveguide. Extension of the theory to two-port devices, such as filters, would be straightforward.

2 Purpose and Scope

The purpose of this paper is to show that it is possible to derive theoretical expressions, using the concept of electromagnetic fields, for the reflexion coefficient and impedance due to a ferrite of narrow resonance linewidth magnetized at or near ferrimagnetic resonance and inside a rectangular waveguide.

The analysis compares the H_{01} modes re-radiated by the ferrite when it is excited by an incident H_{01} mode. Comparison between incident and re-radiated modes yields the reflexion coefficient and hence the normalized impedance.

The analysis regards the ferrite as comprising two orthogonal magnetic dipoles. It employs expressions for the H_{01} modes radiated into a rectangular waveguide by both longitudinal and transverse magnetic dipoles. General expressions for the radiation in a waveguide due to magnetic dipoles have not been found anywhere in published literature and it has been necessary to derive them as a preliminary.

When the analysis was nearly complete it was discovered that A. G. Gurevich² had done something similar. It was decided, however, that it was worth proceeding for two reasons. Firstly, Gurevich's paper had not started from first principles but had quoted the essential equations for the wave radiated from a magnetic dipole from a previous source which was in Russian. Secondly, he dealt only with the case of the ferrite in the centre of the waveguide where it is coupled only to the transverse magnetic field.

2.1 Outline of the Method of Analysis

This section gives a brief physical account of the behaviour of a small magnetized ferrite sphere placed in a waveguide propagating the H_{01} mode. It then outlines the method of analysis adopted later.

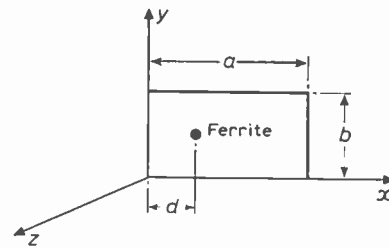


Fig. 1. Location of ferrite in waveguide.

A small ferrite sphere is placed in a waveguide of cross-section $a \times b$ as shown in Fig. 1 and magnetized to near ferrimagnetic resonance by an external d.c. magnetic field applied in the $+y$ direction. An H_{01} mode polarized in the y direction propagates in the $+z$ direction and excites the ferrite. An H_{01} mode contains both transverse (x -directed) and longitudinal (z -directed) components.³ Each one of these components induces alternating magnetization of the ferrite, again in both the x and the z directions. The combined magnetizations in the x direction give rise to a transverse magnetic dipole radiator, and those in the z direction to a longitudinal one. Each one of these separately re-radiates an H_{01} mode and the total re-radiated mode is the sum of the two. Comparison of the total re-radiated mode with the incident one leads to expressions for the magnetic field reflexion coefficients and thence for the input impedance.

The theory outlined above can be expressed in a simple general mathematical form which will point out how to conduct the detailed analysis later. The net fields acting on the ferrite to cause re-radiation are the sums of the incident (H_i) fields and the re-radiated ones (H_r). The magnetization, \mathbf{M} , induced in the ferrite can be expressed as:

$$\mathbf{M} = \mathbf{X} \cdot (\mathbf{H}_i + \mathbf{H}_r) \quad (1)$$

where \mathbf{X} is the tensor susceptibility of the ferrite. In its turn the re-radiated field is linearly related to the magnetization by another tensor relationship:

$$\mathbf{H}_r = \mathbf{R} \cdot \mathbf{M} \quad (2)$$

\mathbf{M} can be eliminated from these two equations leaving a linear equation homogeneous in \mathbf{H}_i and \mathbf{H}_r from which the magnetic reflexion coefficients can be obtained. There are two of these coefficients, $\Gamma_{H(x)}$ for the x components, and $\Gamma_{H(z)}$ for the z components; they differ only in sign. From $\Gamma_{H(x)}$ the waveguide impedance, Z can be calculated from

$$\frac{Z}{Z_0} = \frac{1 - \Gamma_{H(x)}}{1 + \Gamma_{H(x)}} \quad (\text{see for example, reference 3}) \quad (3)$$

where Z_0 is an appropriate characteristic impedance of the waveguide.

Both Γ_H and Z will be calculated as they would be at the plane of the ferrite. They can be transformed to the input or to any other plane between the input and the ferrite by the usual loss-free transmission-line theory. Provided the plane to which the impedance is referred is sufficiently far from the ferrite to be outside the near-field, say at least $\lambda/6$, reactances due to storage fields can probably be ignored.

Both Γ_H and Z will depend upon the location, d , of the ferrite in the x cross-sectional direction. It will be shown that when the ferrite is in the centre of the waveguide it acts as a parallel resonant circuit in series with Z_0 ; at the edge it acts a series resonant circuit in parallel with Z_0 .

From Carter's work an impedance can be calculated for the particular case of the ferrite in the centre of the waveguide. Comparison will be made with this formula to see whether two entirely different methods of analysis yield the same results.

3 The H_{01} Mode in Rectangular Waveguide due to a Magnetic Dipole

In this Section are derived expressions for the field components of the H_{01} mode radiated into a rectangular waveguide by a transverse magnetic dipole and by a longitudinal one. This is a necessary preliminary to the subsequent derivation of the reflexion coefficient. The expressions cater for any location of the dipole in the broad cross-sectional dimensions (a dimension) of the waveguide. Since the H_{01} mode is invariant across the narrow dimension (b) of the waveguide it is assumed that they are independent of the location of the dipole in this dimension.† For convenience the diagrams show the dipole in the centre of the b dimension.

The analyses will be conducted by the method of images as used by Slater⁴ in his analysis for the H_{01} mode radiated by an oscillating electric dipole. Since Slater's analysis is lengthy, and to save repeating much of it in the text, frequent references will be made to his work.

3.1 H_{01} Mode Radiated by a Transverse Magnetic Dipole

3.1.1 The pattern of images

The magnetic dipole m , is disposed in the waveguide cross-section as shown already in Fig. 2. This dipole forms a pattern of images in the x, y plane as shown in

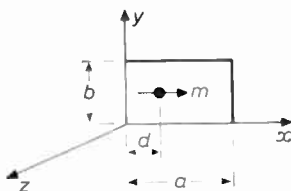


Fig. 2. Transverse dipole orientation.

† This assumption has been checked by calculation. At the longer distances (in terms of λ) down the waveguide from the dipole, where the H_{01} mode is properly formed, the location of the dipole in the b dimension is immaterial. Closer in, where the phase front is still curved, the location enters into the equations as a small correction to the phase. Since we are dealing only with those conditions where the H_{01} mode is fully formed this effect is neglected.

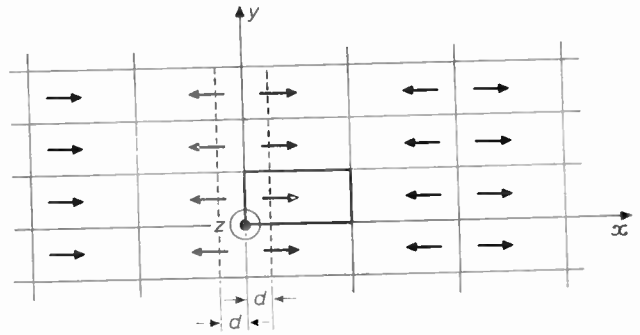


Fig. 3. Transverse dipole, pattern of images.

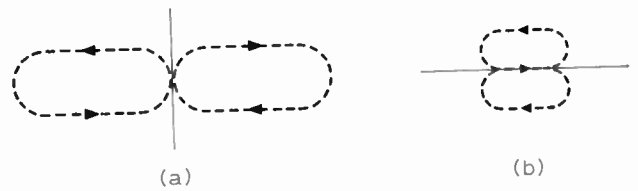


Fig. 4. Sign of images.

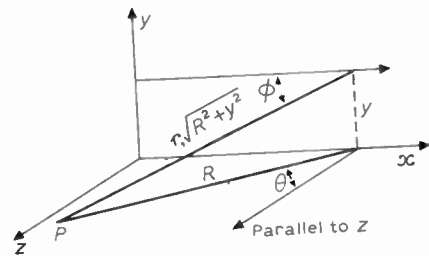


Fig. 5. Transverse dipole, effect of a single column of images.

Fig. 3. Assuming perfectly conducting sidewalls, all the images are equal in strength to the original dipole. That the images are oriented as shown is justified by the necessity for the two sets of magnetic flux lines lying between any pair of adjacent images to turn away from each other so as to be tangential to the surface of the intervening image of the side wall, as depicted in Figs. 4(a) and (b). The images \rightarrow all have x coordinates $2na+d$, where n is an integer including 0. Images \leftarrow have x coordinates $2na-d$.

3.1.2 Effect of a single column of \rightarrow images

Referring to Fig. 5, for an element at a height y ,

$$\cos \phi = \frac{R \sin \theta}{\sqrt{(R^2 + y^2)}}$$

Making the assumption that the spacing between images is small enough, the density of the equivalent continuous distribution of images in the vertical direction is m/b . Therefore the magnetic moment of an elemental length δy of this continuous distribution is $(m/b) \delta y$. The far field of this elemental length at P is given by Slater⁴ in his equation 32.1:

$$\delta H = I_\phi \frac{m \cdot \delta y}{b} \cdot \frac{\pi}{\lambda^2} \cdot \sin \phi \cdot \exp(-jkr). \quad (4)$$

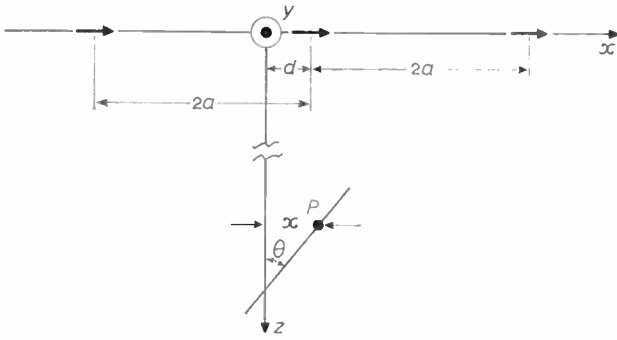


Fig. 6. Effect of all columns of images.

By calculation of the direction cosines, δH can be resolved into:

$$\delta H_x = \frac{m\delta y}{b} \cdot \frac{\pi}{\lambda^2} \cdot \frac{(y^2 + R^2 \cos^2 \theta)}{(y^2 + R^2)^{3/2}} \cdot \exp(-jk\sqrt{(R^2 + y^2)}), \quad (5a)$$

$$\delta H_y = -\frac{m\delta y}{b} \cdot \frac{\pi}{\lambda^2} \cdot \frac{yR \sin \theta}{(y^2 + R^2)^{3/2}} \cdot \exp(-jk\sqrt{(R^2 + y^2)}), \quad (5b)$$

$$\delta H_z = \frac{m\delta y}{b} \cdot \frac{\pi}{\lambda^2} \cdot \frac{R^2 \sin \theta \cdot \cos \theta}{(y^2 + R^2)^{3/2}} \cdot \exp(-jk\sqrt{(R^2 + y^2)}). \quad (5c)$$

To obtain the effect of the total column of images in the direction θ , each of these H should be integrated with respect to y between the limits $\pm\infty$. Following the procedure used by Slater in deriving his equations 37.2-37.6, we obtain by this integration:

$$H_x = \frac{m}{4b} \cdot \frac{k^{3/2}}{\pi^{1/2}} \cdot (1-j) \cos^2 \theta \cdot \frac{\exp(-jkR)}{R}, \quad (6a)$$

$$H_y = 0, \quad (6b)$$

$$H_z = \frac{m}{4b} \cdot \frac{k^{3/2}}{\pi^{1/2}} \cdot (1-j) \cos \theta \cdot \sin \theta \cdot \frac{\exp(-jkR)}{R}. \quad (6c)$$

3.1.3 Integrated effect of all columns of images

In the direction θ . Following the procedure used by Slater in arriving at his equation 37.15, the fields at the point P (Fig. 6) are:

Total

$$H_x = \frac{-jk \cdot m}{4ab} \cdot \cos \theta \times \exp(-jk(d-x) \sin \theta) \cdot \exp(-jkz \cos \theta), \quad (7a)$$

$$H_z = \frac{-jkm}{4ab} \cdot \sin \theta \times \exp(-jk(d-x) \sin \theta) \cdot \exp(-jkz \cos \theta). \quad (7b)$$

In both directions, θ and $-\theta$. Substituting $-\theta$ for θ in the equation (7) and adding corresponding ones we obtain for

$$H_x = \frac{-jkm}{2ab} \cdot \cos \theta \cos \{k(d-x) \sin \theta\} \times \exp(-jkz \cos \theta), \quad (8a)$$

$$H_z = \frac{-km}{2ab} \cdot \sin \theta \cdot \sin \{k(d-x) \sin \theta\} \times \exp(-jkz \cos \theta). \quad (8b)$$

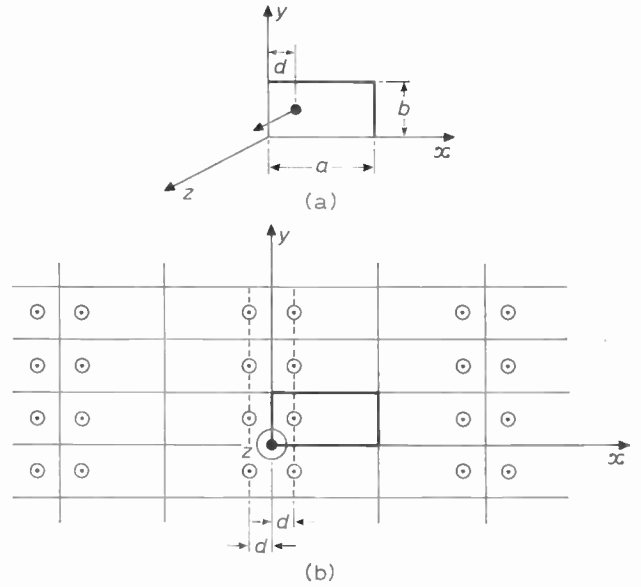


Fig. 7. (a) Longitudinal dipole orientation; (b) Longitudinal dipole, pattern of images.

3.1.4 Total field due to both \rightarrow and \leftarrow images

Equations (8), are for \rightarrow images, i.e. those at $x = 2na + d$. A similar set of equations for \leftarrow images, where $x = 2na - d$, is obtained by substituting $-d$ for d and reversing signs.

$$H_x = -\frac{jkm}{ab} \cdot \cos \theta \cdot \sin(kx \sin \theta) \sin(kd \sin \theta) \times \exp(-jkz \cos \theta), \quad (9a)$$

$$H_z = -\frac{km}{ab} \cdot \sin \theta \cdot \cos(kx \sin \theta) \cdot \sin(kd \sin \theta) \times \exp(-jkz \cos \theta). \quad (9b)$$

This is, in fact, the familiar procedure for deriving the H_{01} mode in a rectangular waveguide by regarding it as composed of two transverse e.m. waves proceeding down the guide in a zig-zag manner by reflexion off opposite narrow (b dimension) walls; $\cos \theta$ is identified with λ/λ_g and $\sin \theta$ with $\lambda/2a$. By writing β for $2\pi/\lambda_g$, equations (9) become

$$H_x = -\frac{jm}{ab} \cdot \frac{2\pi}{\lambda_g} \cdot \sin\left(\frac{\pi x}{a}\right) \sin\left(\frac{\pi d}{a}\right) \cdot \exp(-j\beta z) \quad (10a)$$

$$H_z = \frac{-m}{ab} \cdot \frac{\pi}{a} \cdot \cos\left(\frac{\pi x}{a}\right) \sin\left(\frac{\pi d}{a}\right) \cdot \exp(-j\beta z) \quad (10b)$$

which, by comparison with reference 3 (equations 6.26)

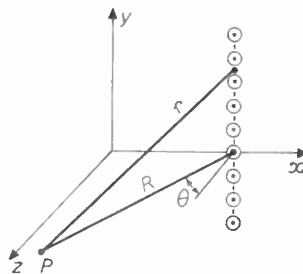


Fig. 8. Longitudinal dipole, effect of a single column of images.

can be seen to represent the H fields of an H_{01} mode propagating in the z direction. As would be expected, the field strength is greatest when the transverse dipole is in the best location for it to provide the transverse H component of the H_{01} mode, i.e. at the guide centre, $d = a/2$. Conversely it is zero where the transverse dipole is at the edge of the guide ($d = 0, a$) where no transverse H field is called for.

3.2 H_{01} Mode Radiated by a Longitudinal Magnetic Dipole

3.2.1 The pattern of images

The dipole is disposed in the waveguide cross-section as shown in Fig. 7(a). The pattern of images formed in the x, y plane is shown in Fig. 7(b). The orientation of images is deduced from the principle that the net magnetic field at the surface of a side-wall, or image of a side-wall, must be tangential. The images lying at distance d to the right of a vertical side-wall all have x coordinates $2na + d$, those to the left, x -coordinates $2na - d$.

3.2.2 Effect of single column of images

Refer to Fig. 8 for the geometry.

The problem is the same as for the column of transverse (\rightarrow) images considered in Section 3.1.2 except that the axes and the angle have been transformed as follows:

$$x \equiv z, z \equiv -x, \theta \equiv \left(\frac{\pi}{2} + \theta\right).$$

We can now write down equations similar to equations (5)

$$\delta H_{(-x)} = -\frac{m\delta y}{b} \cdot \frac{\pi}{\lambda^2} \cdot \frac{R^2 \sin \theta \cos \theta}{(y^2 + R^2)^{3/2}} \times \exp(-jk)\sqrt{(R^2 + y^2)}, \quad (11a)$$

$$\delta H_y = \frac{m\delta y}{b} \cdot \frac{\pi}{\lambda^2} \cdot \frac{yR \cos \theta}{(y^2 + R^2)^{3/2}} \times \exp(-jk)\sqrt{(R^2 + y^2)}, \quad (11b)$$

$$\delta H_z = \frac{m\delta y}{b} \cdot \frac{\pi}{\lambda^2} \cdot \frac{(y^2 + R^2 \sin^2 \theta)}{(R^2 + y^2)^{3/2}} \times \exp(-jk)\sqrt{(R^2 + y^2)}. \quad (11c)$$

Integrating as in Section 3.1.2 to obtain the effect of the whole column:

$$H_{(-x)} = \frac{-mk^{3/2}}{4b\pi^{1/2}} \cdot (1-j) \sin \theta \cos \theta \frac{\exp(-jkR)}{R}, \quad (12a)$$

$$H_y = 0, \quad (12b)$$

$$H_z = \frac{mk^{3/2}}{4b\pi^{1/2}} \cdot (1-j) \sin^2 \theta \cdot \frac{\exp(-jkR)}{R}. \quad (12c)$$

3.2.3 Effect of all columns of images

In the direction θ . By analogy with the procedure of Section 3.1.3 the fields at a long distance down the guide in the $+z$ direction are:

$$H_{(-x)} = +\frac{jk m}{4ab} \cdot \sin \theta \cdot \exp[-jk(d-x) \sin \theta] \times \exp(-jkz \cos \theta), \quad (13a)$$

$$H_z = -\frac{jk m}{4ab} \cdot \frac{\sin^2 \theta}{\cos \theta} \cdot \exp[-jk(d-x) \sin \theta] \times \exp(-jkz \cos \theta). \quad (13b)$$

In both directions θ and $-\theta$. Substituting θ for $-\theta$ in the equations (13) and adding the two yields for:

$$H_{(-x)}, \quad \frac{km}{2ab} \cdot \sin \theta \cdot \sin \{k(d-x) \sin \theta\} \times \exp(-jkz \cos \theta), \quad (14a)$$

$$H_z, \quad \frac{-jk m}{2ab} \cdot \frac{\sin^2 \theta}{\cos \theta} \cdot \cos \{k(d-x) \sin \theta\} \times \exp(-jkz \cos \theta). \quad (14b)$$

3.2.4 Total field due to both sets of images

Equations (14) are for the '+ d ' group of images. A similar pair of equations exist for the '- d ' group; these are obtained by replacing d by $-d$. Doing this and adding gives:

$$H_{(-x)} = \frac{-km}{ab} \cdot \sin \theta \cos(kd \sin \theta) \sin(kx \sin \theta) \times \exp(-jkz \cos \theta), \quad (15a)$$

$$H_z = \frac{-jk m}{ab} \cdot \frac{\sin^2 \theta}{\cos \theta} \cdot \cos(kd \sin \theta) \cos(kx \sin \theta) \times \exp(-jkz \cos \theta). \quad (15b)$$

Again, identifying $\cos \theta$ with λ/λ_g and $\sin \theta$ with $\lambda/2a$, and writing $\beta = 2\pi/\lambda_g$, the equations for the H fields of the H_{01} mode travelling in the z direction are:

$$H_{(-x)} = \frac{-m}{ab} \cdot \frac{\pi}{a} \cdot \cos\left(\frac{\pi d}{a}\right) \cdot \sin\left(\frac{\pi x}{a}\right) \cdot \exp(-j\beta z), \quad (16a)$$

$$H_z = \frac{-jm}{ab} \cdot \left(\frac{\pi}{a}\right)^2 \cdot \frac{\lambda_g}{2\pi} \cdot \cos\left(\frac{\pi d}{a}\right) \cos\left(\frac{\pi x}{a}\right) \times \exp(-j\beta z). \quad (16b)$$

In contrast to the fields due to the transverse dipole, these are a maximum when the dipole is at the edge of the guide ($d = 0, a$) and zero when it is at the centre.

4 Derivation of the Reflexion Coefficients

4.1 Recapitulation

Section 2.1 outlined the proposed method for deriving expressions for the reflexion coefficient and impedance of a small ferrite sphere in rectangular waveguide, magnetized to near ferrimagnetic resonance. Expressions for the magnetic fields of the H_{01} mode radiated into a waveguide by both a transverse and a longitudinal oscillating magnetic dipole are derived in Section 3.

This Section takes these expressions and uses them to derive expressions for the reflexion coefficient. These will cover all locations of the ferrite from the centre of the waveguide to the edge. They will be compared as far as possible with similar ones derived by other workers.

4.2 Magnetization of the Ferrite

The magnetization induced in a ferrite by a uniform magnetic field, H , is given by:

$$\mathbf{M} = \mathbf{X} \cdot \mathbf{H}. \quad (17)$$

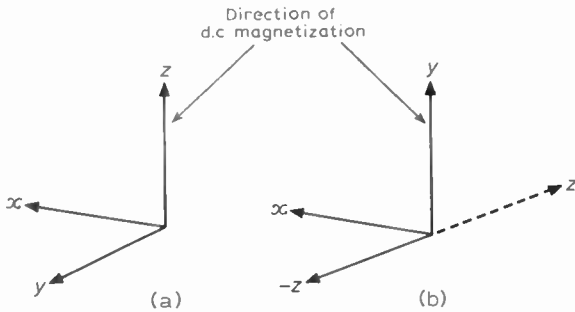


Fig. 9. Change of coordinate axes.

Lax and Button⁶ give \mathbf{X} in Cartesian coordinates for the direction of d.c. magnetization along the z axis (Fig. 9(a)).

For a spherical shape, in which the demagnetizing factors are the same in each direction, and where, as in YIG, the ferrite has little or no magnetic anisotropy, the value of \mathbf{X} is given by:

$$\begin{bmatrix} M_x \\ M_y \\ M_z \end{bmatrix} = \begin{bmatrix} \chi & -j\kappa & 0 \\ j\kappa & \chi & 0 \\ 0 & 0 & 0 \end{bmatrix} \begin{bmatrix} H_x \\ H_y \\ H_z \end{bmatrix} \quad (18)$$

(The more familiar symbols χ and $j\kappa$ have been used instead of χ_{xx} etc. used by Lax and Button.)

In the system of coordinates of this paper the ferrite is magnetized along $+y$ and the tensor has to be transformed to the axes given in Fig. 9(b), becoming:

$$\begin{bmatrix} M_x \\ M_{-z} \\ M_y \end{bmatrix} = \begin{bmatrix} \chi & -j\kappa & 0 \\ j\kappa & \chi & 0 \\ 0 & 0 & 0 \end{bmatrix} \begin{bmatrix} H_x \\ H_{-z} \\ H_y \end{bmatrix} \quad (19)$$

Neglecting storage fields which contribute nothing to the effects observed at some distance from the ferrite the magnetic field in the vicinity of the ferrite is $\mathbf{H}_i + \mathbf{H}_r$ where \mathbf{H}_i is the magnetic field components of the incident H_{01} wave and \mathbf{H}_r is those of the re-radiated wave. Hence the magnetization of the ferrite is given by:

$$\begin{bmatrix} M_x \\ M_{-z} \\ M_y \end{bmatrix} = \begin{bmatrix} \chi & -j\kappa & 0 \\ j\kappa & \chi & 0 \\ 0 & 0 & 0 \end{bmatrix} \begin{bmatrix} H_{xi} + H_{xr} \\ H_{-zi} + H_{-zr} \\ H_{yi} + H_{yr} \end{bmatrix} \quad (20)$$

4.3 The Re-radiated Field, H_r

4.3.1 Due to M_x

See Fig. 10. On the assumption that the ferrite is small† the magnetic moment in the x direction is $M_x v$, where v is the volume of the ferrite. From equations (10) the H_{01} fields due to this magnetic moment are such that $H_{xr} \propto -jM_x v$ and $H_{zr} \propto -M_x v$. However we are more

† For this analysis to be valid it must be possible to assume that the electromagnetic field strengths in the empty waveguide are uniform over the volume to be occupied by the ferrite. To conform with this Gurevich suggests that the diameter should not be more than 0.1λ ; Carter⁷ suggests a maximum of 2.5 mm in an air-filled waveguide at 10 GHz. Both of these are in accordance with the diameter of 1–2 mm often used for work in the 10 GHz band.

interested in the wave re-radiated backwards, in the direction $-z$ and Fig. 10 shows the fields in this direction as well.

Writing down from equations (10), the complete equations for the re-radiated field in the $-z$ direction, we have:

$$H_{xr} = \frac{-jM_x v}{ab} \cdot \frac{2\pi}{\lambda_g} \cdot \sin\left(\frac{\pi x}{a}\right) \cdot \sin\left(\frac{\pi d}{a}\right) \quad (21a)$$

$$H_{-zr} = \frac{-M_x v}{ab} \cdot \frac{\pi}{a} \cdot \cos\left(\frac{\pi x}{a}\right) \cdot \sin\left(\frac{\pi d}{a}\right) \quad (21b)$$

Zero phase angle is given as it is the value of H_r at the ferrite which is required.

4.3.2 Due to M_{-z}

Figure 11(a) shows the H_{01} field components due to a magnetic dipole $M_z v$ at points in both z directions as given by equations (16). For reasons associated with the change of axes for \mathbf{X} it is more convenient to show the magnetic moment oriented in the $-z$ direction as shown in Fig. 11(b). The complete equations for the re-radiated fields in the $-z$ direction are:

$$H_{xr} = \frac{M_{-z} v}{ab} \cdot \frac{\pi}{a} \cdot \cos\left(\frac{\pi d}{a}\right) \cdot \sin\left(\frac{\pi x}{a}\right) \quad (22a)$$

$$H_{-zr} = \frac{-jM_{-z} v}{ab} \left(\frac{\pi}{a}\right)^2 \cdot \frac{\lambda_g}{2\pi} \cdot \cos\left(\frac{\pi d}{a}\right) \cdot \cos\left(\frac{\pi x}{a}\right) \quad (22b)$$

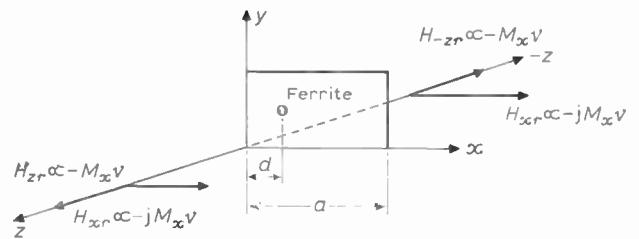


Fig. 10. Radiation from a transverse dipole.

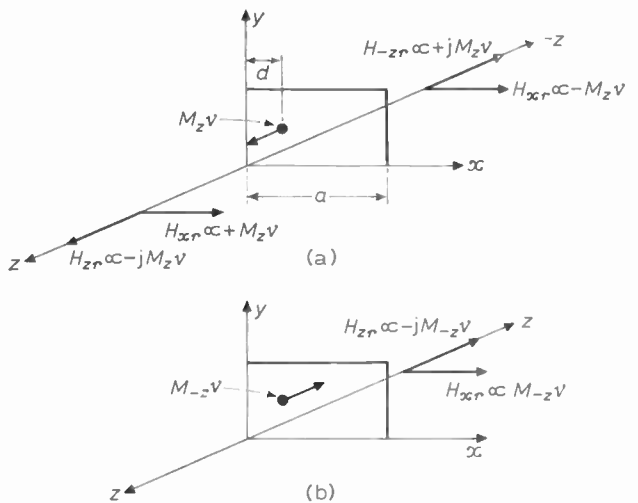


Fig. 11. Radiation from a longitudinal dipole.

4.3.3 Total re-radiated fields

These are obtained by adding equations (21) and (22):

$$H_{xr} = \frac{-jv}{ab} \sin\left(\frac{\pi x}{a}\right) \times \left[M_x \cdot \frac{2\pi}{\lambda_g} \sin\left(\frac{\pi d}{a}\right) + jM_{-z} \cdot \frac{\pi}{a} \cos\left(\frac{\pi d}{a}\right) \right], \quad (23a)$$

$$H_{-zr} = \frac{v}{ab} \cos\left(\frac{\pi x}{a}\right) \times \left[-M_x \cdot \frac{\pi}{a} \sin\left(\frac{\pi d}{a}\right) - jM_{-z} \left(\frac{\pi}{a}\right)^2 \times \frac{\lambda_g}{2} \cos\left(\frac{\pi d}{a}\right) \right]. \quad (23b)$$

4.4 Solution of the Simultaneous Equations for the Re-radiated Fields

Equation (19) for \mathbf{M} , expanded, is:

$$M_x = \chi(H_{xi} + H_{xr}) - j\kappa(H_{-zi} + H_{-zr}), \quad (24a)$$

$$M_{-z} = j\kappa(H_{xi} + H_{xr}) + \chi(H_{-zi} + H_{-zr}), \quad (24b)$$

$$M_y = 0. \quad (24c)$$

Substituting these values for \mathbf{M} into equations (23) yields for H_{xr} :

$$H_{xr} = \frac{-jv}{ab} \sin\left(\frac{\pi d}{a}\right) \cdot \frac{2\pi}{\lambda_g} \times \left[\{\chi(H_{xi} + H_{xr}) - j\kappa(H_{-zi} + H_{-zr})\} \times \sin\left(\frac{\pi d}{a}\right) + j\{j\kappa(H_{xi} + H_{xr}) + \chi(H_{-zi} + H_{-zr})\} \frac{\lambda_g}{2\pi} \cdot \frac{\pi}{a} \cos\left(\frac{\pi d}{a}\right) \right] \quad (25)$$

in which, since we are only concerned with the fields at the location of the ferrite, d has been substituted for x .

Collecting terms on the right-hand side yields:

$$H_{xr} = S[AH_{xi} + AH_{xr} + BH_{-zi} + BH_{-zr}] \quad (26)$$

where, for convenience in writing and manipulation,

$$S \equiv \frac{-jv}{ab} \sin\left(\frac{\pi d}{a}\right) \cdot \frac{2\pi}{\lambda_g},$$

$$A \equiv \left\{ \chi \sin\left(\frac{\pi d}{a}\right) - \kappa \frac{\lambda_g}{2\pi} \cdot \frac{\pi}{a} \cos\left(\frac{\pi d}{a}\right) \right\}$$

$$B \equiv -j \left\{ \kappa \sin\left(\frac{\pi d}{a}\right) - \chi \frac{\lambda_g}{2\pi} \cdot \frac{\pi}{a} \cos\left(\frac{\pi d}{a}\right) \right\}.$$

Substituting for A , B , C , and S gives:

$$\Gamma_{H(x)} = \frac{\frac{-jv}{ab} \cdot \frac{2\pi}{\lambda_g} \left[\left\{ \chi \sin\left(\frac{\pi d}{a}\right) - \kappa \frac{\lambda_g}{2\pi} \cdot \frac{\pi}{a} \cos\left(\frac{\pi d}{a}\right) \right\} \sin\left(\frac{\pi d}{a}\right) + \left\{ \kappa \sin\left(\frac{\pi d}{a}\right) - \chi \frac{\lambda_g}{2\pi} \cdot \frac{\pi}{a} \cos\left(\frac{\pi d}{a}\right) \right\} \frac{\lambda_g}{2a} \cos\left(\frac{\pi d}{a}\right) \right]}{1 - \frac{jv}{ab} \left[\left\{ \kappa \sin\left(\frac{\pi d}{a}\right) - \chi \frac{\lambda_g}{2\pi} \cdot \frac{\pi}{a} \cos\left(\frac{\pi d}{a}\right) \right\} \frac{\pi}{a} \cos\left(\frac{\pi d}{a}\right) - \left\{ \chi \sin\left(\frac{\pi d}{a}\right) - \kappa \frac{\lambda_g}{2\pi} \cdot \frac{\pi}{a} \cos\left(\frac{\pi d}{a}\right) \right\} \frac{2\pi}{\lambda_g} \sin\left(\frac{\pi d}{a}\right) \right]} \quad (36)$$

A similar substitution then yields H_{-zr} :

$$H_{-zr} = \frac{-v}{ab} \cos\left(\frac{\pi d}{a}\right) \cdot \left(\frac{\pi}{a}\right) \times \left[\{\chi(H_{xi} + H_{xr}) - j\kappa(H_{-zi} + H_{-zr})\} \times \sin\left(\frac{\pi d}{a}\right) + j\{j\kappa(H_{xi} + H_{xr}) + \chi(H_{-zi} + H_{-zr})\} \frac{\pi}{a} \cdot \frac{\lambda_g}{2\pi} \cos\left(\frac{\pi d}{a}\right) \right]. \quad (27)$$

Writing C for $-v/ab \cdot \cos(\pi d/a) \pi/a$ and collecting terms on the right-hand side:

$$H_{-zr} = C[AH_{xi} + AH_{xr} + BH_{-zi} + BH_{-zr}]. \quad (28)$$

Equations (26) and (28) are a pair of simultaneous equations for H_{xr} and H_{-zr} in terms of H_{xi} and H_{-zi} whose solutions are:

$$H_{xr} = \frac{S(AH_{xi} + BH_{-zi})}{(1 - CB - AS)}, \quad (29)$$

$$H_{-zr} = \frac{C(AH_{xi} + BH_{-zi})}{(1 - CB - AS)}. \quad (30)$$

The expressions for H_{xi} and H_{-zi} , the fields of the incident H_{01} wave in the region of the ferrite, are obtainable from many standard works, e.g. reference 3, and are:

$$H_{xi} = H_0 \sin\left(\frac{\pi d}{a}\right) \quad (31)$$

$$H_{-zi} = jH_0 \frac{\lambda_g}{2a} \cos\left(\frac{\pi d}{a}\right), \quad (32)$$

taking phase angle as being zero at the plane of the ferrite.

Substituting these values in equations (29), (30), gives:

$$H_{xr} = \frac{SH_0 \left\{ A \sin\left(\frac{\pi d}{a}\right) + Bj \frac{\lambda_g}{2a} \cos\left(\frac{\pi d}{a}\right) \right\}}{(1 - CB - AS)}, \quad (33)$$

$$H_{-zr} = \frac{CH_0 \left\{ A \sin\left(\frac{\pi d}{a}\right) + Bj \frac{\lambda_g}{2a} \cos\left(\frac{\pi d}{a}\right) \right\}}{(1 - CB - AS)}. \quad (34)$$

4.5 The Reflexion Coefficients

4.5.1 $\Gamma_{H(x)}$

This is defined as H_{xr}/H_{xi} . Since both H_{xr} and H_{xi} have the same x dependence, $\sin(\pi x/a)$, it does not matter at what value of x it is specified; specifying at $x = d$ gives from equations (33) and (32):

$$\Gamma_{H(x)} = \frac{S \left[A \sin\left(\frac{\pi d}{a}\right) + Bj \frac{\lambda_g}{2a} \cos\left(\frac{\pi d}{a}\right) \right]}{\sin\left(\frac{\pi d}{a}\right) (1 - CB - AS)}. \quad (35)$$

For the particular case where the ferrite is in the centre of the guide $d = a/2$ and:

$$\Gamma_{H(x)} = \frac{-j \frac{v}{ab} \cdot \frac{2\pi}{\lambda_g} \chi}{1 + j \frac{v}{ab} \cdot \frac{2\pi}{\lambda_g} \chi} \quad (37)$$

which agrees with Gurevich's equation 29.²

4.5.2 $\Gamma_{H(z)}$

Inspection of equations (29) and (30) for H_r and of equations (31) and (32) for H_i yields the expected result that $\Gamma_{H(-z)}$, which is given by H_{-zr}/H_{-zi} , is equal to $-\Gamma_{H(x)}$. Reversing the sign of the suffix in both numerator and denominator does not affect the sign of the reflexion coefficient, therefore:

$$\Gamma_{H(z)} = -\Gamma_{H(x)}. \quad (38)$$

5 The Impedance Presented by the Ferrite, and the Equivalent Circuit

By ordinary transmission line theory, the normalized impedance, Z/Z_0 is given by:

$$\frac{Z}{Z_0} = \frac{1 - \Gamma_{H(x)}}{1 + \Gamma_{H(x)}} \quad (39)$$

Since $\Gamma_{H(x)}$ is a function of location, d , in the broad dimension of the waveguide, it follows that the impedance also is. Equation (36) shows that a general expression is likely to be complicated but four particular locations in the broad dimension yield simple results. They are, centre, edge and the two planes of circular polarization of H .

5.1 Ferrite in the Centre of the Broad Dimension of the Waveguide

For the simple case where the ferrite is in the centre of the broad (a) dimension of the waveguide, substituting equation (37) into equation (39) yields:

$$\frac{Z}{Z_0} = 1 + 2\chi \frac{v}{ab} \cdot \frac{2\pi}{\lambda_g} \quad (40)$$

which is equivalent to the series circuit in Fig. 12. Since the waveguide is assumed to be terminated in a matched load, $Z/Z_0 = 1$ and the ferrite couples in the normalized series impedance $2j\chi(v/ab) \cdot (2\pi/\lambda_g)$. It is shown in the Appendix, equation (52), that for a small sphere

$$\chi = -\frac{j\chi_r''}{1 + j\left(\frac{y}{2\alpha}\right)}$$

where χ_r'' is the imaginary part of the complex suscepti-

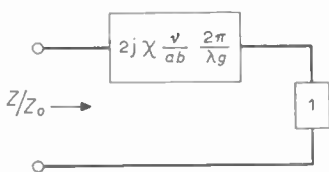


Fig. 12. Ferrite in the centre of the waveguide, equivalent circuit.

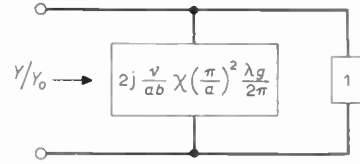


Fig. 13. Ferrite at the edge of the waveguide, equivalent circuit.

bility (diagonal component) at ferrimagnetic resonance, α is the Landau-Lifshitz damping parameter and y is the frequency parameter ($\omega/\omega_r - \omega_r/\omega$). (ω_r is the resonant frequency in rad/s and ω is the actual frequency of operation.) Hence the normalized coupled impedance due to the ferrite is:

$$\frac{Z}{Z_0} = \frac{\chi_r'' \frac{2v}{ab} \cdot \frac{2\pi}{\lambda_g}}{1 + j\left(\frac{y}{2\alpha}\right)} \quad (41)$$

This may be compared with the impedance of a parallel resonant circuit which is of the form $R_D/(1 + jyQ_u)$. (R_D is the resonant parallel resistance and Q_u is the unloaded Q factor of the circuit.) The two are similar in form from which it may be concluded that the ferrite couples in series with the guide a parallel resonant circuit of normalized resonant resistance, $\chi_r'' \cdot 2v/ab \cdot 2\pi/\lambda_g$ and of Q factor $1/2\alpha$. Both of these can be related to the ferrite properties by observing that χ_r'' for a sphere is $M_s/\Delta H$ (see equation (53)), where M_s is the saturation magnetization of the ferrite and ΔH is the resonance line width; $1/2\alpha = Q_u = \omega_r/\gamma\Delta H$ (see equation (54)), where γ is the gyromagnetic ratio for electron spin.

It is interesting to compare this value of impedance with that deduced by Carter.¹ He shows (equation II-10(a)) by an equivalent circuit analogy that the absolute open circuit impedance of a two-port filter using a ferrite as the resonant element is given by:

$$Z = j\omega\mu_0 v K^2 \chi \quad (42)$$

where K for a ferrite located in the centre of the a dimension of a waveguide carrying the H_{01} mode is $\pi/2a$ (reference 1, equation II-20).

On the assumption that the only impedance in the guide in this case is the ferrite (i.e. there is a short-circuit, or transferred short-circuit at the plane of the ferrite), Z is the impedance of the ferrite with the second port an open-circuit. This should be compatible with the value of normalized series impedance, $2j\chi \cdot v/ab \cdot 2\pi/\lambda_g$ deduced above. It is, provided that one chooses the correct value of characteristic impedance for the waveguide. Since a ferrite is a current operated device the use of Waldron's⁸ power-total series current definition seems appropriate. For an H_{01} mode in air-filled rectangular waveguide this is

$$Z_0 = \frac{\pi \cdot b \cdot \lambda_g}{8 \cdot a \cdot \lambda} \sqrt{\frac{\mu_0}{\epsilon_0}} \quad (43)$$

Dividing equation (42) by equation (43) yields the same normalized value of ferrite impedance, $2j\chi(v/ab) \cdot 2\pi/\lambda_g$, as that deduced in this paper.

5.2 Ferrite at the Edge of the Broad Dimension of the Waveguide†

Inserting $d = 0$ or $d = a$ into equation (36) yields:

$$\Gamma_{H(x)} = \frac{+ \frac{jv}{ab} \chi \left(\frac{\pi}{a}\right)^2 \frac{\lambda_g}{2\pi}}{1 + \frac{jv}{ab} \chi \left(\frac{\pi}{a}\right)^2 \frac{\lambda_g}{2\pi}} \quad (44)$$

By analogy with equation (39) the equation for the normalized admittance is:

$$\frac{Y}{Y_0} = \frac{1 + \Gamma_{H(x)}}{1 - \Gamma_{H(x)}} \quad (45)$$

hence, from (44),

$$\frac{Y}{Y_0} = 1 + 2 \frac{jv}{ab} \cdot \chi \cdot \left(\frac{\pi}{a}\right)^2 \cdot \frac{\lambda_g}{2\pi} \quad (46)$$

showing that the equivalent circuit is as given in Fig. 13.

Remembering that $\chi = (-j\chi_r)/(1 + jyQ_u)$ and assuming that the waveguide is correctly terminated, it follows that the ferrite places in parallel with the waveguide an admittance

$$\frac{2v}{ab} \chi_r'' \left(\frac{\pi}{a}\right)^2 \cdot \frac{\lambda_g}{2\pi} \cdot \frac{1}{1 + jyQ_u}$$

This may be compared with the admittance of a series resonant circuit which is of the form $G/(1 + jyQ_u)$, where G is the conductance at resonance. It is concluded that the ferrite places in parallel with the waveguide a series resonant circuit of resonant conductance

$$\frac{2v}{ab} \cdot \chi_r'' \left(\frac{\pi}{a}\right)^2 \cdot \frac{\lambda_g}{2\pi}$$

and a Q factor again $1/2\alpha$.

5.3 Ferrite in the Planes of Circular Polarization of the Magnetic Field of the H_{01} Mode

The two planes of circular polarization of the magnetic field H , of the H_{01} mode occur at values of d given by:

$$\frac{\lambda_g}{2a} \cos\left(\frac{\pi d}{a}\right) = + \sin\left(\frac{\pi d}{a}\right); \quad 0 < d < \frac{a}{2} \quad (47)$$

and

$$\frac{\lambda_g}{2a} \cos\left(\frac{\pi d}{a}\right) = - \sin\left(\frac{\pi d}{a}\right); \quad \frac{a}{2} < d < a. \quad (48)$$

They are of particular interest because the precessing electron spins react best to a rotating magnetic field of constant amplitude, i.e. to a circularly polarized magnetic field.

Substituting the positive value into the equation for $\Gamma_{H(x)}$ (36) gives $\Gamma_{H(x)} = 0$, i.e. there is a perfect match. The positive sign implies that the magnetic field of an H_{01} mode travelling in the $+z$ direction is anti-clockwise circularly polarized with respect to the y axis, and thus

with respect to the direction of the d.c. magnetic field. Simple gyromagnetic theory of electron spin shows that a magnetic field of this sense of polarization does not couple to the electron spin precession with the ferrite. The ferrite does not interfere with the wave, which proceeds unhindered to the matched termination beyond the ferrite.

Substituting the negative value also yields $\Gamma_{H(x)} = 0$. But in this case the H_{01} mode magnetic field is clockwise circularly polarized with respect to the d.c. magnetic field and is coupled strongly to the ferrite. The explanation is that the ferrite absorbs part or even all of the mode without reflexion; whatever is not absorbed passes onto the matched load.

6 Discussion

An expression has been derived for the reflexion coefficient due to a small narrow linewidth ferrite sphere biased at or near ferrimagnetic resonance. The expression covers all locations of the ferrite in the broad cross-sectional dimension of the waveguide from the centre to the edge. It agrees with that deduced by Gurevich² for the particular case of the ferrite in the centre of the waveguide.

From the reflexion coefficient the normalized impedance coupled into the waveguide has been calculated for four particular locations of the ferrite; in the centre, at the edge and in each one of the two planes of circular polarization of the waveguide magnetic field. The expressions obtained all give the physical pictures expected. In the centre of the waveguide the ferrite couples wholly to the transverse component of magnetic field, and hence to the series currents in the waveguide wall. It behaves here as a parallel resonant circuit in series with the waveguide and inserts a near open-circuit at resonance. At the edge the ferrite couples wholly to the longitudinal component of magnetic field, and hence to the shunt currents. It behaves here as a series resonant circuit in parallel with the waveguide across which it places a short-circuit at resonance. In the plane of clockwise circular polarization of the waveguide magnetic field with respect to the d.c. biasing magnetic field, complete interaction occurs between the waveguide magnetic field and the precessing electron spins within the ferrite. The wave is absorbed wholly, or partly, without reflexion. In the other plane of circular polarization no interaction occurs and the wave passes unhindered down the waveguide to be absorbed in the termination.

Quantitative corroboration of the correctness of this analysis is forthcoming from the work of P. S. Carter *et al.*¹ From Carter's work an absolute impedance can be derived for the case of the ferrite in the centre of the waveguide. Provided that the characteristic impedance chosen is the power flux-total series current one, the normalized impedance derived here is in agreement with this.

7 Conclusion

The equations derived here fill a gap in the theoretical literature. They are presented as giving an adequate physical and quantitative account of the behaviour of a

† In practice this cannot be realized exactly. To avoid mutual coupling between the ferrite and its image, the sphere should be no closer to the wall of the waveguide than about two diameters.

magnetic dipole radiating an H_{01} mode into a rectangular waveguide, and of that of a magnetized ferrite sphere in the waveguide. Comparison with other work shows that care is needed in choosing an appropriate waveguide characteristic impedance.

8 Acknowledgments

The help of R. P. Owens in checking the analyses and in giving advice about the appropriate choice of waveguide characteristic impedance is gratefully acknowledged. Thanks are due to Professor P. C. J. Hill for his helpful criticisms and for his suggestions about the layout of the paper.

9 References

1. Carter, P. S. *et al.*, 'Design criteria for microwave filters and coupling structures, Chapter II, Electronically tunable filters employing garnet resonators', Stanford Research Institute, Project 2326, Technical Report No. 8, Oct. 1959.
2. Gurevich, A. G. 'Ferrite ellipsoid in a waveguide', *Radio Engineering and Electronic Physics*, 8, pp. 799-808, January-June 1963.
3. See, for example, Glazier, E. V. D. and Lamont, H. R. L., 'Transmission and Propagation', Chap. 6 (H.M. Stationery Office, London, 1958).
4. Slater, J. C., 'Microwave Transmission', Chap. 7 (Dover, New York, 1942).
5. *Ibid.*, Chap. 3.
6. Lax, B. and Button, K. J., 'Microwave Ferrites and Ferrimagnetics', equation 4.14 (Mc-Graw-Hill, New York, 1962).
7. Carter, P. S., Jr., 'Magnetically tunable, microwave filters using single-crystal yttrium-iron-garnet resonators', *IRE Transactions on Microwave Theory and Techniques*, MTT-9, pp. 252-60, May 1961.
8. Waldron, R. A., 'The Theory of Guided Electro-Magnetic Waves', Chap. IV.E, paragraph 33 (Van Nostrand Reinhold, New York, 1970).

10 Appendix : The Ferrite Susceptibility

Lax and Button⁶ give a formula for the external value of χ , which is the one we are concerned with here. For the case of a sphere, in which the demagnetizing factors are all equal to $\frac{1}{3}$, this formula reduces to

$$\chi = \frac{\omega_m[\omega_r + j/T]}{\omega_r^2 - \omega^2 + \frac{2j\omega_r}{T}} \quad (49)$$

where ω_r is given by Lax and Button's equation 4.30.

For the purpose of this analysis it is slightly easier to use the Landau-Lifshitz damping parameter, α , rather than the Bloch-Blombergen one, T . The two are related by $\alpha\omega T = 1$. Furthermore, for a narrow resonance line width ferrite, $\alpha \ll 1$. Using these two facts (49) can be re-written:

$$\chi = \frac{\omega_m \omega_r}{\omega_r^2 - \omega^2 + 2j\omega\omega_r\alpha} \quad (50)$$

At resonance, $\omega = \omega_r$:

$$\chi_r = \frac{-j\omega_m}{2\omega_r\alpha} \quad (51)$$

In general χ is complex, $\chi' - j\chi''$. At resonance it is wholly imaginary, $\chi'' = \omega_m/2\omega_r\alpha$. Substituting this in (50) and writing

$$y = \left(\frac{\omega}{\omega_r} - \frac{\omega_r}{\omega} \right),$$

then

$$\chi = - \frac{j\chi''}{1 + j(y/2\alpha)} \quad (52)$$

Lax and Button give $\Delta H = 2/\gamma T$; in terms of α , $\Delta H = 2\alpha\omega_r/\gamma$. ω_r is written instead of just ω since ΔH is measured by varying H_{dc} about the resonant frequency. Substituting γM_s for ω_m and substituting this formula for ΔH gives

$$\chi'' = \frac{M_s}{\Delta H} \quad (53)$$

Since $1/2\alpha = Q_u = \omega_r/\gamma\Delta H$, where Q_u is the unloaded Q of the ferrite resonator,

$$Q_u = \frac{\omega_r}{\gamma\Delta H} \quad (54)$$

Manuscript first received by the Institution on 15th August 1973, and in final form on 20th March 1974. (Paper No. 1603/CC 209.)

© The Institution of Electronic and Radio Engineers, 1974

Signal recovery from repetitive non-uniform sampling patterns

J. DUNLOP, Ph.D., M.Sc.*

and

V. J. PHILLIPS, Ph.D., B.Sc.(Eng.)†

SUMMARY

This paper describes a technique for using amplitude samples which have been taken at non-uniform intervals of time. The method is essentially indirect, as the non-uniform samples are first converted into uniform samples, the conversion being based upon the impulse response of a practical realizable filter. The problems encountered in the process are analysed, and a procedure for determining the optimum parameters in any given case is suggested.

* Formerly at University College of Swansea; now at University of Strathclyde.

† Department of Electrical and Electronic Engineering, University College of Swansea, University of Wales, Singleton Park, Swansea SA2 8PP.

List of Symbols

$f(t)$	input signal
W	bandwidth of input signal
T	interval between uniform samples
$n; m$	general integers 1, 2, 3 . . .
$s(t)$	output signal from 'memory filter'
t_{NE}	memory length of normalized filter
t_E	de-normalized 'memory length'
$P(t)$	response of 'memory filter' to unit sample
$P(\tau_m - t_n); P(m, n)$	response at time τ_m due to unit sample at t_n
$A(n)$	uniform samples of $f(t)$
$b(m)$	non-uniform samples of $f(t)$
$B(m)$	non-uniform samples of $s(t)$
$V(x, y)$	terms in inverted P matrix
$E(n)$	errors in regenerated uniform samples
$K(n), Q(n), R(n), Y(n)$	error constants

1 Introduction

The sampling theorem states¹ that a signal $f(t)$ which is limited to a maximum frequency bandwidth of W Hz can be completely recovered from amplitude samples which are spaced at intervals of $1/2W$ seconds or less, i.e. from samples taken at a minimum rate of $2W$ samples/second. The theorem in this restricted form is expressed by:

$$f(t) = \sum_{n=-\infty}^{+\infty} A(n) \cdot \frac{\sin \left\{ 2\pi W \left(t - \frac{n}{2W} \right) \right\}}{2\pi W \left(t - \frac{n}{2W} \right)} \quad (1)$$

where $A(1), A(2), \dots, A(n)$ are the values of the samples. Equation (1) shows that the signal $f(t)$ can be recovered from its samples by multiplying each sample by a function of the general form $\sin \omega t / \omega t$ and summing these products over all time. The sample values $A(n)$ may be preserved by using them to amplitude-modulate a train of pulses of unit height and very short duration, and it is convenient to think of the samples in this way. It may be shown that if a network has a response to one of these unit pulses which lasts for a long time compared with the duration of the pulse, then its output response to that pulse is virtually identical (apart from a simple multiplying constant) to its response to a Dirac impulse function $\delta(t)$. Since an ideal low-pass filter with an infinitely steep-cut-off has an impulse response which is a $\sin \omega t / \omega t$ function, the signal recovery may be thought of as simply passing the samples through such a filter having its cut-off at W Hz.

Yen² has considered the case where the samples do not occur at uniformly spaced intervals of time, and it has been shown that the signal may be recovered without error from non-uniform samples of this sort provided that the samples occur at an average rate which is twice

the highest frequency in the signal. The functions used for signal recovery will not now be of the form $\sin \omega t / \omega t$ but will be different for each sample, and will be highly complicated in shape, as Yen's paper has shown. Thus, if one wishes to devise systems which transmit irregularly spaced samples or samples arranged in bunched patterns, one would need to generate these complicated functions at the receiver of the system in order to achieve signal recovery. The complexity of the instrumentation would preclude the use of these systems from a practical point of view.

The purpose of the present paper is to suggest a more practical method of using non-uniformly spaced samples. One particular case where the principle could be of use is in the system described by Flood and Hoskins.³ If wide-band signals are sent over a t.d.m. system designed originally for narrow-band signals, the use of several narrow-band channels for transmission can result in non-uniform sampling, and hence in distortion of the received signal. Another possible application will be mentioned later.

1.1 Extension of Sampling Theorem to Non-Uniform Sampling

The recovery problem may be approached from a somewhat different viewpoint, as follows. Since the original function $f(t)$ can be obtained completely and without error from the uniform samples $A(n)$ taken at times $t = n/2W$, it follows that other non-uniform sample values taken at times not equal to $n/2W$ can also be obtained from the $A(n)$ values:

$$b(m) \text{ (a sample at time } \tau_m) = \sum_{n=-\infty}^{\infty} A(n) \frac{\sin \left\{ 2\pi W \left(\tau_m - \frac{n}{2W} \right) \right\}}{2\pi W \left(\tau_m - \frac{n}{2W} \right)}. \quad (2)$$

The summations in such expressions have infinite limits because the $\sin \omega t / \omega t$ functions exist from $t = -\infty$ to $t = +\infty$. The effect of any given sample $A(n)$ thus persists for all time, and that sample must be included in the expression for $f(t)$. Furthermore, since all the $A(n)$ values determine $f(t)$ without error, an infinite number of equations such as those in (2) above would constitute a set of simultaneous equations from which the values $b(m)$ could be obtained. Conversely, knowledge of an infinite number of samples $b(m)$ would enable the samples $A(n)$ to be obtained and would thus also specify $f(t)$ without error.

One might attempt to limit the number of equations in order to render such a calculation feasible. For example, this could be done by assuming that the value of $f(t)$ at a time τ_m is determined by a finite number of samples $A(n)$ in the region of time τ_m . In effect, one is truncating the $\sin \omega t / \omega t$ function and assuming that it falls to zero after a finite time. Although these functions are zero at $t = \pm \infty$, the decay to zero is quite slow (e.g. after 50 cycles of the sinusoid the peaks are still attaining about 0.3% of the value at $t = 0$) and the number of equations

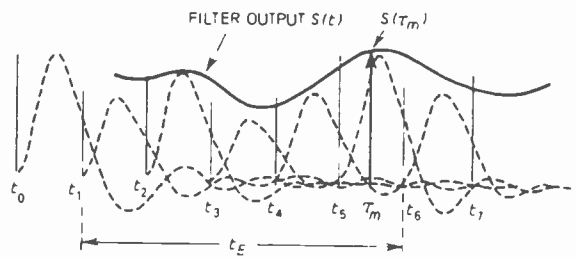


Fig. 1. Filter output given by superposition of individual responses.

must remain large if gross errors are to be avoided. It is perhaps worth noting that the recovery functions used by Yen² in the previously quoted reference are also of infinite duration, and analogous problems would arise when using his method of recovery.

The question of using non-uniformly spaced samples will now be reformulated in such a way as to avoid these functions of infinite duration. First consider that the band-limited signal $f(t)$ has been uniformly sampled in the normal 'classical' manner. Let these samples $A(n)$ be passed through a practical, realizable, low-pass filter. The output of this filter will be a waveform $s(t)$ which can be expressed as the sum of the responses to each individual sample (Fig. 1). The important point to note here is that a practical filter has an impulse response which is causal; that is to say no output will appear until an input sample has been applied and the response will die away to zero in some time which, although theoretically infinite, will normally be much more rapid than that of the ideal filter previously discussed. For all practical purposes it may be assumed to have decayed to below some chosen value after a time t_E has elapsed. If, purely for the sake of illustration, it is assumed that t_E is equal to, say, five uniform sampling intervals, then the output of the filter at some time τ_m (Fig. 1), is given by:

$$B(m) = s(\tau_m) = \sum_{n=1}^5 A(n) P(\tau_m - t_n) \quad (3)$$

where the $A(n)$ functions are the uniform sample values; $P(t)$ is the response of the filter to a sample of unit height, and $P(\tau_m - t_n)$ is the response at time τ_m due to a sample which occurred at t_n . Note that the limit of the summation is now set by the time t_E . The longer the time t_E considered for any given filter, the more accurate will be the result of the calculation. The important point is that by selection of t_E , we have the ability to carry out the calculation to any specified accuracy which we may require. It is assumed that after a time t_E has elapsed, the filter will have 'forgotten' the existence of that sample, and this time will henceforth be referred to as the 'memory length' of the filter. The exact effects of the selection of t_E for a given filter will be discussed in detail in a later Section of the paper.

Let the filter output waveform $s(t)$ be sampled in any particular non-uniform way which may be required for the transmission system being devised. Using equation (3), each of these non-uniform samples $B(m)$ may be expressed in terms of a finite number of input uniform samples $A(n)$ which have been derived from the original

function $f(t)$. The samples $B(m)$ are transmitted to the receiver of the system, and provided that the distribution in time of samples $B(m)$ relative to samples $A(n)$ is known, the P values in the equation will be known, and samples $A(n)$ can be recovered by solution of those equations. The requirement to know the distribution in time of the samples precludes the use of samples which occur at completely random times, but allows the use of samples which are distributed non-uniformly according to some known pattern. More will be said about sample distribution patterns in the next Section.

What has been done here is to transform the samples $A(n)$ into other samples $B(m)$. An infinite number of such transformations could, of course, be envisaged by selecting the P terms in the equations in different ways. We have elected to do this in one particular way which represents the easily-arranged uniform sampling-filtering-non-uniform sampling process, and so values of P used in this case will be determined by the impulse response of the 'memory' filter we have chosen.

It is perhaps worth pointing out that the processes involved have been described purely in the time domain. It is possible to describe them in the frequency domain also. Assume that the input signal $f(t)$ occupies the spectral range zero to 4 kHz. The uniform samples going into the 'memory' filter would have a spectrum consisting of the same base-band, together with sets of double-sidebands situated about the harmonics of the sampling frequency (which would be nominally 8 kHz). The spectrum of the output signal $s(t)$ would again consist of the base-band modified somewhat according to the amplitude and phase responses of the filter. In general, one would wish to keep the 'memory length' t_E short in order to limit the number of equations used. This, in turn, would imply a filter with no prolonged ringing effects in its impulse response, and therefore one with a fairly gradual cut-off in its amplitude/frequency response. The signal $s(t)$ would thus contain some of the sidebands in addition to the base-band. It might be thought that filtering the uniform samples of a signal is equivalent to filtering the signal itself, but this is not so. We have shown that $s(t)$ is neither identical to $f(t)$, nor to the base-band modified in amplitude and phase but contains sideband terms as well. Thus we may not merely put $f(t)$ into the 'memory filter' and take non-uniform samples $B(m)$ of the output signal, because the sideband terms would be absent, and the mathematics developed for the time domain would not then apply.

1.2 Types of Non-Uniform Sampling

The method of solution involved in the calculation of the uniform samples from the non-uniform samples will depend on the distribution of the samples in time. The distributions shown in Fig. 2 will illustrate the processes involved. It will be assumed quite arbitrarily at this point, and purely for purposes of illustration, that the 'memory filter' used has a 'memory' length t_E equal to twelve uniform sampling intervals; i.e. equal to $12T$ where $T = 1/2W$.

In the type of situation shown in Fig. 2(a), one non-uniform sample of $s(t)$ occurs in each interval between

two uniform samples of $f(t)$. Remembering that $t_E = 12T$, the twelfth non-uniform sample can be expressed by means of an equation similar to equation (3), as:

$$B(12) = A(1) \cdot P(\tau_{12} - t_1) + A(2) \cdot P(\tau_{12} - t_2) \dots + A(12) \cdot P(\tau_{12} - t_{12}) \quad (4)$$

where $P(\tau_m - t_n)$ is the response at non-uniform sample time τ_m produced by a uniform sample of unit amplitude at t_n . For convenience, this will be written $P(m, n)$. Using this notation, the non-uniform samples of Fig. 2(a) may be written:

$$B(12) = A(1) \cdot P(12, 1) + A(2) \cdot P(12, 2) \dots + A(12) \cdot P(12, 12) \quad (5a)$$

$$B(13) = A(2) \cdot P(13, 2) + A(3) \cdot P(13, 3) \dots + A(13) \cdot P(13, 13) \quad (5b)$$

$$B(14) = A(3) \cdot P(14, 3) + A(4) \cdot P(14, 4) \dots + A(14) \cdot P(14, 14) \quad (5c)$$

etc.

These equations are characterized by the displacement of one uniform sample value in sequence in successive equations as a result of the fact that there is one non-uniform sample in between each pair of uniform samples.

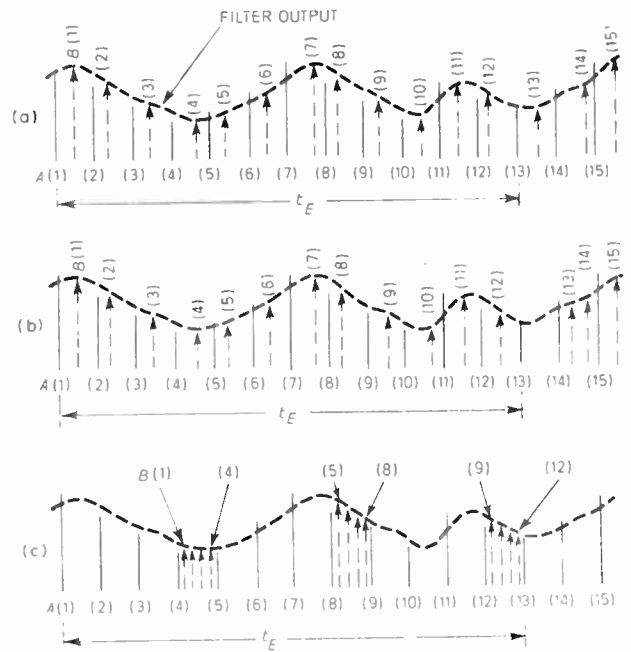


Fig. 2. Various non-uniform sampling patterns.

Two obvious conditions must be met before equations (5) can be solved for uniform samples $A(n)$ in terms of known non-uniform samples $B(n)$. The first condition is that the non-uniform sample arrangement must be known in advance so that the $P(m, n)$ values may be computed. The second is that in order to calculate any particular uniform sample value from one of the equations (5) all other uniform sample values appearing in the equation must be known.

Taking equation (5a) and assuming that the values $A(1)$ to $A(11)$ are already known:

$$A(12) = \frac{B(12) - X(12)}{P(12, 12)} \quad (6)$$

where

$$X(12) = \sum_{n=1}^{11} A(n) \cdot P(12, n).$$

Subsequent samples $A(13)$, $A(14)$, etc. may then be computed by similar means. A calculation of this sort is a continuing process, but it has to be started off somewhere. One way of doing this is to assume that all samples before $A(1)$ are zero. In this case $B(1)$ is given by:

$$B(1) = A(1) \cdot P(1, 1)$$

from which

$$A(1) = \frac{B(1)}{P(1, 1)} \quad (7)$$

This value may now be used in the computation of $A(2)$ and so on. The values of $A(1)$ to $A(11)$ are calculated in this way from a knowledge of $B(1)$ to $B(11)$. It is to be hoped that such a process will always converge from the assumed zero samples to give eventually the correct values of $A(n)$. The detailed mathematics of this convergence process involves not only the coefficients $P(m, n)$ but also the sample values themselves; but at least the system is such that the 'incorrect' zero samples are forgotten after the interval of time t_E . This convergence process is discussed in more detail in Appendix 1.

A somewhat different sample distribution is shown in Fig. 2(b) where the two non-uniform samples $B(13)$ and $B(14)$ are bunched together in one uniform sampling interval. The equations for this case now become:

$$\begin{aligned} \text{(a) } B(12) &= A(1) \cdot P(12, 1) + A(2) \cdot P(12, 2) \dots \\ &\quad + A(11) \cdot P(12, 11) + A(12) \cdot P(12, 12) \\ \text{(b) } B(13) &= A(3) \cdot P(13, 3) + A(4) \cdot P(13, 4) \dots \\ &\quad + A(13) \cdot P(13, 13) + A(14) \cdot P(13, 14) \\ \text{(c) } B(14) &= A(3) \cdot P(14, 3) + A(4) \cdot P(14, 4) \dots \\ &\quad + A(13) \cdot P(14, 13) + A(14) \cdot P(14, 14) \\ \text{(d) } B(15) &= A(4) \cdot P(15, 4) + A(5) \cdot P(15, 5) \dots \\ &\quad + A(14) \cdot P(15, 14) + A(15) \cdot P(15, 15) \end{aligned} \quad (8)$$

These can no longer be solved singly in turn, as before. Equation (8a) can be solved for $A(12)$. $B(13)$ and $B(14)$ are, however, expressed in terms of the same set of uniform sample values, and thus $A(13)$ and $A(14)$ must be calculated from a simultaneous solution of (8b) and (8c). Having solved for these, $A(15)$ follows from (8d):

$$A(15) = \frac{B(15) - X(15)}{P(15, 15)}$$

where

$$X(15) = \sum_{n=4}^{14} A(n) \cdot P(15, n) \quad (9)$$

Continuing this bunching up of non-uniform samples leads to the type of distribution illustrated in Fig. 2(c), where a number of non-uniform samples (four in this example) are grouped within one uniform sampling

interval, yielding the equations:

$$\begin{aligned} B(9) &= A(1) \cdot P(9, 1) + A(2) \cdot P(9, 2) \dots \\ &\quad + A(11) \cdot P(9, 11) + A(12) \cdot P(9, 12) \\ B(10) &= A(1) \cdot P(10, 1) + A(2) \cdot P(10, 2) \dots \\ &\quad + A(11) \cdot P(10, 11) + A(12) \cdot P(10, 12) \\ B(11) &= A(1) \cdot P(11, 1) + A(2) \cdot P(11, 2) \dots \\ &\quad + A(11) \cdot P(11, 11) + A(12) \cdot P(11, 12) \\ B(12) &= A(1) \cdot P(12, 1) + A(2) \cdot P(12, 2) \dots \\ &\quad + A(11) \cdot P(12, 11) + A(12) \cdot P(12, 12) \end{aligned} \quad (10)$$

Assuming that uniform samples $A(1)$ to $A(8)$ are known from previous calculations, equations (10) are solved simultaneously to give $A(9)$ to $A(12)$. Subsequent samples are also obtained by solution of sets of simultaneous equations of this sort.

Two conditions in addition to those mentioned previously must be met if conversions of non-uniform samples are to be possible.

(i) During the time interval over which the conversion is carried out the number of uniform samples must equal the number of non-uniform samples. Put in another way, the non-uniform samples must occur at an average rate equal to the rate of the uniform samples.

(ii) At least one non-uniform sample of $s(t)$ must occur during the interval t_E after any uniform sample of $f(t)$. If this is not the case, then the uniform sample in question cannot contribute to any non-uniform sample, and cannot subsequently be obtained from a knowledge of the non-uniform samples. This sets a limit to the degree of bunching of samples which is permitted for a filter of given 'memory length'.

1.3 Cumulative Errors

The equations in the foregoing analysis were derived on the assumption that the filter used had a 'memory length' $t_E = 12T$. The obvious disadvantage of these equations is that in any individual calculation the values of previously calculated uniform samples must be used. Any errors in computation, arising from whatever cause, would therefore be carried on into the next calculation. Although one would hope that these errors would die out in time due to the finite 'memory', the situation is a complicated one, and there is no guarantee that with given unfavourable sample values the whole process would not become unstable, giving progressively worse and worse errors as time went on. All things considered, it would be very advantageous to avoid passing on errors from stage to stage in the calculation.

If a filter were selected having a memory length $t_E = 4T$, then equations (10) would reduce to:

$$\begin{aligned} B(9) &= \sum_{n=9}^{12} A(n) \cdot P(9, n) \\ B(10) &= \sum_{n=9}^{12} A(n) \cdot P(10, n) \\ B(11) &= \sum_{n=9}^{12} A(n) \cdot P(11, n) \\ B(12) &= \sum_{n=9}^{12} A(n) \cdot P(12, n) \end{aligned} \quad (11)$$

In this case, knowledge of $A(1)$ to $A(8)$ is no longer required for solution of the equations to give $A(9)$ to $A(12)$, so that errors will not be handed on. A 'memory length' of much less than $4T$ cannot be used as the situation could arise where $A(9)$ for example would not contribute to any of the non-uniform sample values, thereby violating condition (ii) of Section 1.2. It would therefore seem that in order to use the simple equations (11), and in order to avoid violating the condition just mentioned, we would be forced in this example to select a memory filter with 'memory length' equal to $4T$ or thereabouts.

There is, however, one other alternative which could be explored. For the same arrangement of samples in groups of four we might prefer (for reasons which will appear later) to select a filter having a memory length equal to some other value—say $7T$, for example. Equations (11) were derived on the assumption that the memory length was $4T$, so it would be incorrect to use these equations for the case where the impulse response persists for a time $7T$. Use of the equations in this way would effectively terminate the response too soon and this would lead to errors. However, since the response would be dying away fairly rapidly after a time $4T$, the error thus introduced might be small and could perhaps be tolerated in order to avoid any possibility of cumulative errors handed on from previous calculations.

The next section will contain a detailed analysis of the various factors involved in selection of the 'memory length'. First, however, it will be convenient to introduce matrix notation and to represent equations (11) in the form:

$$\begin{bmatrix} B(9) \\ B(10) \\ B(11) \\ B(12) \end{bmatrix} = \begin{bmatrix} P(9,9) & P(9,10) & P(9,11) & P(9,12) \\ P(10,9) & P(10,10) & P(10,11) & P(10,12) \\ P(11,9) & P(11,10) & P(11,11) & P(11,12) \\ P(12,9) & P(12,10) & P(12,11) & P(12,12) \end{bmatrix} \begin{bmatrix} A(9) \\ A(10) \\ A(11) \\ A(12) \end{bmatrix} \quad (12)$$

Since the aim is to recover the $A(n)$ values, given the $B(m)$ values, the P matrix may be inverted to give:

$$\begin{bmatrix} A(9) \\ A(10) \\ A(11) \\ A(12) \end{bmatrix} = \begin{bmatrix} V(9,9) & V(9,10) & V(9,11) & V(9,12) \\ V(10,9) & V(10,10) & V(10,11) & V(10,12) \\ V(11,9) & V(11,10) & V(11,11) & V(11,12) \\ V(12,9) & V(12,10) & V(12,11) & V(12,12) \end{bmatrix} \begin{bmatrix} B(9) \\ B(10) \\ B(11) \\ B(12) \end{bmatrix} \quad (13)$$

For any given repetitive pattern of pulses this matrix inversion would only have to be carried out once, and it will be noted that the actual physical process of calculating the $A(n)$ values consists simply of adding the $B(m)$ values in the proportions indicated by these equations, i.e. the process normally referred to as 'matrixing'.

2 Initial Simulation of a System Employing Non-Uniform Samples

There is an infinite number of possible arrangements of non-uniform samples, but in order to illuminate any possible problems arising in the signal recovery process, one particular arrangement of samples (namely that of Fig. 2(c)) has been selected for further study. This pattern was chosen because it could have a practical

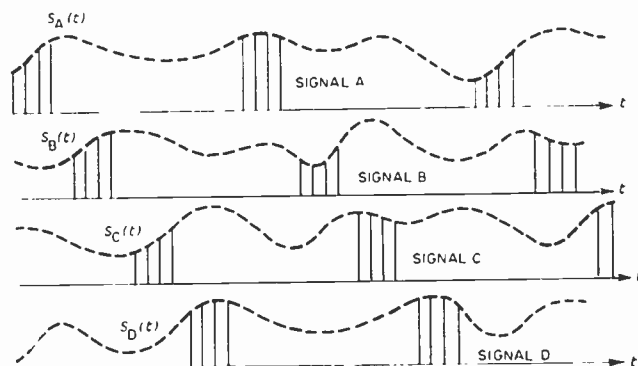


Fig. 3. Four-channel t.c.m. incorporating non-uniform sampling.

application in the form of signal transmission known as 'time-compression-multiplexing' (t.c.m.) described by Flood and Urquhart-Pullen⁴. In the usual form of time-division-multiplex transmission, adjacent samples are derived from different speech (or other information) channels, and must be separated by a guard interval to reduce inter-symbol cross-talk caused by imperfections in the transmission channel. In the t.c.m. system, uniform samples from each speech channel are stored and sent together in groups; these groups being interleaved with sample groups from other speech channels. The efficiency of transmission is improved because relatively large guard intervals are now needed only between groups and not between individual samples.

A possible alternative approach is illustrated in Fig. 3. Each band-limited speech signal is first sampled in the classical uniform manner, and the samples from each signal are passed through memory filters to produce signals $s(t)$ —one for each speech signal. Each $s(t)$ is then sampled non-uniformly, as in Fig. 3, in order to provide groups of, say, four samples directly. These groups are then time-multiplexed by adding them together. Synchronizing information is added as required, and a suitable signal for transmission is thus formed. At the receiver, the groups are separated, and each group is converted back into uniform samples using the technique described in the previous section. Simple low-pass filtering then recovers the continuous speech signals. A block diagram of the system is shown in Fig. 4. One channel only is shown, the multiplexing arrangements having been omitted for simplicity. At the receiver, the incoming $B(m)$ samples are stored, and after the correct number of samples in a frame (four in our example) have arrived, they are added together (matrixed) in the proportions indicated by equations (13). The results of these computations, $A(1)$, $A(2)$, $A(3)$ and $A(4)$, are again stored and are then read out in turn by a switch in order to produce a train of uniform samples. The continuous signal is then produced by the final low-pass recovery filter.

2.1 Choice of 'Memory Filter' and Estimation of 'Memory Length'

Since the recovery method depends on the response of the memory filter, the selection of this filter is a matter of some importance. As mentioned in Section 1, if the sample pulses are of small duration then

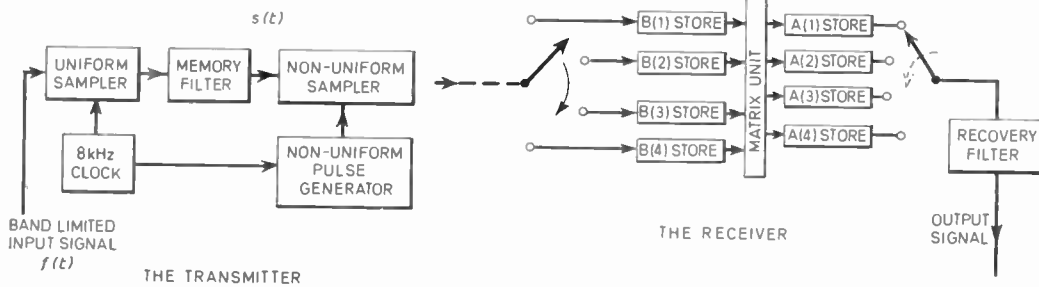


Fig. 4. Proposed system.

(apart from a simple multiplying constant) the response $P(t)$ to a sample of unit height is virtually identical to the impulse response. Use of the impulse function simplifies the algebra involved in calculating the response and the functions $P(t)$ used in this paper have been calculated in this way. The terms 'response to a unit sample' and 'impulse response' are used interchangeably in this sense. Many standard types of low-pass filter exist and are described in the literature. For example, Chebyshev filters and Bessel filters have impulse responses which can be thought of as being near the opposite ends of a scale of impulse-response types. Chebyshev filters are designed primarily to have steep cut-off characteristics and have impulse responses which are highly oscillatory in nature. Bessel filters^{5,6}, on the other hand, are designed specifically to have linear phase characteristics. They have relatively slow rates of cut-off in their amplitude response characteristics, and as a consequence exhibit virtually no ringing in their impulse responses.

Having chosen the type of filter to be used, it then remains to select the order of the filter. However, it can be shown (Appendix 2) that the maximum number of independent equations such as equations (12) which can be written, relating input samples and output of a network is equal to the order of the impulse response. For a solution to exist for the four equations (12), the filter must be at least fourth-order. If this is not the case, the P matrix will be singular, and it will not be possible to invert it.

The two types of filter selected for the initial investiga-

Table 1. Coefficients of impulse response equation for normalized fifth-order filters.

	Bessel	Chebyshev
(α)	3.6467	0.3631
(β)	3.3519	0.1122
(γ)	1.7427	1.0118
(θ)	2.3247	0.2937
(ϕ)	3.5710	0.6253
(V)	20.8634	0.3884
(W)	-23.8703	0.0800
(X)	12.6862	-0.1863
(Y)	3.0067	-0.4684
(Z)	-5.3337	0.3072

tion were 5th-order Chebyshev and Bessel filters. The impulse response for both filters is of the form of equation (14), the values of the constants being given in Table 1.

$$P(t) = V e^{-\alpha t} + e^{-\beta t} [W \cos(\gamma t) + X \sin(\gamma t)] + e^{-\theta t} [Y \cos(\phi t) + Z \sin(\phi t)] \quad (14)$$

The impulse responses of the two filters, normalized to a cut-off frequency of 1 rad/s, were calculated on a digital computer, and the resulting curves are shown in Figs. 5(a) and (b). (Note the different time scales of these curves.)

The 'memory lengths' t_{NE} of these normalized filters were estimated by calculation in the following way, using a digital computer. A sinusoidal input signal was first sampled uniformly. These samples were then assumed to be the input to the 'memory filter', and the output from the filter at various times was calculated by summing the products of the 'input sample' and 'impulse response'. The impulse response was obtained from equation (14). The first time the calculation was carried

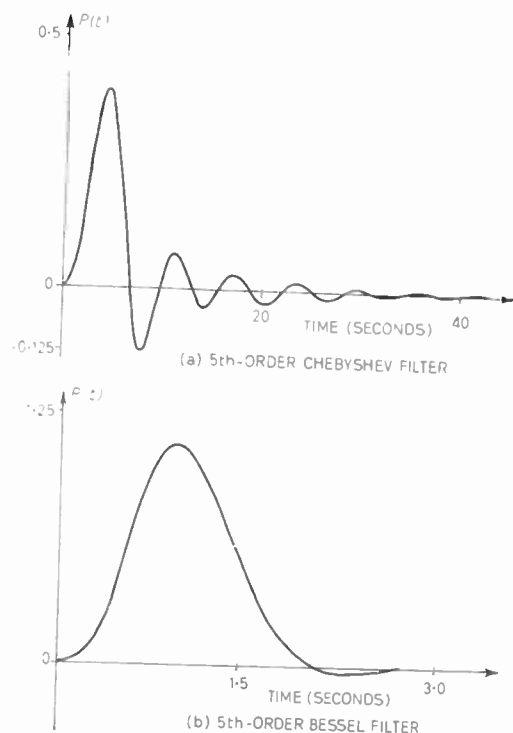


Fig. 5. Normalized impulse responses.

out, the impulse response was assumed to become zero after some very short time t_c , and only the first t_c seconds of the response were used in the calculation. This severe truncation of the impulse response meant that the computation was seriously in error. A second computation was then carried out identical with the first except that the response was assumed to last for a somewhat longer time, t_c . The output voltages calculated were not the same as before, being a better approximation to what would actually be produced in a practical experiment. The computation was repeated over and over, each time for a longer t_c . Eventually, when t_c was very long, the output waveform calculated was an extremely good approximation to the experimental case, and there would be hardly any difference between the values obtained in successive computations. As previously explained, the 'memory length' has to be defined according to some arbitrary criterion, and the one adopted was to examine the successive computations of the various points on the output waveform and to take as the normalized 'memory length' t_{NE} the value of t_c when the computations became the same to five significant figures.

2.2 Computer Simulation of the Proposed System

The system of Fig. 4 was simulated on a digital computer. Calculations were carried out for both the Chebyshev and the Bessel filter, both being denormalized so as to have a memory length equal to four uniform-sample periods ($4T$). A simple sinusoidal signal $f(t)$ was first uniformly sampled at a rate of 8 kHz. These samples were used as the input to the 'memory filter', and were also stored for eventual comparison with those obtained by calculation at the receiver of the system. The non-uniform samples $B(m)$ of the filter output waveform were then calculated. At this stage in the computation the representation of equations (10) was used; these equations take account of the impulse response for up to twelve sample periods, so this meant that there was effectively no truncation of the response, and the output waveform obtained from the memory filter would simulate the practical filtering process with negligible error.

The matrixing process at the receiver was simulated using equations (11), (12), and (13) assuming that the memory length was truly $4T$, and neglecting the impulse response beyond this interval. The uniform samples thus calculated could then be compared with the stored correct values in order to assess the effectiveness of the recovery process. To help in this comparison, a computer graph-plotter was used to provide a visual display. A fifth-order Chebyshev recovery filter (having a cut-off frequency of 3 kHz) was simulated on the computer. The correct stored samples $A(n)$ were applied to this filter, and its output was computed at closely spaced points so that the graph plotter was able to interpolate and produce a continuous output curve. The recovered samples at the receiver were then put into the recovery filter, and its output was again determined. In order to facilitate comparison of the two signals, the difference between the two signals was plotted.

Figure 6 shows the results obtained for input sinusoids of 1.7 kHz and 3 kHz. The correct outputs are shown together with the errors which result from the use of fifth-order Chebyshev and Bessel 'memory filters' with $t_E = 4T$.

It will be noted that in each case the error produced by the Bessel filter is the smaller. The input levels of the two sinusoids were originally equal; the difference in amplitudes of the correct signals is due to the selective attenuation of the recovery filter. The Bessel filter error signal is approximately -34 dB (2%) relative to the 1.7 kHz signal, and -30 dB (3%) for the 3 kHz signal.

The equivalent figures for the Chebyshev filter are -20 dB (10%) and -21 dB (9%) respectively.

Thus it may be concluded that the system is capable of reproducing the sinusoidal inputs with very reasonable error, particularly when the Bessel filter is used. The exact mechanisms which give rise to the errors will be analysed in the next section, the Bessel filter alone being considered, since it produces a better result than the Chebyshev.

3 Sources of Error

So far, it has been assumed that there are two sources of error which could be encountered in a system of this

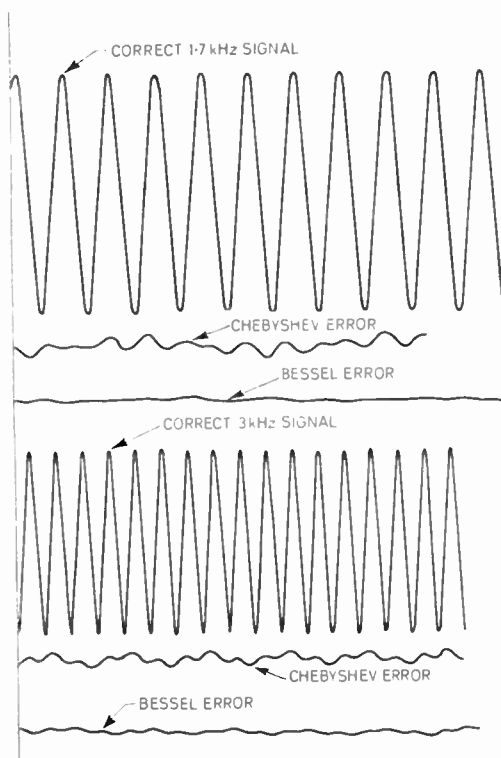


Fig. 6. Errors produced by using denormalized 'memory lengths' $t_E = 4T$.

The normalized 'memory lengths' for the two fifth-order filters were:

Chebyshev filter—96 seconds; Bessel filter—6 seconds

If a filter is denormalized to have its cut-off frequency at some other angular frequency ω_c its memory length will then be $t_E = t_{NE}/\omega_c$. Conversely, if a filter is required having a memory length equal to some particular value, the cut-off frequency needed can be obtained from the same formula.

type. There is the cumulative error previously mentioned, where errors in one set of calculations are handed on to the next when using equations (10). This can be avoided by using equations (11) or (12) where the impulse response is truncated, i.e. is assumed zero after some finite time. This, in turn, means that equations (12) are a less exact representation of the process, so that other errors called 'truncation errors' arise from this cause. Additionally, however, in any practical transmission system, there will always be small errors in the $B(m)$ values arriving at the receiver due to imperfections in transmission, and the effects of these errors must also be considered.

3.1 Truncation Errors

In the computer simulation which led to the results presented in Fig. 6, the errors are a direct result of the fact that the impulse response is assumed to have fallen to zero after four inter-sample intervals, the memory lengths of the filters having been denormalized to $4T$.

The full equations for the non-uniform samples, assuming no truncation (i.e. an infinitely long impulse response), would be similar to equations (10), taking account of all samples back to the $A(-\infty)$. These may be rewritten:

$$\begin{aligned}
 B(9) &= \left\{ \sum_{n=-\infty}^8 A(n) \cdot P(9, n) \right\} + A(9) \cdot P(9, 9) + A(10) \cdot P(9, 10) + A(11) \cdot P(9, 11) + A(12) \cdot P(9, 12) \\
 B(10) &= \left\{ \sum_{n=-\infty}^8 A(n) \cdot P(10, n) \right\} + A(9) \cdot P(10, 9) + A(10) \cdot P(10, 10) + A(11) \cdot P(10, 11) + A(12) \cdot P(10, 12) \\
 B(11) &= \left\{ \sum_{n=-\infty}^8 A(n) \cdot P(11, n) \right\} + A(9) \cdot P(11, 9) + A(10) \cdot P(11, 10) + A(11) \cdot P(11, 11) + A(12) \cdot P(11, 12) \\
 B(12) &= \left\{ \sum_{n=-\infty}^8 A(n) \cdot P(12, n) \right\} + A(9) \cdot P(12, 9) + A(10) \cdot P(12, 10) + A(11) \cdot P(12, 11) + A(12) \cdot P(12, 12)
 \end{aligned}$$

and hence:

$$\begin{vmatrix} A(9) \\ A(10) \\ A(11) \\ A(12) \end{vmatrix} = \begin{vmatrix} V(9, 9) & V(9, 10) & V(9, 11) & V(9, 12) \\ V(10, 9) & V(10, 10) & V(10, 11) & V(10, 12) \\ V(11, 9) & V(11, 10) & V(11, 11) & V(11, 12) \\ V(12, 9) & V(12, 10) & V(12, 11) & V(12, 12) \end{vmatrix} \cdot \begin{vmatrix} B(9) - \sum_{n=-\infty}^8 A(n) \cdot P(9, n) \\ B(10) - \sum_{n=-\infty}^8 A(n) \cdot P(10, n) \\ B(11) - \sum_{n=-\infty}^8 A(n) \cdot P(11, n) \\ B(12) - \sum_{n=-\infty}^8 A(n) \cdot P(12, n) \end{vmatrix} \quad (15)$$

It will be observed that 'early' relatively large values of the impulse response are involved in the V matrix, whereas 'late' smaller values of the tail of the response appear in the last matrix of equation (15). If calculations are carried out according to equation (13), there will be an error in the value of $A(9)$ designated $E(9)$ given by:

$$\begin{aligned}
 E(9) &= V(9, 9) \sum_{n=-\infty}^8 A(n) \cdot P(9, n) + \\
 &+ V(9, 10) \sum_{n=-\infty}^8 A(n) \cdot P(10, n) + \\
 &+ V(9, 11) \sum_{n=-\infty}^8 A(n) \cdot P(11, n) + \\
 &+ V(9, 12) \sum_{n=-\infty}^8 A(n) \cdot P(12, n) \quad (16)
 \end{aligned}$$

This error depends on the particular values of $A(n)$ involved and also on the V and P values which are derived from the impulse response. It is therefore convenient to rewrite equation (16) in the form:

$$E(9) = \sum_{n=-\infty}^8 A(n) \cdot K(n) \quad (17)$$

where

$$\begin{aligned}
 K(n) &= V(9, 9) \cdot P(9, n) + V(9, 10) \cdot P(10, n) + \\
 &+ V(9, 11) \cdot P(11, n) + V(9, 12) \cdot P(12, n)
 \end{aligned}$$

The numbers $K(n)$ will be referred to as the error constants, and they are a property of the impulse response alone. Similar error constants $Q(n)$, $R(n)$ and $Y(n)$ may be derived for $A(10)$, $A(11)$, and $A(12)$:

$$\begin{aligned}
 E(10) &= \sum_{n=-\infty}^8 A(n) \cdot Q(n) \\
 E(11) &= \sum_{n=-\infty}^8 A(n) \cdot R(n) \quad (18) \\
 E(12) &= \sum_{n=-\infty}^8 A(n) \cdot Y(n)
 \end{aligned}$$

For a repetitive non-uniform sampling pattern such as that considered here, the error constants will have identical values for successive groups of samples.

As shown above, in any given calculation the error involved will depend on the sample values and the error constants as in equation (17). Nothing can be done about the sample values, but it would seem to be a reasonable assumption that in order to minimize the error, the error constants should be kept as small as possible. This, in turn, means that for a start the P values in the error constants should be kept small, i.e. the impulse response should fall to zero very quickly after the interval t_E , which is only common sense. The results of Fig. 6, of course, verify this, since the decay of the Bessel filter is rapid, whereas that of the Chebyshev filter is not.

It follows from this discussion, and again from common sense, that the errors produced by this truncation effect could be reduced by taking a longer length of the normalized impulse response as being memory length t_{NE} and denormalizing this new increased length to the interval $4T$, thereby increasing the accuracy of the equations. There is, however, another factor which needs to be considered before this is done.

3.2 Conditioning of the Matrix and its Effect on Transmission Errors

It will be evident from Fig. 2(c) that the contribution to each bunch of non-uniform samples by the most remote uniform sample in the interval $4T$ is very small. For example, the contribution of $A(9)$ to $B(9)$ is smaller than the contribution of $A(11)$ or $A(12)$ to $B(9)$. Because of this the coefficients in the first column of the P matrix will be much smaller than the other coefficients. A typical P matrix for a fifth-order Bessel filter with memory length $t_{NE} = 6$ seconds denormalized to $4T$, the regular sampling rate being 8 kHz, is given in Table 2. (The coefficient $P(9, 12)$ is zero here because in this particular example $B(9)$ is assumed coincident with $A(12)$.) The inverted V matrix is also given in Table 2, and it will be seen that the first column of small P coefficients has given rise to a first row of large V coefficients. Such a row of large coefficients demands very high accuracy in the values of the non-uniform samples and in the computation itself, since the first uniform sample is calculated from the sums and differences of very large numbers; in other words, the P matrix is ill-conditioned. It also means, incidentally, that the P coefficients themselves must be known to a high degree of precision.

It should be made clear that this 'conditioning' error now being discussed has not appeared at all in the results of Fig. 6 since the calculations were carried out on a digital computer to a very high precision. If the matrixing operation of Fig. 4 were to be realized using practical adding circuits, such considerations of accuracy and conditioning would be extremely important, and the success or otherwise of the scheme would depend upon these factors.

If a longer period than 6 s of the normalized response were to be taken as the 'memory length', as suggested in Section 3.1, this ill-conditioning effect would be exaggerated even further, since the numbers in the first column of the P matrix would be smaller still. One way of increasing these numbers would be to denormalize the $t_{NE} = 6$ s to some longer interval than $4T$. As an example, Table 3 shows the P and V matrices for a fifth-order Bessel filter denormalized to $10T$. The V matrix in this case has a much smaller range of values and is much better from a point of view of accuracy. Clearly, this denormalization to $10T$ will increase the truncation error involved if a 4×4 matrix solution is still used to avoid cumulative errors.

3.3 Optimization of Impulse Response

To summarize, therefore, there are two conflicting requirements in the selection of the filter impulse response to be used. On the one hand it is desirable that t_{NE} be denormalized to as short a time as possible so as to avoid the truncation errors implicit in equations (12); on the other hand, it should be denormalized to a long time to avoid the ill-conditioned matrix and the resulting practi-

Table 2. P and V matrices for fifth-order Bessel filter with 'memory length' $4T$.

P Matrix			
-0.214478E-04	0.339996E-02	0.450564E+00	0.000000E+00
0.703470E-04	0.181668E-02	0.714486E-01	0.234572E+00
0.183945E-04	-0.352656E-03	-0.209894E-01	0.953996E+00
-0.835564E-05	-0.416421E-03	-0.727582E-02	0.982818E+00
V Matrix			
0.289302E+04	-0.670389E+04	0.583665E+05	-0.550549E+05
-0.279943E+03	0.110595E+04	-0.324503E+04	0.288591E+04
0.446960E+01	-0.866463E+01	0.272654E+02	-0.243978E+02
-0.609284E-01	0.347455E+00	-0.676864E+00	0.159156E+01

Table 3. P and V matrices for fifth-order Bessel filter with 'memory length' $10T$.

P Matrix			
0.120397E+00	0.893833E+00	0.691647E+00	0.000000E+00
0.348978E-01	0.675557E+00	0.953996E+00	0.124566E-01
-0.747406E-02	0.450564E+00	0.107921E+01	0.123610E+00
-0.209894E-01	0.259228E+00	0.104794E+01	0.375429E+00
V Matrix			
0.388265E+02	-0.101798E+03	0.908791E+02	-0.265443E+02
-0.672135E+01	0.223914E+02	-0.217033E+02	0.640289E+01
0.337332E+01	-0.112167E+02	0.122281E+02	-0.365394E+01
-0.260436E+01	0.101573E+02	-0.140660E+02	0.695786E+01

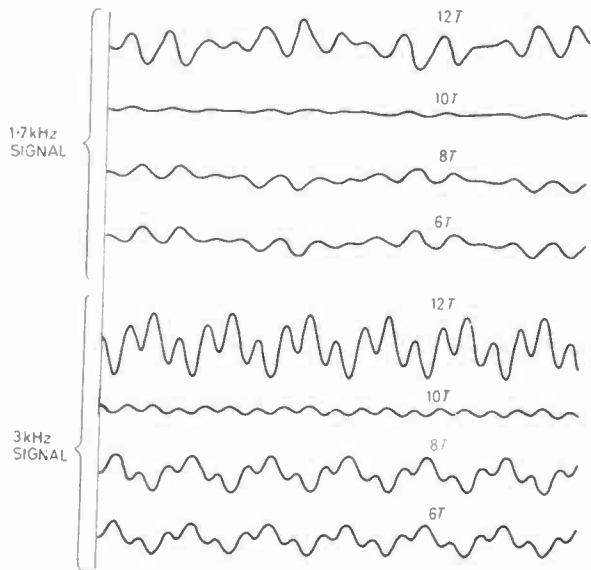


Fig. 7. Errors produced by Bessel filters of various denormalized memory lengths.

cal problems. There is one mitigating circumstance here; if equation (17) is consulted it will be seen that the error coefficients are the sums of products of P values and V values, so that to some extent at least if the P values are increased to improve conditioning, the V values decrease, thereby moderating the truncation errors produced.

The problem is one of some complexity, and in order to shed some further light on the process and to see if any optimum situation exists, the curves of Fig. 7 were produced. These show the errors produced in the 1.7 kHz and 3 kHz signals when the 4×4 matrix solution of equation (12) was used as before, but with the Bessel filter $t_{NE} = 6$ s denormalized to $6T, 8T, 10T$ and $12T$. An interesting effect is immediately apparent here in that compared with the $4T$ denormalization of Fig. 6, the errors are larger but there does seem to be a very noticeable decrease in error for the $10T$ case. Can any reason be found for this?

Consider first the error constants which describe the truncation error. These have been computed for 'memory lengths' in the range of denormalized $t_E = 4T$

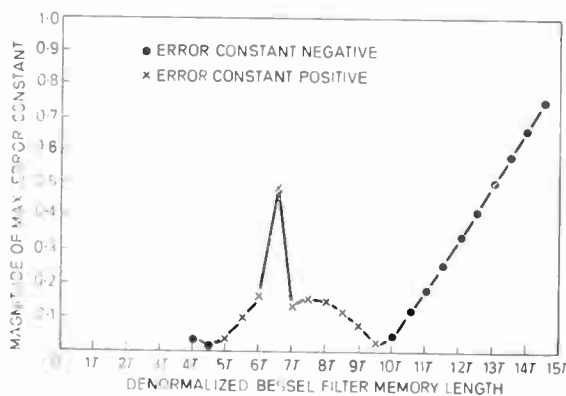


Fig. 8. Magnitude of maximum error constants for various denormalized memory lengths (Bessel filter).

to $15T$. In every case $K(8)$ turned out to be the largest of the coefficients; this is not surprising since $K(8)$ is the coefficient concerned with the truncation error due to neglect of $A(8)$ which is the sample immediately preceding the group $B(9)$ to $B(12)$. The value of $K(8)$ is plotted in Fig. 8, and it will be seen that the two smallest values of this curve occur at around $4T$ and $10T$. This suggests that truncation errors would be small if t_{NE} were denormalized to either of these values; hence agreeing with the observations of Fig. 7. There is a sharp maximum in the curve of Fig. 8 at about $t_E = 6T$. Discussion of this will be deferred for the moment.

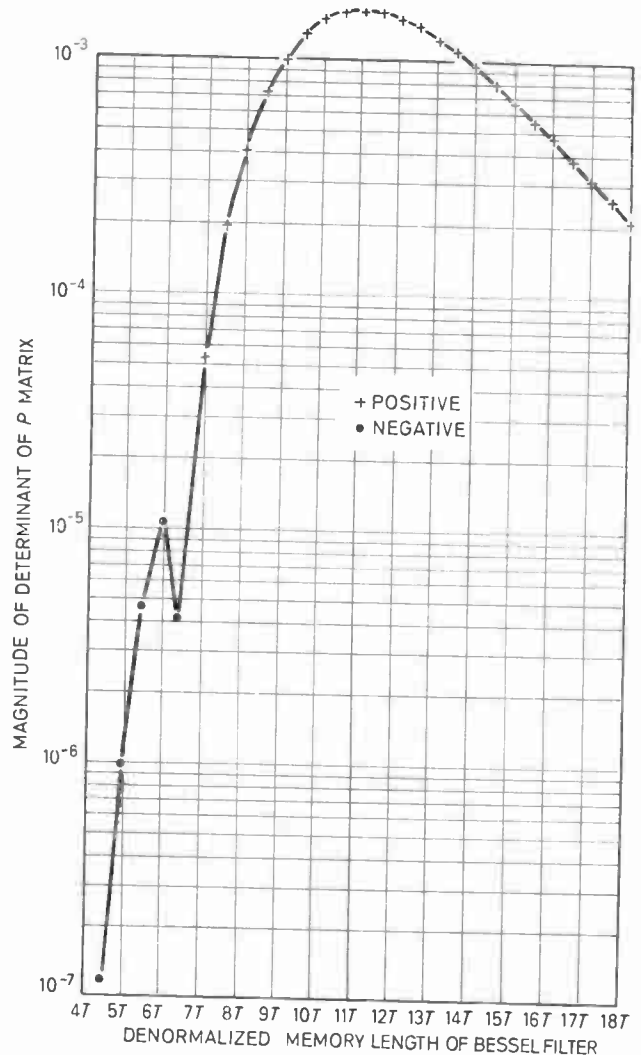


Fig. 9. Determinant of P matrix for various denormalized memory lengths. (Bessel filter.)

Consider next the conditioning of the P matrix to be solved. It is well known that if the determinant of a matrix becomes small compared with some of the terms in the matrix, the matrix is ill-conditioned and demands high accuracy for satisfactory solution.^{7,8} The coefficients in the P matrix themselves must always have values in the range approximately -0.1 to 1.25 , since they are read off the response curve of Fig. 5(b). Thus the determinant itself may be used directly as a measure of the conditioning of matrices of such P values,

and determinants have been computed for matrices which arise from denormalized 'memory lengths' in the range $t_E = 4T$ to $18T$. These are plotted in Fig. 9. It is clear that the determinant is very small indeed compared with unity when $t_E = 4T$, so that this particular P matrix is very ill-conditioned and demands high accuracy. As the denormalized t_E increases, the determinant rises very markedly to reach a maximum at $t_E = 11T$, falling gradually beyond this point. There is again a curious disturbance in the curve at around $6T$.

All these phenomena can be explained in physical terms. First, it should be noted that the normalized impulse response of the 5th-order Bessel filter of Fig. 5(b) has a 'memory length' t_{NE} (as previously determined in Section 2.1) of 6 s. However, most of the significant part of the waveform is over by $t = 3$ s; the values beyond that time are too small to be reasonably plotted on a graph.

Now refer to Fig. 10. This shows the sampling patterns together with the impulse responses (as in Fig. 1) for the regular samples, drawn to scale for denormalized $t_E = 4T, 6T, 10T$ and $12T$. For ease in drawing, the impulse responses are shown as being of fixed size and the time axis calibration is altered, but in each case the interval between uniform samples is $125 \mu\text{s}$.

Consider first the determinant of the P matrix. When $t_E = 4T$ the value of, say, $P(11, 9)$ is very small indeed, whereas $P(11, 12)$ is quite large. The P matrix will therefore contain a large number of small coefficients together with some large ones, which will mean that on the whole the determinant is likely to be small. When $t_E = 10T$ on the other hand, all the responses of $A(9)$ to $A(12)$ at the non-uniform samples $B(9)$ to $B(12)$ will be reasonably large in value, with one or two exceptions, so that the determinant will be much larger than before. As t_{NE} is denormalized to greater lengths than this, e.g. to $20T$, the P values used will be on the leading edge of the response curve and will become smaller, leading to a gradual decrease in the determinant, as in Fig. 9.

When t_E is $6T$, an interesting phenomenon occurs which is a property of the particular impulse response curve being used. It will be seen from Fig. 10(b) that the

Table 4. First rows of P matrices for t_E in the range $4.5T$ to $7.5T$. (Numbers have been rounded off so as to show magnitudes involved more clearly.)

t_E	$P(9, 9)$	$P(9, 10)$	$P(9, 11)$	$P(9, 12)$
$4.5T$	-0.0005	-0.005	0.70	0
$5.0T$	0.0002	-0.019	0.89	0
$5.5T$	0.0027	-0.018	1.02	0
$6.0T$	0.0034	0.017	1.07	0
$6.5T$	-0.001	0.08	1.08	0
$7.0T$	-0.010	0.19	1.06	0
$7.5T$	-0.019	0.32	1.01	0

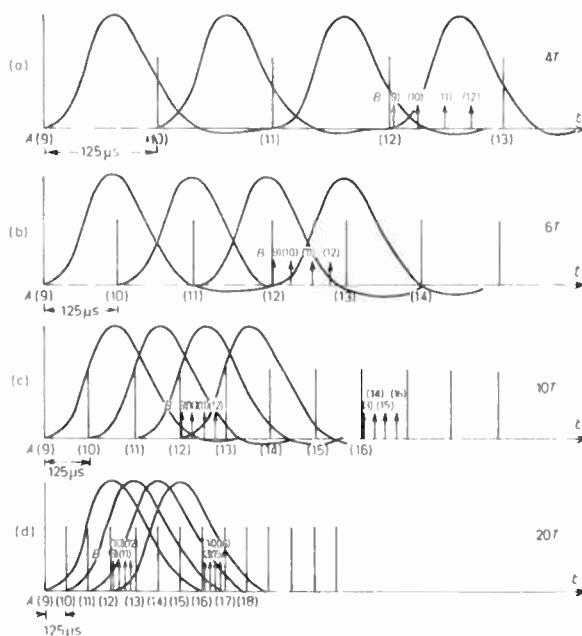


Fig. 10. Superposition of impulse responses of Bessel filter for various denormalized 'memory lengths' (drawn to scale).

responses at $B(9)$ due to $A(9), A(10)$ and $A(12)$ (i.e. $P(9, 9), P(9, 10)$ and $P(9, 12)$ are all nearly zero.)

Table 4 shows the first rows of the P matrices for values of $t_E = 4.5T$ to $7T$. It will be seen that $P(9, 9)$ and $P(9, 10)$ are both changing sign together, and hence will both have small values in the region of 6 to $6.5T$. There is thus a temporary cessation in the general rise in the values of coefficients, giving rise to the dip in the determinant value at this point, as in Fig. 9. No other such unpropitious coincidence of events seems to occur, and thereafter the determinant curve appears to have no further dips of this sort.

Consider next the truncation error in the light of Fig. 10. In the case of $t_E = 4T$ the error in $B(9)$ due to neglect of $A(8)$ (or in $B(13)$ due to neglect of $A(12)$) is very small and there is little truncation error involved in using a simple 4×4 matrix of equations. Going to the other extreme of $t_E = 20T$, the truncation error due to neglecting the effect of $A(12)$ on $B(13)$ would be very large indeed.

Looking at the intermediate case of $t_E = 10T$, the effect of $A(12)$ on $B(13)$ is small, but no longer negligibly so, and is becoming significant. This suggests a rise in the truncation errors as t_E is increased beyond about $10T$ because the significant first half of the 'memory length' is beginning to affect the next group of non-uniform samples. This conclusion is in accordance with the phenomenon observed in Fig. 8.

The expression for the error constant $K(8)$ written out in full is:

$$K(8) = V(9, 9) \cdot P(9, 8) + V(9, 10) \cdot P(10, 8) + V(9, 11) \cdot P(11, 8) + V(9, 12) \cdot P(12, 8) \quad (19)$$

The P values appearing here express the effect of $A(8)$ on the non-uniform samples in the group $B(9)$ to $B(12)$.

These P values will in general increase as t_E is increased from $4T$. When $t_E = 6T$, these P values themselves will be small, but it has already been shown that in this region the P matrix used in the computation is ill-conditioned, and hence the V matrix will contain very large coefficients. In fact, for $t_E = 6.5T$, $V(9, 11) = -18933$, which is comparable with the numbers in the V matrix of Table 2, and certainly very much larger than those in Table 3. This localized rise in the values of the V matrix coefficients at $t_E = 6.5T$ thus seems to overcome the small P values and causes a rise in $K(8)$ for this case, which implies large truncation errors, as suggested by the peak in the curve of Fig. 8.

The analysis of the error coefficients and the matrix determinants thus shows that for this particular non-uniform sampling pattern and for this particular 'memory filter', there exists an optimum denormalization of t_{NE} to about $10T$.

Other sampling patterns and other memory filters would require different denormalization of 'memory lengths' for best results, but the technique of examining the determinant of the P matrix and the error coefficients would again enable optimum parameters to be selected in any given case.

4 Conclusions

This paper has suggested an indirect method of using amplitude samples distributed non-uniformly in time. Uniform samples of the signal are passed through a practical, realizable low-pass filter and the output of this filter is sampled in a non-uniform manner. These samples are then used for whatever purpose they are required (e.g. for transmission over a communications channel) and are then converted back to the uniform samples using the known impulse response characteristics of the filter. Recovery of the signal from these uniform samples is then simply achieved by low-pass filtering in the classical manner. One particular non-uniform sample distribution which could have a possible practical application has been analysed in detail in order to illustrate the various sources of error inherent in the process.

Cumulative errors carried on from sample to sample can be avoided with certain types of sampling pattern. There remain, however, two other sources of error. The first is truncation error due to the assumption that the impulse response of the filter is of finite duration; the second is error which arises in practical implementation of the scheme due to ill-conditioning of the matrix used in the conversion, leading to a demand for very high accuracy of computation. The conditions necessary for reduction of these two types of error are, to a certain extent, contradictory, but a method for seeking the optimum parameters for best signal recovery in any particular case has been outlined.

5 References

1. Schwartz, M., 'Information, Transmission, Modulation and Noise', Sect. 4 (McGraw-Hill, New York, 1959).
2. Yen, J. L., 'On non-uniform sampling of bandwidth limited signals', *IRE Trans. on Circuit Theory*, 3, pp. 251-7, December 1956.

3. Flood, J. E. and Hoskins, R. F., 'T.d.m. transmission of programme channels', *Proc. IEE*, 112, No. 8, pp. 1483-1491, August 1965.
4. Flood, J. E. and Urquhart-Pullen, D. I., 'Time compression multiplex transmission', *Proc. IEE*, 111, No. 4, p. 647, April 1964.
5. Storch, L., 'Synthesis of constant time-delay ladder networks using Bessel polynomials', *Proc. IRE*, pp. 1666-75, November 1954.
6. Kuo, F. F., 'Network Analysis and Synthesis', Chap. 13 (Wiley, New York, 1966).
7. Hartree, D. R., 'Numerical Analysis', Chap. 8 (Oxford University Press, 1962).
8. Redish, K. A., 'Introduction to Computational Methods', p. 8ff (English Universities Press, 1962).

6 Appendix 1: Discussion of Convergence

Equation (6) may be written in full:

$$A(12) = \frac{B(12)}{P(12, 12)} - A(1) \cdot \frac{P(12, 1)}{P(12, 12)} - A(2) \cdot \frac{P(12, 2)}{P(12, 12)} \dots - A(11) \cdot \frac{P(12, 11)}{P(12, 12)} \quad (20)$$

The P ratios which appear in this equation will, for the most part, be less than unity to the decaying nature of the impulse response. However, if $P(12, 12)$ represents a value on the impulse curve before that curve has reached its maximum value it is quite possible for the ratio $P(12, 11)/P(12, 12)$ to be greater than unity. This means that any error in $A(11)$ will appear magnified in $A(12)$. If, in the next stage of computation, $P(13, 12)/P(13, 13)$ is again greater than unity the error will again be increased when it appears in $A(13)$.

If this process is allowed to continue the errors will clearly become very large indeed. It is important to see, therefore, that the non-uniform samples are distributed in such a way that the final P ratio will, on the whole, be less than unity. An occasional departure from this rule can be tolerated as it will then cause only a temporary increase in error.

7 Appendix 2: Requirements for the Existence of an Inverse of the P Matrix

A filter with a first-order transmission function has an impulse response which can be expressed as

$$P(t) = \exp(-at) \quad (21)$$

If an impulse of weight X is incident at the input of such a filter at time t_1 , the output of the filter at any time $t > t_1$ is given by

$$S(t) = X \exp[-a(t-t_1)] \quad (22)$$

The magnitude of X can be determined by sampling $S(t)$ at any instant (e.g. t_2) after the occurrence of X . The value of $S(t)$ at time t_2 is Z which is given by

$$Z = X \exp[-a(t_2-t_1)] \quad (23)$$

From a knowledge of times t_1 and t_2 the magnitude of X can be determined

$$X = \frac{Z}{\exp[-a(t_2-t_1)]} \quad (24)$$

If two different impulses of different magnitude X_1 and

X_2 are incident at the filter input at times t_1 and t_2 the output of the filter is given by the superposition of the outputs due to the individual impulses.

If the output signal of the filter is sampled at times t_3 and t_4 these samples can be expressed in terms of X_1 and X_2 by equation (25):

$$\begin{bmatrix} Z_1 \\ Z_2 \end{bmatrix} = \begin{bmatrix} C_{11} & C_{12} \\ C_{21} & C_{22} \end{bmatrix} \cdot \begin{bmatrix} X_1 \\ X_2 \end{bmatrix} \quad (25)$$

where

$$C_{11} = \exp[-a(t_3 - t_1)] \quad C_{12} = \exp[-a(t_3 - t_2)]$$

$$C_{21} = \exp[-a(t_4 - t_1)] \quad C_{22} = \exp[-a(t_4 - t_2)]$$

In order that equation (25) can be solved for X_1 and X_2 the matrix containing the exponentials must have an inverse. This requires the equations relating Z_1 and Z_2 with X_1 and X_2 to be linearly independent. If this condition is fulfilled, the matrix of equation (25) will have a non-zero determinant.

The determinant of the matrix is given as

$$D = C_{11} \cdot C_{22} - C_{21} \cdot C_{12} \quad (26)$$

which becomes

$$D = \exp[-a(t_3 + t_4 - t_2 - t_1)] - \exp[-a(t_3 + t_4 - t_1 - t_2)] \quad (27)$$

i.e. $D = 0$ independent of the values t_1, t_2, t_3 and t_4 . This implies that two independent equations relating input and output cannot be derived for a first-order network. A network with a second-order impulse response can be expressed in the most general way as

$$P(t) = \exp(-at) + B \exp(-bt). \quad (28)$$

If the second-order network is given the same inputs X_1 and X_2 occurring at times t_1 and t_2 and samples of the output Z_1 and Z_2 are taken at times t_3 and t_4 , the relationship between input and output can once again be expressed as equation (25) where

$$\begin{aligned} C_{11} &= \exp[-a(t_3 - t_1)] + B \exp[-b(t_3 - t_1)] \\ C_{12} &= \exp[-a(t_3 - t_2)] + B \exp[-b(t_3 - t_2)] \\ C_{21} &= \exp[-a(t_4 - t_1)] + B \exp[-b(t_4 - t_1)] \\ C_{22} &= \exp[-a(t_4 - t_2)] + B \exp[-b(t_4 - t_2)] \end{aligned} \quad (29)$$

The determinant in this case is given by

$$D = B \{ \exp[-a(t_3 - t_1) - b(t_4 - t_2)] + \exp[-a(t_4 - t_2) - b(t_3 - t_1)] - \exp[-a(t_4 - t_1) - b(t_3 - t_2)] - \exp[-a(t_3 - t_2) - b(t_4 - t_1)] \} \quad (30)$$

$D = 0$ when $a = b$ or when $B = 0$ or when $t_1 = t_2$ or when $t_3 = t_4$. Hence provided $B \neq 0$ and $a \neq b$ the determinant will have a non-zero value if $t_1 \neq t_2$ and $t_3 \neq t_4$.

This means that, for a second-order system, two linearly independent equations relating input and output can be derived, subject to the conditions given above. For a second-order system the conditions $B \neq 0$ and $a \neq b$ are automatically fulfilled by definition. The conditions $t_1 \neq t_2$ and $t_3 \neq t_4$ are trivial since independent impulses occur at different times and also the output is sampled at two different instants.

It has been shown for a first-order system that only one equation relating input and output can be derived. This can be increased to two equations when the network is a second-order one. It would therefore seem reasonable to assume that for an n th-order system the maximum number of linearly independent equations relating input and output is restricted to n .

No formal proof of this generalized statement was attempted as the analysis for networks with transmission functions of higher order than two becomes extremely tedious. However, computer results have shown that if a matrix of order $(n+1) \times (n+1)$ is derived from a polynomial of order n , then this matrix is singular. This was shown to be the case for values of n up to 5. Thus, observations suggest that the proof given for the first and second-order case applies to n th-order systems also.

Manuscript first received by the Institution on 10th April 1973, in revised form on 2nd November 1973 and in final form on 5th March 1974. (Paper No. 1604/Com. 98.)

Thick film techniques for hybrid integrated microwave circuits

W. FUNK*

and

W. SCHILZ, Dr. rer. nat.*

Based on a paper presented at the IERE Conference on Hybrid Microelectronics held in Canterbury on 25th to 27th September 1973

SUMMARY

The applicability of thick film technique has been investigated for frequencies above 1 GHz. By using a special technique (direct metal foil screens) integrated microwave circuits for frequencies up to 10 GHz have been fabricated. The special requirements for microwave thick film circuits are discussed and the electrical and technological properties of three selected microwave circuits are reported in detail.

* Philips Forschungslaboratorium Hamburg GmbH, 2 Hamburg 54, Germany.

1 Introduction

The application of hybrid integration techniques, both thick film and thin film is a well-established method in the v.h.f. and u.h.f. range. The microwave integrated circuit (m.i.c.) which has been recently developed can be thought of as an extension of this technology to the higher frequency bands and for many applications replaces the commonly used waveguide and stripline technique. It makes use of the microstrip transmission line, which consists of a narrow conductor, evaporated onto a dielectric substrate with high dielectric constant, such as alumina, ferrite or boron nitride. The back of the substrate is metallized (see Fig. 1). The microwave travels along this microstrip and the main part of the r.f. field is concentrated in the substrate beneath the strip. Due to the high dielectric constant, the wavelength of microwaves is remarkably reduced, thus allowing miniaturization of microwave components.

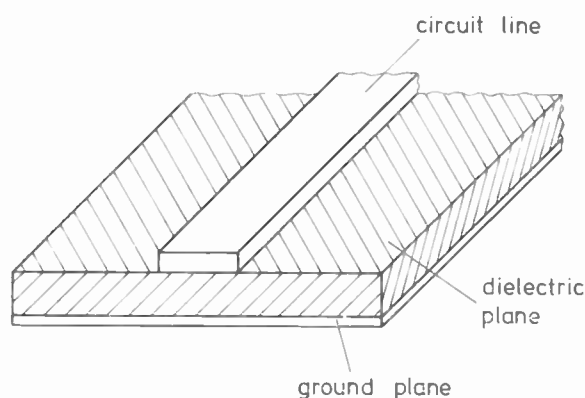


Fig. 1. The microstrip transmission line.

These components, for example, couplers, filters, resonators, mixers, power splitters, etc., are realized by combining sections of transmission lines having well-defined lengths and impedances. In this technique several components can be placed on a single substrate forming a very compact microwave sub-system. Since it is a planar technology, it is well suited for low price mass production. Furthermore due to the small size of microstrip these passive components are compatible with microwave semiconductors—Gunn diodes, mixer diodes, p.i.n. diodes—which can be favourably incorporated into the microstrip sub-system by thermo-compression bonding or soldering techniques. Three examples of microstrip sub-systems are shown in Fig. 2. In these cases a non-magnetic ferrite is used as a substrate.

The performance of m.i.c.s is determined by the electrical (dielectrical constant, losses) and mechanical (surface polish) properties of the substrate and by the conductivity and accuracy of the microstrip lines. Since the r.f. current in the microstrip is concentrated near the edges a good edge definition is required. All these requirements are higher when frequency is increased. The microstrip technique can be used for frequencies up to at least 50 GHz.

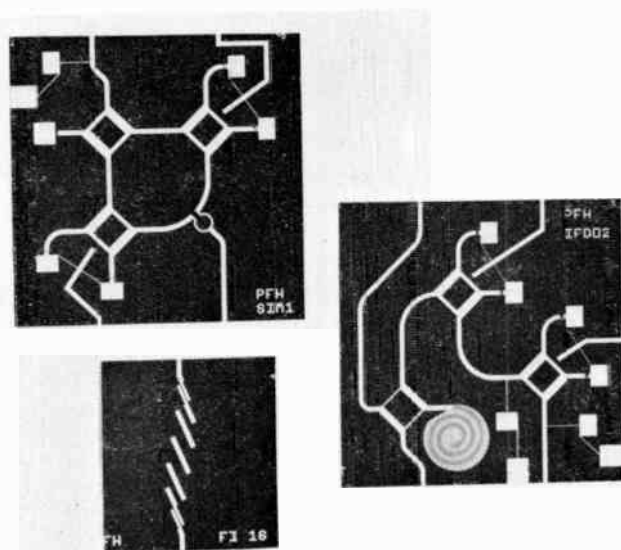


Fig. 2. Examples of microwave integrated circuits.

Usually the thin film technique is applied for the fabrication of m.i.c.s. As compared with this rather complicated and expensive technology, the thick film technique offers the possibility of a low cost mass production of m.i.c.s, if it can fulfil the requirements of m.i.c.s with respect to accuracy and losses. This has been investigated by several authors¹⁻³ and it was found, that at least for frequencies up to 12 GHz the performance of thick film transmission lines is comparable with the thin film counterpart.

Furthermore, thick film has the advantage of an extremely good adhesion both on Al_2O_3 and on polished ferrite substrates. The availability of thick film pastes of different conductivity and resistivity and of insulating materials allows the design of a variety of new m.i.c. components. We will now first discuss the special processing of m.i.c. thick film and then discuss in detail three selected microwave components which demonstrate the advantages of the thick film technique.

2 Microstrip Lines

The width of microstrip lines usually ranges from 0.03 to 0.6 mm. A suitable electrical performance is obtained when the deviations of the strip width are less than 10%. To meet these requirements high demands are imposed on the screen printing technique and the pastes employed. The necessary sharp line definition can be obtained with direct metal foil screens; only such screens produce the required results. A copper beryllium foil 45 μm thick is etched 35 μm deep from one side with the pattern and 10 μm deep from the other side with a screen configuration similar to a 325 mesh screen. The holes of the screen should be accurately aligned to the pattern as seen in Fig. 3. Also the hole-to-wire ratio has to be distributed uniformly over the whole pattern. Bent conductors or spiral coils in particular require such a distribution. On-contact printing is necessary for direct metal foil screens so that a precise

and accurately adjustable screenprinter is required. We have used a slightly modified Aremco Model 3100 printer. A soft squeegee blade is useful; the squeegee pressure and the distance between the screen and the substrate should be adjusted so that a few microns snap-off remains.

The main property required of the pastes to realize low-loss lines is a high conductivity, thus restricting the choice to gold or silver pastes. The viscosity has to be pseudo-plastic, so that the printed line will exhibit sharp edges without flow. We have achieved good results using gold pastes EMCA 282 and ESL 8831 and 8835. The optimum firing temperature for these pastes is 1000°C. No degradation of the polished substrate surfaces was observed after firing both for Al_2O_3 and ferrite substrates. Although the structure of the screen, through the pseudo-plastic viscosity, causes a rough surface, the skin effect will be essentially undisturbed because the pattern-to-screen ratio of 35 to 10 μm in the metal foil makes the roughness small on the conductor line. For some applications a better conductivity is necessary. This can be achieved by overprinting the fired conductors with pure gold. The very precise screen printer allowed quadruple overprinting, resulting in a conductor thickness of 60 μm fired. Such a conductor is shown in Fig. 4; this is a flat coil used for fast modulation of YIG filters and oscillators. The thick film version results in an extremely high mechanical stability as well as good heat dissipation.

Also pastes with low conductivity such as PdAg offer advantages for r.f. shielding in m.i.c.s and as solder pads. Gold cannot be used because of its extensive diffusion into solder. Solder materials containing gold have high melting temperatures and are expensive, so they are not recommended. The possibility of printing resistors and capacitors in thick film is another advantage. Using resistor inks currently on the market the requirements for T-networks, attenuators and inductorless dummy loads can be fulfilled. The right choice of the dielectric materials enables capacitors to be printed with a sufficiently high Q -value also at microwave frequencies.

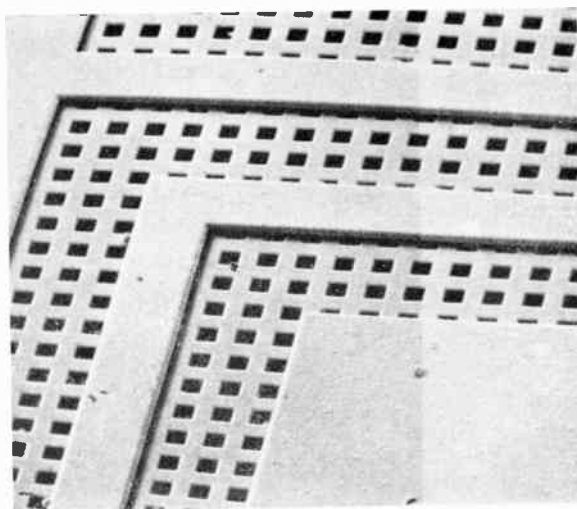


Fig. 3. REM-photograph of a direct metal foil screen.

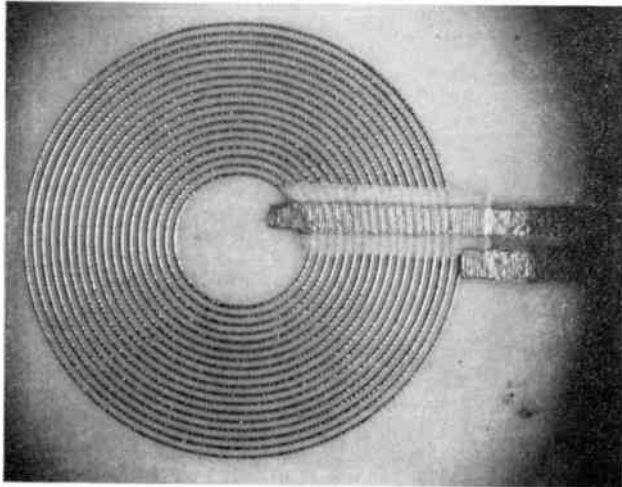


Fig. 4. Flat coil on alumina substrate.

3 Examples of Thick Film M.I.C.s

As examples of thick film m.i.c.s that we have fabricated we will now discuss a meander-line phase shifter, a proximity coupler—both operating at X-band—and the integrated part of a phase-locked-loop system, operating at 3 GHz.

The use of electronically-controlled phase shifters in so-called phased arrays is of increasing interest in radar systems in order to replace the mechanically-moved scanning antenna by an electronically-scanned array which is very fast and can be controlled by a computer. In such arrays large numbers of phase shifters are needed, typically 10^4 . This makes clear that low cost and good reproducibility are essential conditions for the introduction of these advanced systems. Besides the waveguide phase shifter—which is too bulky for many applications—and the p-i-n-diode phase shifter, the planar ferrite phase shifter is an interesting device. This component has been investigated in our laboratory and a miniaturized working model for digital phase shift operation is shown in

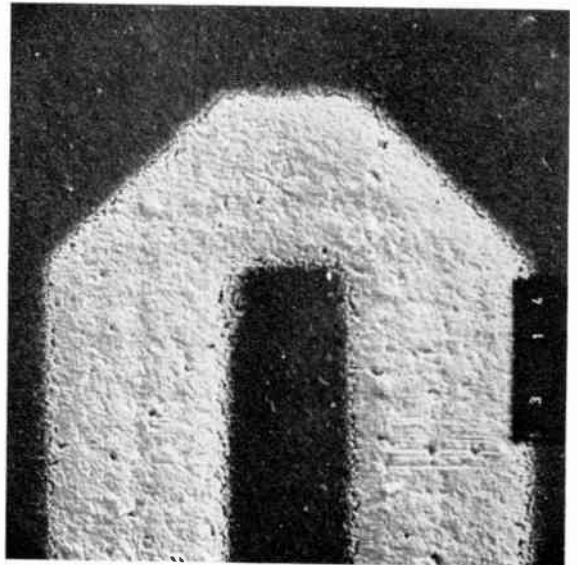


Fig. 6. R.e.m.-photograph of one bend of the printed meander.

Fig. 5. We will here only consider the microstrip part, the meander-line conductor which is placed on a non-magnetic ferrite or an Al_2O_3 substrate. This part has been made in thick film with only 10–15% increase of losses as compared with the thin film counterpart. High accuracy of the bends of the meander and narrow slots between adjacent strips are required. The obtained accuracy can be seen from the enlarged section photograph in Fig. 6.

One disadvantage of m.i.c.s is the relatively low power handling capability. Especially at high peak powers, which are often used in radar systems, the power is limited by sparking between adjacent conductors. The onset of this sparking can be shifted to higher levels when the microstrip is overprinted with a dielectric layer, which reduces the peak field strength at the sharp edges of the microstrip lines. This has been applied for a meander-line ferrite phase shifter. The structure was

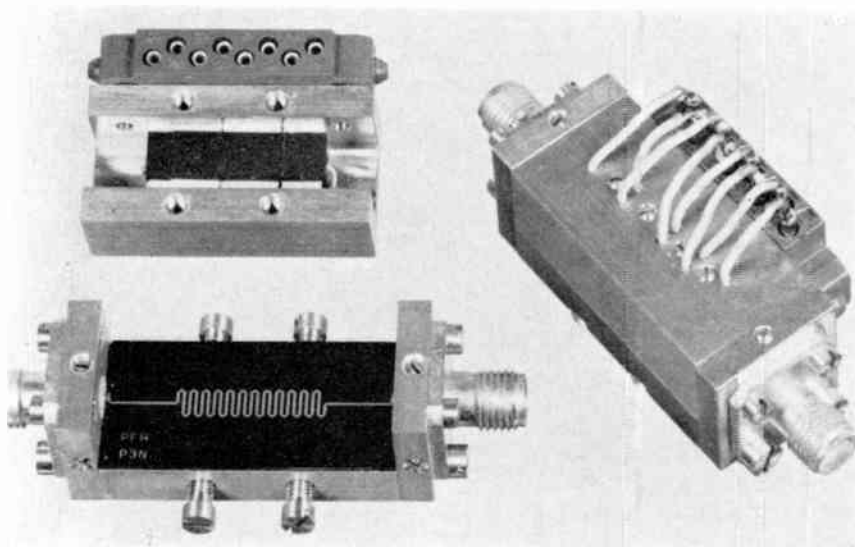


Fig. 5. Meander-line latching ferrite phase shifter operating at 10 GHz.

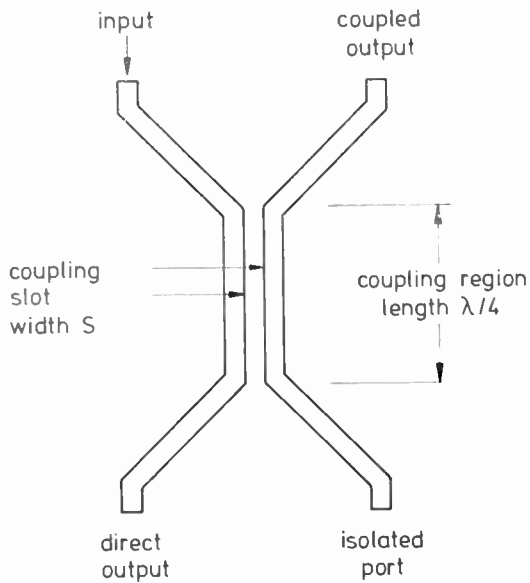


Fig. 7. Principle of the design of a proximity coupler.

overprinted with a 50 μm thick dielectric layer of ESL 4608 paste with a dielectric constant $\epsilon_r = 10$. The onset of sparking was shifted to at least 10 kW peak power at 10 GHz as compared with 1 kW in the open microstrip case. No increase of attenuation due to the dielectric could be measured.

Most microstrip sub-systems contain couplers in order to combine two signals or to split one signal into two or more output branches with different phase (0°, 90°, 180°) and different power ratio (20 dB ... 3 dB). The fundamental coupler types in m.i.c. are the hybrid ring, the rat-race, and the proximity coupler. The proximity coupler—its principle of design is shown in Fig. 7—is of special interest for the following reasons:

- (i) it can be made to work over a relatively broad band,
- (ii) matching and directivity are frequency independent,
- (iii) the power splitting ratio can be varied over a wide range.

The coupling to the two output arms is determined mainly by the distance between the two microstrips in the coupling region. High coupling requires very narrow slots and therefore the 3 dB coupler (equal power at both output ports) cannot be realized in a pure planar technique. One possibility to overcome this difficulty is to apply overlay technique, that is to increase the coupling by a partial overlapping of the two microstrips in the coupling region. The two strips are then separated by a thin insulating foil. This however requires a rather complex technology in thin film technique and therefore thick film technique can be favourably used here.

We have made couplers of this kind by applying three subsequent printing processes. In the first step one microstrip is printed, then the coupling region is covered with a dielectric paste, and finally the second microstrip is printed. In this application the electric

field is concentrated in the dielectric layer and therefore the electric performance, especially the loss factor of the material, is very important. A wide range of dielectric pastes is available, fabricated by different manufacturers. We obtained also in this case best results with ESL 4608 because the dielectric constant of this paste is nearly equal to that of the substrate. The paste is fired at 1000°C and the thickness after firing, which determines the degree of coupling, was 70 μm. Since the two microstrips are on different printing screens, the coupling ratio can easily be controlled by varying the degree of overlapping.

In the example shown in Fig. 8 this effect is demonstrated. The parameter S is the distance between the adjacent strips which are 0.4 mm wide in the coupling region. A negative value of S means overlapping. With decreasing S , the power coupled to the direct output decreases and the power in the coupled output increases. As can be seen from the diagram in Fig. 8, a 3 dB coupler requires $S = -0.1$, i.e. 25% overlapping.

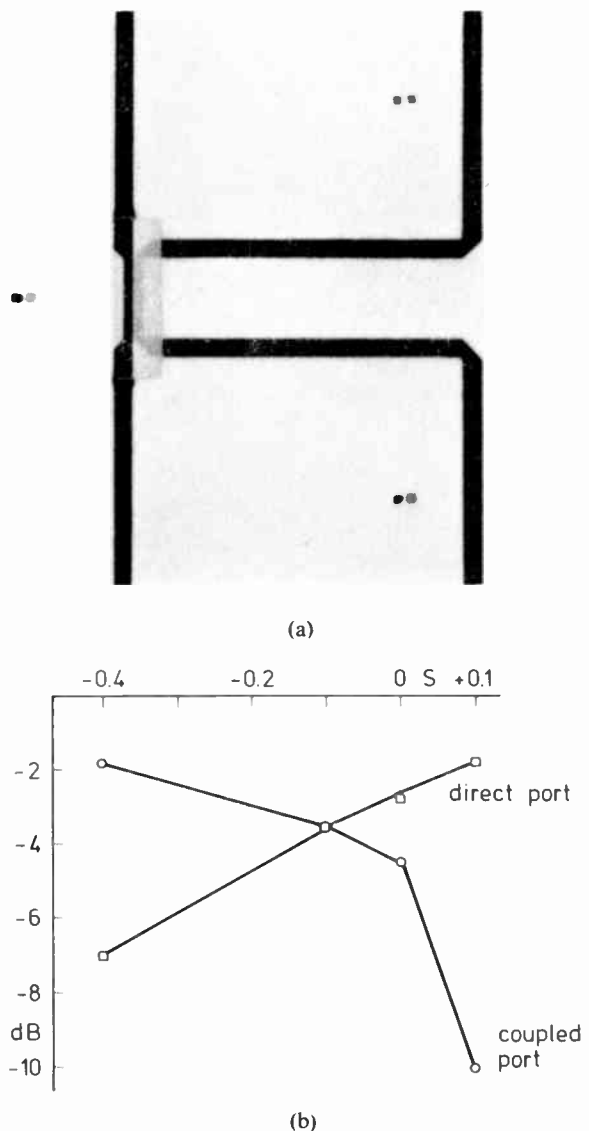
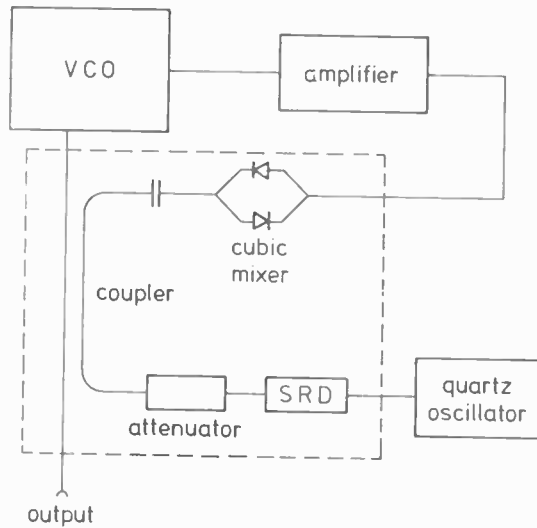
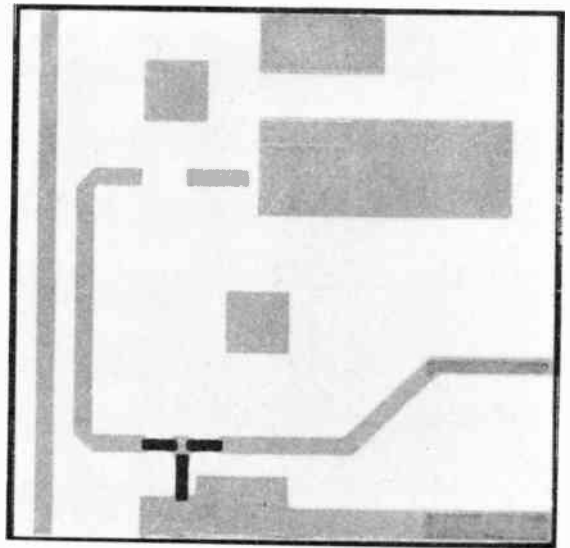


Fig. 8. Power splitting between the two output ports vs. degree of overlapping ($S = -0.4$: total overlapping).



(a) Block diagram of a phase locked loop system.



(b) Printed passive part of the system.

Fig. 9.

The insertion loss of this coupler is of the order of 1 dB, which is comparable with thin-film couplers.

Frequency stabilization of voltage controlled oscillators (v.c.o.) by phase locking is a commonly used technique also at microwave frequencies. By using harmonic mixers the multiplication network can be avoided and direct phase locking of the microwave-v.c.o. with a 50 MHz quartz oscillator can be achieved. With such a system, the block diagram of which is shown in Fig. 9, we have obtained stable operation of a 2...3 GHz v.c.o. using the 60th harmonic of a quartz. The passive part of the system (inside the broken line) comprising the step recovery diodes, the matching attenuator, the 3 GHz proximity coupler, the coupling capacitor and the cubic mixer is well suited for thick film integration. The printed chip is shown in the same Figure. To complete this circuit, bonding and soldering technique have to be applied which require the use of different thick film pastes. Furthermore the incorporation of the T-network attenuator, which is necessary for the stable operation of the step recovery diodes could easily be realized by printed resistors.

4 Conclusion

The thick film technique is applicable for microwave integrated circuits at frequencies up to at least 10 GHz,

when the slight degradation of performance as compared with thin film devices can be tolerated. In this case it offers the possibility of low-price mass production.

Independent of this consideration thick film m.i.c.s have some advantages—as our examples have shown—which favour the use of thick film technique for special microwave applications.

5 References

1. Lake, B. and O'Donnell, E. R., 'Thick film microwave components', Proceedings of the 1973 Microwave Conference, Brussels, B.6.5.
2. Woodcock, K. W. and Barnwell, P. G., 'The effect of some process and material variables on the properties of thick film microwave transmission lines', IERE Conference on Hybrid Microelectronics, Canterbury, 1973, p. 115. (IERE Conference Proceedings No. 27.)
3. Robertson, R. J. and Bainbridge, P. L., 'Low noise hybrid microwave amplifier and mixer using thick film techniques', *ibid.*, p. 139.

Manuscript first received by the Institution on 15th May 1973 and in final form on 3rd May 1974 (Paper No. 1605/CC210).

© The Institution of Electronic and Radio Engineers, 1974

Colloquium on Signal Processing in Feedback Control Systems

Middlesex Hospital Medical School,
London

2nd April 1974

Session 1. Determination and Realization of Compensation Filters

Computer-aided synthesis of compensation filters required to obtain a specified performance from a closed-loop system incorporating a given plant

By Dr. T. KONWERSKI (*University of Surrey*)

The main steps in any design process are:

- (i) Choice of the hardware the system needs, on the basis of power requirements, size and weight restrictions, availability, cost etc. The resulting hardware will be called the plant.
- (ii) Identification of the plant dynamic characteristics, theoretically or by experimental measurement.
- (iii) Translation of a general specification of the performance required from the system into a set of usable performance indices.
- (iv) Design or synthesis of compensation filters which must be used with the plant in order to obtain a system whose performance satisfies the indices.

In the method presented, system performance is specified by seven commonly used indices, four relating to the transient response, and three to the frequency response. Systems are characterized by four parameters plus the asymptotic slope of their frequency response (or pole-over-zero excess); from this the corresponding transfer function is found in a straightforward manner. The constraint of the pole-over-zero excess of the plant is introduced at the outset, ensuring that any compensation calculated by the method does not call for physically unrealizable networks with an excess of zeros in their transfer functions.

Compensation filter design via low-order modelling

By Lt. Cdr. M. J. ASHWORTH, RN (*Royal Naval Engineering College*)

It is well known that high-order complex systems can be adequately modelled by low-order transfer functions and, in particular, for many systems, dynamic performance may be matched using a zero velocity lag coefficient plane model. In

This one-day colloquium organized by the Institution's Automation and Control Systems Group Committee drew an attendance of some 80 engineers from industry, universities, the Services, and Government departments. The session chairmen were Professor D. R. Towill (UWIST), Mr. D. E. O'N. Waddington (Marconi Instruments), Cdr. D. J. Kenner RN (Ret.), (Redbridge Technical College), and Mr. M. T. Challenger (Smith's Industries). The call for papers for the colloquium was so over-subscribed that a second colloquium, this time to be held in conjunction with the IERE Communication Group, is planned for the near future.

practice, it is found that irrespective of the initial design technique used, the model coefficients lie within a small region of the coefficient plane. A computer-aided design procedure based on this model has been developed to determine the compensation filter required for a given plant transfer function. In theory, for a high-order plant transfer function, the compensation filter will also be of high order. However, the paper showed that a simple low-order model of the exact filter satisfactorily compensates the system in achieving the desired performance. The low-order filter model is derived using a constrained least squares error curve fit algorithm based on the Sanathanan and Koerner iterative extension of Levy's method.

Digital realization of linear and parametric networks

By F. G. A. COUPE and Dr. J. I. SEWELL (*University of Hull*)

Investigation into the design of a digital machine to realize an N -port active network is currently yielding some intriguing results. This technique is applicable to networks of a great variety including, in particular, linear and parametric systems. The digital implementation enables the control of parameters in a much less restricted way than in conventional analogue circuits. The range of variation of parameters covers elements of both polarities. One typical example is a digital gyrator producing a truly time-varying reactance, which leads to a tunable parametric filter. The machine can be computer controlled, which is useful in the field of adaptive equalizers and filters. Analogue or previously digitized signals can be manipulated with equal ease. As the investigation is into an N -port machine, a tunable digital N -port parametric filter is a final possibility.

Session 2. Process Control Applications

Signal adaptive three-term controller for Culham High Energy Laboratory thermo-nuclear CLEO experiment

By P. ATKINSON and A. J. ALLEN (*University of Reading*)

In order to contain the plasma in a toroid for the CLEO stellerator experiments, it is necessary to produce an accurately timed current pulse of up to 12 000 amperes in an inductive helical winding. The desired accuracy of $\pm 0.2\%$ is to be achieved in spite of winding resistance increase of 12% due to the 0.5 second current pulse which also causes a 4% reduction of generator speed. The generator and load can be approximately described by a second-order differential equation, and so the control problem appears trivial. In

order to meet the steady-state 'flat top' specification it is shown that a three-term controller is required. However, to cope with the initial transient specification, a local feedback loop with signal-controlled non-linearities is also essential. Digital computer studies of the linearized system were employed to produce an initial design for the controller. The complete system was then simulated on an analogue computer with parallel logic facilities and the optimum non-linear parameters determined. The controller has been tested using the actual s.c.r. power amplifier and generator with a simulated load. The overall system was fully tested in March 1974 when the helical winding was finally assembled on site at Culham.

The Design of an adaptive filter for use in process control

By Dr. R. J. SMITH-SAVILLE (*Cambridge Consultants*)

The principles of non-contact velocity measurement by laser Doppler techniques were reviewed briefly, and the application of such techniques to length measurement by velocity integration was discussed with particular reference to process control. An instrument using these techniques suitable for control applications must be capable of adapting both to signal amplitude and frequency and must be designed to measure the frequency of intermittent narrow band noise-like signals with maximum statistical accuracy. The design of a frequency tracking adaptive filter which meets these requirements was described, and incorporates a broad band preamplifier with automatic gain control for signal normalization. This is followed by a tracking homodyne filter which is tuned by a local oscillator. This oscillator in turn is automatically tuned to the same frequency as the input signal by a first order feedback loop incorporating a novel wideband frequency discriminator. Because the frequency tracking errors in this system are very small, direct integration of the frequency of this oscillator may be used for length measurement. Finally alternative techniques of interfacing this processor with control systems requiring length measurement were discussed.

Session 3. Servomechanism Applications

Hardware design of adaptive digital filters using L.S.I. and TTL chips

By Dr. D. R. WILSON, D. F. NEALE and M. BURL (*Polytechnic of Central London*)

Hardware required for the construction of digital filters is considerable and two methods were outlined: (1) special-purpose l.s.i. and (2) TTL (m.s.i./s.s.i.) logic. Special-purpose l.s.i. circuits offer the advantages of requiring only a small number of chips. However, the external hardware is significant and includes the provision of a four-phase clocking signal, two ladder networks and amplifiers for the analogue/digital converter, and a number of supply voltages and interface circuits. Circuit details were described, including the functional components of the filter:

- (a) multipliers
- (b) converter unit
- (c) shift register adder
- (d) external l.s.i. hardware, and examples of servo signal processing circuits presented.

Adaptive series compensation of stable platform

By Lt. Cdr. R. WILSON, RN (*ASWE*)

This paper illustrated the basic gimbal system for a shipborne two-axis stable platform for a large surveillance radar antenna. The design of the linear actuators and the general drive configuration were also illustrated. The antenna presents a time-varying inertial load to the gimbal axes as it rotates in the azimuth plane; this effect is shown in the predicted rate loop response in the form of a moving resonance and anti-resonance. From the drive transfer function with the load outside the measurement transducer, the significance of the resonance in the position loop is evident. An adaptive digital notch filter was proposed as a series compensator.

Session 4. Transportation Applications

Design and assessment of signal processing filters for adaptive, automatic control of aircraft

By R. G. HARRISON (*A & AEE Engineering, formerly BAC*)

In this paper, a study was made of the design and assessment of signal processing filters for adaptive, automatic control of aircraft. These comprise:

- (i) An optimal feedback controller to minimize touchdown dispersion and maximize passenger comfort.
- (ii) A state estimator to learn the current value of state with unknown initial conditions. This is to allow the pilot to make arbitrary, initial beam joining manoeuvres.
- (iii) Error signal observability to ensure error signal detection whose processing provides future adaptive control. This is to combat sensor noises, deterministic and random with incomplete statistics, and low-altitude gusting.
- (iv) A Bayes detector to identify a class of unknown signals. The covariance of the input error signal to the Bayes changes with time when the entire system is providing adaptation. For a constant probability of detection error, the time-varying covariance leads to an adaptive system, Bayes within an adaptive system.
- (v) An analogue feedback algorithm which combines the Bayes output and the filter gains of the estimator to provide stable, adaptive control.

The study included both theoretical and experimental results and an assessment of the controlled aircraft performance under worst case conditions.

The use of a discrete Kalman-Bucy filter to estimate the misalignment angles of a ship's inertial navigation system at sea

By Dr. M. HEALEY (*University College, Cardiff*)

The position of a ship is determined, using SINS, by double integration of two orthogonally mounted accelerometers, pointing due North and East. A failure at sea means that the SINS must be realigned to 'point North'. In harbour the two accelerometer outputs are due entirely to misalignment, but at sea they are due to misalignment plus ships manoeuvres. A filter is therefore required to extract the misalignment data, which is in practice much smaller than the manoeuvring data. Misalignment equations were presented as a problem in stochastic control and the results of using a Kalman-Bucy filter to estimate the misalignment shown. The algorithm for the control computer was stated and the plausibility of using such a complex signal processor discussed.

IERE

News and Commentary

Visitors to Bedford Square from Overseas

Professor Harold W. Shipton (Fellow) who was in England during a European tour earlier this year, is Director of the Bioengineering Resource Facility in the College of Medicine of the University of Iowa. Professor Shipton will be known to many members particularly for his work on electro-physiological display techniques while at the Burden Neurological Institute where he was for some eight years before going to Iowa in 1957.

Professor A. N. Daw, M.Sc., D.Phil. (Member) was warmly welcomed at the Institution during his recent visit to London. Professor Daw has been a member of the Institution's Indian Advisory Council for many years and more recently was made Honorary Treasurer of the Indian Division. He is the author of several text books and a member of the Science and Engineering Faculty of the University of Calcutta.

In discussing education and engineering standards he related that in this present year the University of Calcutta has set examinations for over 300,000 undergraduates and examined theses and other engineering work of no less than 15,000 postgraduates. The majority of those examinees were concerned with the humanities and social services.

Lord Blackett and Dr. Vannevar Bush

Within a fortnight, in July last, the deaths were reported of two eminent scientists, one American and the other English, who both contributed in considerable measure to the scientific direction of the Second World War.

Lord Blackett, who was a former President of the Royal Society, is probably best known for his original work on the design of large cloud chambers for cosmic ray research which he started while at the Cavendish Laboratory, continued at Birkbeck College and subsequently took to Manchester University, where he was Langworthy Professor of Physics from 1937 to 1953. This work ultimately led to his being awarded the Nobel Prize for Physics in 1948 which was specifically linked to his discovery of the positive electron fifteen years earlier.

During the war years, as Professor P. M. S. Blackett, he developed the new science of operational research and he later took an active part, as an elder statesman of science, in the controversies associated with the military and civil applications of nuclear physics.

Dr. Vannevar Bush was President Roosevelt's chief scientific adviser during the Second World War and he was closely associated with the development of the atomic bomb.

To members of this Institution, however, he will be most familiar for his work leading to the modern electronic computer which he carried out in the early 1940s and the possibilities of which were first disclosed, in this country, by Lord Mountbatten in his first presidential address in 1946.

BUPA Group for IERE Members

We would like to remind members that the Institution operates a Group Scheme with BUPA, so as to help members who, in the event of illness, would like to have private treatment for themselves and their families. Group membership enables a member to obtain a rebate of 10% on the basic rate of subscription, plus immediate cover upon acceptance instead of the usual three months' waiting period.

Present members of the IERE Group are advised by BUPA to re-examine their level of cover before their annual renewal date in view of the recent increases in Hospital charges. For a London Teaching Hospital the private accommodation charge is £172.90 per week while a Provincial Teaching Hospital charge for accommodation is £145.60 per week.

There are two schemes which are currently operated by BUPA which are also available to members. The World Wide Travel Scheme provides up to £1000 for medical expenses incurred abroad, for only £1.50 for 16 days. This scheme has an optional extra in that for an additional 80p one can have cover for loss of baggage, money deposits and personal liability in the case of accident.

The Medical Centre in King's Cross, London, provides facilities for complete health checks. Subscribers of the Group may avail themselves of a complete screening at this unique fully automated clinic for a specially reduced fee.

Further details for joining BUPA or any of the extra schemes may be obtained from Mr. D. R. Andrews, Branch Manager, BUPA (IERE Group), 24 Newport Road, Cardiff CF2 1SF. (Telephone Cardiff (0222) 44851).

Plan to attract Indian Scientists to return

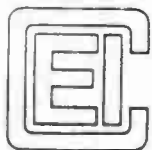
The Indian Government has approved a scheme prepared by the Council of Scientific and Industrial Research to attract Indian scientists, technologists and engineers currently employed in responsible positions in research and development and manufacturing establishments in foreign countries.

This scheme would promote the return to India of those scientists, engineers and technologists who have completed their studies or research abroad and have taken up jobs in production departments or management positions in industrial firms abroad owing to lack of employment opportunities in India.

The facilities offered under this scheme would be: first, scientists or technologists who are abroad will be permitted to keep the foreign exchange earned by them in their foreign bank account for a period of three years instead of 30 days; secondly, permission will be given to use this foreign exchange for importing equipment, machinery, capital goods and raw material; thirdly, a simplified procedure will be adopted for licensing, capital goods, clearance, and issue of an import licence.

CSIR will set up a bureau to offer advice to the scientist or technologist returning from abroad to match his skills with the local market needs and facilities. Financial institutions will be requested to extend their present facilities to include entrepreneurial loans on special terms. CSIR will be the implementing agency to the scheme.

Indian scientists abroad may contact the appropriate Indian Embassy or the Chief (Technology Utilization) CSIR in Delhi for further details for processing their proposals.



Notes and News for Members

Election of Chairman and Vice-Chairman of CEI for 1975-76

At CEI's Board Meeting on 25th July the Chairman, Sir Leonard Atkinson, put forward nominations to the Board for Chairman and Vice-Chairman of CEI to take office with effect from the Annual Meeting in January 1975. This followed his consultations with the Presidents of Constituent Members.

The nomination for Chairman was Professor J. F. Coales (CEI's present Vice-Chairman) and that for Vice-Chairman, Mr. G. A. Dummett, a past President of the Institution of Chemical Engineers. The election of both was agreed unanimously.

Professor John Flavell Coales, C.B.E., M.A., Hon.D.Sc., C.Eng., F.I.C.E., F.I.E.E., F.R.S., is Professor of Engineering (Control), University of Cambridge. His industrial experience includes that of research director with Elliot Bros. (London) Ltd. and as a consultant on research and development, particularly in the field of control and automation, to a large number of industrial groups. He was a member of the R & D Board of Tube Investments Limited from 1957-1961 and Deputy Chairman of the Governing Body of B.S.A. Group Research Centre from 1967 to 1971. Professor Coales was elected to Fellowship of the Royal Society in 1971 and was President of the IEE for 1971-72.

Mr. George Anthony Dummett, M.A., C.Eng., F.I.Chem.E., has extensive experience in the chemical engineering industry, notably as Deputy Managing Director of A.P.V. Co. Ltd. and as a director of various other companies. A former Board Member of CEI, Mr. Dummett was President of the Institution of Chemical Engineers for 1968-69 and is Chairman of its Overseas Committee. Last year he became the Chairman of the British National Committee for FEANI—the federation of professional engineering institutions in Europe—and in 1972 was elected Chairman of the European Federation of Chemical Engineers.

CEI Local Committee for S.E. England

The Council of Engineering Institutions has established a new Local Committee to serve Kent and Sussex, to be known as the CEI Kent and Sussex Committee. The Chairman of the new Committee is Mr. R. G. Mattocks, C.Eng., F.I.E.E., Tokai-so, Madeira Road, Littlestone, Kent, and the Hon. Secretary is Mr. F. J. Halligey, C.Eng., F.I.Mech.E., M.I.E.E., 44 Senlac Way, St. Leonards-on-Sea, Sussex TN37 7JG.

This brings the number of CEI Local Committees so far formed up to fifteen, in addition to five CEI Junior Committees which operate in the interests of graduates and students admitted to membership of Constituent Member institutions or societies.

In broad terms, the function of a CEI Local Committee is to co-ordinate, and to stimulate interest in, the activities of the local Branches or Centres of Constituent Members in its area, and to publicise the work of the Council and its Constituent Members through relations with local authorities, educational and other local bodies, and the Press.

New Executive Committee

The Composition of CEI's new Executive Committee was confirmed, as follows, by the Board at its meeting on 25th July. The new Executive will hold its first meeting on 24th October.

CEI OFFICERS

Sir Leonard Atkinson	Chairman of CEI and Chairman of Executive.
Professor J. F. Coales	Vice-Chairman of CEI.
Sir Angus Paton	Immediate Past Chairman of CEI.

ELECTED BY THE BOARD FROM NOMINATIONS FROM ANY CONSTITUENT MEMBER

Sir Norman Rowntree
 Sir St. John Elstub
 Professor H. J. King

NOMINATED ON A GROUP BASIS

Nomination	Group
Mr. W. McClimont	Marine/Naval Architect
Mr. R. N. Bruce	Chemical/Fuel/Gas
Mr. K. Severn	Civil/Municipal/Structural
Mr. A. R. O. Williams	Mining/Mining and Metallurgy
Dr. G. S. Hislop	Aeronautical/Mechanical/ Production
Dr. P. A. Allaway	Electrical/Electronic and Radio

Joint Royal Society—CEI Education Committee

CEI has agreed to the establishment, jointly with the Royal Society, of a new committee to be officially designated the Joint Royal Society/CEI Education Committee on the Teaching in Schools of Science and Mathematics related to the needs of Engineering and Industry. This development follows meetings with the Royal Society attended by CEI's Vice-Chairman, Professor J. F. Coales. These discussions stemmed from the Royal Society's anxiety to set up a joint Education Committee with CEI so that problems relating to science teaching in schools and colleges of further education—already under review by various Royal Society joint committees in other scientific fields—could take fully into account the relevance of such problems to the future of engineering.

The committee will not be concerned with issues in the university field or other areas of tertiary education relating to engineering. Its sole concern will be with matters in schools and colleges which could affect both the supply of potential engineers and the educational attainments of those about to enter engineering courses at all levels.

The Committee, which will report to the Council of the Royal Society and the Council of Engineering Institutions, will advise on:-

- (a) Matters affecting the content and teaching arrangements in schools' and technical colleges' courses in order to create a greater awareness of the applications of science and mathematics to the needs of the engineering profession and of industry.

- (b) Associated problems at the earlier stages of polytechnic and university courses.
- (c) Problems of teacher supply and attitudes of teachers to the applications of science and mathematics.

The new Joint Committee will comprise thirteen members and two observers (from the Department of Education and Science and the Scottish Education Department). Seven members will be practising teachers and lecturers in the relevant field, drawn from a variety of different types of educational institutions. Three members will be appointed from the Royal Society, being Fellows and working in the field of engineering; and three members will be appointed to represent CEI. The Chairmanship and Vice-Chairmanship of the Committee will alternate between the Royal Society and CEI. A Royal Society nominee, Professor D. W. Holder, a Chartered Engineer and Professor of Engineering at the University of Oxford, will be the first chairman of the Committee and Professor Coales—a nominee of CEI—its Vice-Chairman.

Informal Board Meeting Discusses Professional Competence

A wide-ranging discussion on professional competence took place at a recent informal CEI Board Meeting. Chaired by Sir Leonard Atkinson, the discussion centred around the Report of ICE's Working Party on Professional Competence (Sir Kirby Laing, Chairman, Sir Norman Rowntree and Mr. A. Paterson) set up to consider whether that Institution—since it has Rules for Professional Conduct and accepts responsibility for regulating such conduct—has similar responsibility in respect of incompetence or negligence of its members.

In outlining some of the points in the Report, Sir Kirby said that it was important to distinguish between professional conduct, professional negligence and professional competence. Professional negligence occurred when an engineer failed to exercise the degree of care and skill properly to be expected of him. A breach of duty to take care could arise from causes ranging from inadequate engineering knowledge, that is to say engineering incompetence, to personality weaknesses and human failings. In cases arising from such a breach, he felt that the Institution was not equipped either to provide the forum or to decide such issues, as these involved a lengthy examination of facts and evidence and the making of value judgements on matters not easily quantified. Those injured had their remedies in the courts of law existing for that purpose.

On the other hand, he felt that the Institution had a responsibility for assisting members to acquire engineering knowledge and as such recommended that the Institution should provide guidance to its members to make them fully aware of their responsibilities for maintaining their engineering competence throughout their careers. Incompetence could stem from lack of fundamental engineering knowledge, from lack of up-to-date specialized knowledge, or from insufficient practice and inadequate experience. The means currently employed by the Institution to ensure the competence of its members were, firstly, by regulating through CEI the academic standards of the Associate Member [Graduate member in IERE] and through recognized training controlling the practical qualifications of the young engineer. At the Professional Interview the candidate was judged and admitted to membership if thought competent. Secondly, the Institution encouraged members at large to keep abreast of technological advances by attendance at meetings, informal discussions, conferences and so on; and by publishing technical papers and promoting and recommending courses of mid-career training.

Sir Kirby pointed out that the Report referred to the fact that at no stage after the Professional Interview did the Institution concern itself with the continuing competence of its members individually and that it had gone on to say that 'we believe that it should do so in the public interest'. Additionally, the Report had recommended that when considering applications for transfer from Member to Fellow the Membership Committee should have regard to the steps taken by candidates to benefit from mid-career training.

Guidelines suggested by the Report which should apply to all members whether self-employed, employers or employees, were that: (1) It is the responsibility of a member to keep up-to-date his knowledge in those fields of engineering in which he is engaged so that he may maintain his competence in those fields. (2) It is the responsibility of a member before undertaking work in fields of engineering beyond his knowledge and experience to obtain competent advice or appropriate knowledge. (3) It is the responsibility of a member to ensure that sufficient attention can be given to all work carried out under his charge.

The Report had concluded by pointing out that the ability of a member to maintain his competence is dependent not only on his own efforts but on the extent to which new knowledge can be made available to him. There are therefore parallel responsibilities falling on education and training authorities and the learned societies to be aware of needs and to make reasonable efforts to meet those needs. At a time of rapidly changing technology the cooperation of employers will also be needed as adult education and mid-career training become increasingly important as means by which a member can respond to the Guidelines.

A variety of views were expressed by Board members on these matters when the meeting was opened up for discussion. Some members emphasized the great value that could be gained to industry, as well as by the profession itself, in actively encouraging their engineers to attend courses and symposia through which they could update their knowledge of technological developments. While this was already done by some firms, others especially the smaller ones, were sometimes reluctant or found it difficult to release staff for this purpose while they were otherwise engaged on current projects for their Company.

Common Engineering Qualifications

At question time in the House of Commons during June, Mrs. Linda Chalker (Cons., Wallasey) asked the Secretary of State for Industry what progress he had made in his discussions with the Council of Engineering Institutions in recognition of a common standard qualification such as that granted for the Institution of Heating and Ventilating Engineers, and if he would make a statement on the progress of harmonization of standards concerning the acceptability in Europe of the common qualification granted in the United Kingdom.

The Parliamentary Under-Secretary of State, Industry, Mr. Michael Meacher, stated in a written Parliamentary answer that no common standard qualification had yet been agreed with the Council of Engineering Institutions, which was examining a proposal put to it by his Department. There had been no directly related negotiations yet in the EEC.

CEI's Royal Charter and By-Laws

A new edition of CEI's Royal Charter and By-laws has been published. Copies can be obtained from CEI, 2 Little Smith Street, London SW1P 3DL, price 50p each.

Members' Appointments

CORPORATE MEMBERS

Mr. J. E. Betteridge (Fellow 1972, Member 1970, Graduate 1954) who has been Chief Engineer with Steering Systems Inc. of Covington, Louisiana, since last year, has been appointed Director and General Manager of the Company. He was previously Chief Engineer with the American and Canadian associated companies of Decca Radar Ltd.

Mr. N. L. Garlick, M.Sc.(Eng.) (Fellow 1966, Member 1961) who went to Brighton College of Technology (now Polytechnic) in 1963 as Head of the Department of Electrical and Electronic Engineering and has been for the past four years Dean of Student Affairs has now been appointed Assistant Director. He is a past member of the Council of the Institution and of the Examinations Committee and currently serves on the Membership Committee.

Col. I. W. Peck, RA (Fellow 1966, Member 1959) has been appointed Project Co-ordinator — Military Systems with EASAMS Ltd., Camberley.

Mr. B. E. P. Ritson (Fellow 1953, Member 1947) retired from the Telecommunications Department of the States of Jersey in August and is now a Consulting Engineer. Mr. Ritson was appointed Chief Telecommunications Engineer in 1949 following some 10 years with the Ministry of Aircraft Production and the Ministry of Civil Aviation.

Mr. G. W. Sparks, P.Eng. (Fellow 1968, Member 1951) has been appointed Manager of Defence Program Development, Aerospace and Government Systems with RCA Ltd. in Quebec. Mr. Sparks joined RCA in 1961 as Manager of the Ottawa Office following service with the RAF during the war and held appointments with various Canadian Companies between 1951 and 1961.

Mr. C. H. Vincent, Ph.D., M.Sc. (Fellow 1964) has been awarded the degree of Doctor of Science by the University of Edinburgh. Dr. Vincent is a Superintendent in the Applied Physics Department of the Atomic Weapons Research Establishment. He has recently published a book on 'Random Pulse Trains'.

Mr. W. F. Allen (Member 1973) who joined Hawker Siddeley Dynamics Ltd. in 1964 and was latterly Senior Engineer concerned with on-board computers for satellites has moved to the British Aircraft Corporation, Stevenage, as Electronics Engineer.

Wing Cdr. A. R. Atkins, RAF (Ret.) (Member 1967) whose last service appointment was Elect. Eng. 1 (RAF) at the Ministry of Defence, has been appointed a Lecturer of the Army Apprentice College at Arborfield.

Mr. R. Backhouse (Member 1973, Graduate 1969) who was a Lecturer at Salford College of Technology, has been appointed Instructor Officer in H.M.S. *Collingwood*.

Major D. E. Blenkinsop, REME (Ret.) (Member 1972) has been appointed Principal Engineer with the Department of Posts and Telecommunications, Fiji; his last service appointment was officer in charge of the Aircraft Technical Service Unit REME at the Army Aviation Centre, Middle Wallop.

Sqn. Ldr. T. Briggs, RAF (Member 1968, Graduate 1962) who has been Officer Commanding Electrical Engineering Squadron, RAF Wattisham, is now Electrical Engineering Member of the Ministry of Defence Advisory Team to the Kingdom of Saudi Arabia based in Riyadh.

Major P. C. Coderre (Member 1971, Graduate 1967) is now at the Electrical Engineering Department at the Royal Military College of Canada, Kingston, Ontario, following a staff appointment at the Headquarters of Canadian Forces Communication Command, Ottawa.

Lt. Col. G. Corden, R. Signals (Member 1974) has been posted to the NATO Integrated Communication System Management Agency in Brussels. He was previously at the National Defence College.

Mr. B. K. Curant (Member 1974) has joined Tektronix (UK) Ltd. as a Field Engineer. He was previously an Area Sales Manager with Burndept Electronics Ltd.

Mr. J. K. Draper (Member 1949, Associate 1946) is now with Magnetic Components Ltd., Farnham.

Mr. A. T. Fernandes (Member 1961) has been appointed Manager of Quality Assurance with the E.I. Company Ltd., Shannon, Ireland, which is a subsidiary of the (American) General Electric Company.

Mr. C. H. Garnett (Member 1963) has left the Meteorological Office and is now working on quality assurance in design with the Defence Quality Assurance Board Executive in the Ministry of Defence, Procurement Executive.

Mr. B. T. Graham (Member 1963), formerly Chief Electronic Engineer with Associated Automation Ltd., has joined Thorn Consumer Electronics Ltd. as Chief Television Development Engineer at the Enfield factory.

Sqn. Ldr. D. F. Grimston, RAF (Member 1971) has completed a tour of duty at RAF Gan and is now at Headquarters of 46 Group at RAF Upavon as Elect. Eng. 2.

Flt. Lt. R. M. Harrison, RAF (Member 1973, Graduate 1968) has been posted to Headquarters of RAF Germany as Elect. Eng. 2B1, following an advanced maintenance engineering course at the RAF College, Cranwell.

Mr. D. F. Hill (Member 1965) has joined Elnode Ltd. of Luton as Managing Director.

Mr. K. C. Jones, M.Phil. (Member 1971, Graduate 1961) who has been Education and Training Officer at the Institution of Electrical Engineers since 1965, has been appointed to the new post of Director of Qualifications.

Mr. F. F. Kemp (Member 1973, Graduate 1968), formerly a Senior Electronic Engineer concerned with digital circuitry development with Hawker Siddeley Dynamics Ltd. has joined the Allen Clark Research Centre of the Plessey Company as an Electronic Development Engineer.

Mr. M. G. Kervell (Member 1966, Graduate 1960) is now Chief Development Engineer of the Audio Products Division of Pye Ltd. at Stevenage.

Lt. Cdr. J. Lewcock, RN (Ret.) (Member 1973) has joined GEC Gas Turbines Ltd., Whetstone, Leicester, as Contracts Officer; for the past two years he was at the RN Aircraft Yard, Fleetlands, and responsible for forward planning of overhaul and repair of avionic equipments fitted to military helicopters.

Mr. A. M. Nurmohamed (Member 1970, Graduate 1967) who joined Elliott Brothers (London) Ltd., Rochester in 1966 as a Development Engineer, has recently been appointed a Project Manager with Marconi-Elliott Avionics Systems Ltd.

Cdr. R. Payne, RN (Ret.) (Member 1973) is now the Projects Manager in the Support Services Department of Vosper Thornycroft Ltd., Fareham; he was at H.M. Dock Yard, Portsmouth prior to his retirement.

Mr. H. J. H. Perry, B.Sc. (Member 1961) has been appointed Director of Quality Assurance and Reliability for Bio-Medical Services Inc., Fairfield, New Jersey. He was formerly Quality Control Manager, U.S. Group, for Loctite Corporation of Newington, Conn.

Mr. B. Poole (Member 1971, Graduate 1966) is in charge of a section concerned with applied research and development at the Rotherham factory of Air Products Ltd. He was previously on the staff of the Electricity Council Research Centre, Capenhurst, Chester.

Mr. M. B. Roles (Member 1970) who was with Associated Semiconductor Manufacturers Ltd., Mullard, Southampton Works as a Development Engineer, is now Lecturer in Nautical Studies at Southampton School of Navigation.

Group Capt. S. J. Stephens, RAF (Member 1959) has moved to HQ Allied Forces Central Europe, as Commander of the Regional Signals Support Group; for the past two years, he has been Command of Trade Standards Officer at the H.Q. Training Command, at RAF Brampton.

Mr. C. R. Tyner (Member 1970) has been appointed Director of the Centre for Ocean Technology at the Nova Scotia Research Foundation, Dartmouth, Nova Scotia.

NON-CORPORATE MEMBERS

Mr. A. Anastasiou (Graduate 1970) who was with International Computers Ltd. has now returned to Cyprus and is Broadcasting Engineer with the British Forces Broadcasting Service in Dhekelia.

Mr. G. W. Briton (Graduate 1971) who has been with Plessey South Africa Ltd. in Plumstead, Cape Province, for the past two years has been promoted to Senior Equipment Engineer.

Mr. R. Carpenter (Graduate 1970) has been promoted to Area Telecommunications Engineer with the Southern Electricity Board. He joined the Board in 1960 as a Craft Apprentice Fitter and has been a 4th Assistant Engineer (Telecommunications) since 1969.

Mr. J. D. Chestnutt (Graduate 1966) is now a Development Engineer with Ultra Electronics Ltd. at Greenford, Middlesex. Before joining the Company in July he was a Design Engineer with Marconi Instruments Ltd., St. Albans.

Mr. T. Davis (Graduate 1967) has been appointed Engineering Support Manager (National) with Hewlett-Packard Ltd. and is concerned with field installation and maintenance of computer and calculator systems. He was previously Regional Service Supervisor for the Company in the North of England.

Lt. W. J. Lloyd, REME (Graduate 1970) has been appointed Instructor Officer at the Army Apprentices College, Chepstow.

Mr. A. P. Newman, B.Sc., M.Sc. (Graduate 1972) has moved from the Sperry Gyroscope Division of Sperry Rand Ltd., Bracknell, where he was an Electronic Engineer, to Marconi Elliott Avionics Ltd., Rochester, as a Project Engineer in the Flight Controls Division.

Mr. B. K. Pendlebury (Graduate 1973) who was a Technical Officer with the Post Office in Manchester, has joined International Computers Ltd., West Gorton, as Computer Systems Commissioning Engineer.

Mr. R. O. Roberts, B.Sc. (Graduate 1968) has been appointed Lecturer II in Electrical Engineering at Widnes and Runcorn College of Further Education. He was previously an Assistant Lecturer at Denbighshire Technical College, Wrexham.

Mr. O. K. C. Obasi (Associate Member 1973) is now a Higher Technical Officer with the Medical Research Council of Nigeria.

Mr. V. C.-H. Hung (Associate 1969) has been appointed Engineering Manager with Sylvania Far East Ltd., Hong Kong.

Mr. L. Hassall (Associate 1972), who has been with the BBC since 1954, latterly as Acting Assistant to the Engineer-in-Charge at the Tatsfield Receiving Centre, is now On Station Instructor at the Receiving Station at Caversham Park, Reading.

Mr. C. A. Rowley (Associate 1968) has taken up the appointment of Engineering Liaison Officer with Racial Electronics (S.A.) Ltd. in Pretoria. He was previously Chief Engineer in the Broadcasting and Information Department of the Government of Swaziland.

Mr. J. N. Slater (Associate 1969) has been appointed Engineer in the Engineering Information Department of the BBC. He was previously a Schedule Engineer with BBC External Broadcasting.

Mr. W. E. Taylor (Associate 1956) who has been a Divisional Manager within the Electronics Group of Siemens Ltd. for three years, has been appointed Group Liaison Manager, Special Projects. Before joining the Company's British agents, Cole Electronics Ltd., in 1965, Mr. Taylor was Industrial Valve Product Manager with Associated Electrical Industries and from 1961 to 1965 he was Sales Manager with Rank Electronic Tubes Ltd. In 1958 he contributed a paper on Vapotron system of cooling high power valves to the Journal.

Lt. Col. M. R. C. Weiner, R. Signals (Associate 1970) has been posted to Procurement Executive of the Ministry of Defence as GSOI(W) in the *Ptarmigan* Project Office. For the past three years he was with C and E Division, HQ NORTHAG.

STANDARD FREQUENCY TRANSMISSIONS—July 1974

(Communication from the National Physical Laboratory)

July 1974	Deviation from nominal frequency in parts in 10 ¹⁰ (24-hour mean centred on 0300 UT)			Relative phase readings in microseconds NPL—Station (Readings at 1500 UT)		July 1974	Deviation from nominal frequency in parts in 10 ¹⁰ (24-hour mean centred on 0300 UT)			Relative phase readings in microseconds NPL—Station (Readings at 1500 UT)	
	GBR 16 kHz	MSF 60 kHz	Droitwich 200 kHz	*GBR 16 kHz	†MSF 60 kHz		GBR 16 kHz	MSF 60 kHz	Droitwich 200 kHz	*GBR 16 kHz	†MSF 60 kHz
1	0	0	-0.1	695	593.6	17	0	-0.1	-0.1	698	597.7
2	0	0	-0.2	695	593.9	18	0	0	0	698	597.7
3	0	+0.1	-0.1	695	593.4	19	0	+0.1	-0.1	698	597.1
4	0	0	-0.2	695	593.3	20	0	0	-0.1	698	596.7
5	—	0	-0.1	—	593.5	21	0	0	-0.1	698	596.4
6	—	-0.1	-0.1	—	594.1	22	0	0	-0.1	698	596.6
7	0	0	-0.2	695	593.9	23	0	0	-0.1	698	596.8
8	0	0	-0.2	695	594.2	24	-0.1	-0.1	-0.1	699	597.6
9	0	-0.1	-0.2	695	594.8	25	0	0	-0.1	699	597.9
10	0	0	-0.2	695	595.0	26	0	0	-0.1	699	598.0
11	-0.1	0	-0.2	696	595.2	27	0	0	-0.1	699	598.4
12	0	0	-0.1	696	595.4	28	0	0	-0.1	699	598.8
13	0	0	-0.1	696	595.6	29	0	0	-0.1	699	598.8
14	0	0	-0.1	696	595.8	30	0	0	-0.1	699	599.0
15	-0.1	-0.1	-0.1	697	596.7	31	0	0	-0.1	699	599.2
16	-0.1	0	-0.1	698	596.9						

All measurements in terms of H-P Caesium Standard No. 334, agrees with the NPL Caesium Standard to 1 part in 10¹¹.

* Relative to UTC Scale; (UTC_{NPL} - Station) = + 500 at 1500 UT 31st December 1968.

† Relative to AT Scale; (AT_{NPL} - Station) = +468.6 at 1500 UT 31st December 1968.

Letter to the Editor

The Institution's Council does not necessarily agree with views expressed by correspondents.

Correspondence of a technical nature, or on any matter of interest to electronic and radio engineers, is welcomed.

From: A. M. Sandman, C.Eng., M.I.E.R.E.

Qualifications of an Engineer

Surely the qualifications of an engineer is basically an intellectual problem which should be approached from the broadest viewpoint?

The basic fact of the matter is that the ability to obtain a degree to a large extent depends on the ability to organize past knowledge. Indeed, our whole educational system with happy exceptions is geared to this narrow facet of human thought.

But what is often wanted in an engineer is creativity, the ability to invent something new. Quite often the best inventors have either had no degree or only a rather low class of pass.

Not only the simple ground of justice to individuals but the general ground of maintaining a high level of inventive ability should make us very chary of narrowing the gate to 'Chartered Engineer' any more. Indeed, I would argue that we have, recently, gone too far in 'raising membership standards' and may well have effectively frozen out creative individuals and laid the foundations of ossification.

Since first composing this letter the proposals to take over the existing chartered institutions examination setting functions by an enlarged CEI have become public. One result of this would be firstly to 'broaden the syllabus', i.e. to include even more irrelevant material to be learnt by rote and forgotten as soon as possible and to further 'raise standards', i.e. to ensure that the chances of creative individuals passing the highly organized irrelevances of the exams or getting in by 'a side door' were still further reduced.

This and the general inefficiency of large organizations should surely condemn the entire 'Parkinsonian' idea of increasing the status of the CEI.

A. SANDMAN

Research Department of Anaesthetics,
Royal College of Surgeons of England,
35-43 Lincoln's Inn Fields, London WC2A 3PN
4th September 1974.

Automation Takes Over in Test Equipment

The use of automatic test equipment (ATE) is beginning to grow rapidly. The major industrial countries of Western Europe spent about £12.3 M on ATE in 1972-73. By 1978 spending is forecast to increase to £78.6 M.

These estimates are made in a new report, 'European Markets for Automatic Test Equipment', by the Market Research Section of Sira Institute. The report, available from Ovum Ltd., shows that in some sectors such as the British electronics industry, 60% of all the companies contacted are already using ATE in some form.

But this is only a beginning. 'Automatic production testing is in its infancy in the majority of manufacturing industries in Europe,' says the report. 'Even in the electronics sector, there is far more growth in the use of automatic testing to come than we have seen hitherto, both in terms of market size and product development.'

The report defines ATE as equipment which takes more than one reading from the item under test, without manual intervention, and then takes some sort of decision about the quality of the item. This definition embraces a huge range of equipment.

Examples include printed-circuit board testers marketed by companies such as General Radio, Membrain, and Teradyne in the range from £10,000 to £40,000; elaborate equipment for testing complete systems such as that sold by British Aircraft Corporation at prices up to £250,000 or more; and much cheaper circuit testers from companies such as Wayne Kerr and Rosemount Engineering costing as little as £1,000. 'Automatic' is not necessarily synonymous with 'expensive' in the authors' opinion.

ATE can be applied at all stages of the manufacturing process, but there is a growing tendency to test at earlier stages as products grow more complex. For example, one large company cut the cost of product failures on final test

from 20% to only 3% of manufacturing cost by weeding out faulty printed-circuit boards at the sub-assembly stage.

The case for ATE is primarily economic, but the biggest single reason given for its adoption by the companies surveyed was to alleviate the shortage of skilled testers. Others, in descending order of importance, were, to reduce labour costs, to reduce overall costs, to increase the speed of testing, to reduce the cost of finished product failures and, in some cases, that there was simply no other way of testing the product concerned.

Big savings in testing times and costs have been achieved, although the medium-sized company may find itself in a difficult position where it cannot justify the cost of the more elaborate systems, yet has outgrown the capabilities of the simpler ones. On the whole, companies are aiming to see their investment in ATE returned within two to three years, though a surprising number are prepared to wait five years or even longer.

Looking at Western Europe as a whole, Britain is currently the biggest single market for ATE, with sales of £5.7 M in 1972-73. (About 45% of this is accounted for by companies producing equipment for their own needs.) But West Germany already leads Britain in some areas, such as the automatic test of electrical systems in cars, and the German market is expected to rise from £3.3 M in 1972-73 to £28 M in 1978, leaving Britain in second place with sales of £20.4 M.

On this occasion, the depth survey, involving personal and telephone interviews and a postal questionnaire, was confined to the UK. Estimates from the rest of Europe were extrapolated from the British results with the help of published data and expert comment. American and British companies have tended to dominate the ATE market so far, and many British-based companies cover the whole of Europe.

'European Markets for Automatic Test Equipment' is available from Ovum Ltd., 22 Grays Inn Road, London WC1, price £75.

Forthcoming Institution Meetings

London Meetings

Tuesday, 29th October

JOINT MEETING OF COMMUNICATIONS GROUP AND AUTOMATION AND CONTROL SYSTEMS GROUP

Colloquium on SIGNAL PROCESSING IN COMMUNICATIONS SYSTEMS

IERE Lecture Room, 10 a.m.

Advance registration necessary. For further details and registration forms, apply to Meetings Secretary, IERE.

Some examples of adaptive signal processing using tuneable filters

By R. C. Weston (*SRDE*)

An adaptive detection system for time varying pulse signals

By V. McKinley and Dr. F. C. Monds (*Queen's University, Belfast*)

Adaptive techniques for high resolution spectrum estimation

By Dr. T. S. Durrani and D. Farrier (*Southampton University*)

Comparison of optimal delta modulators for low bit-rate transmission.

By D. W. W. Rogers and Dr. R. Barrett (*Hatfield Polytechnic*)

Optimum filters for digital amplitude and phase modulation systems

By Dr. M. Tomlinson (*Plessey*)

Some considerations relating to the properties of the Hadamard transformation and its application in data compression

By Dr. L. F. Turner (*Imperial College*)

Digital demodulation for linearly modulated signals

By Professor A. M. Rosie and A. J. Ruddell (*University of Strathclyde*)

Iterative detection processes

By A. Clements and Dr. A. P. Clark (*Loughborough University*)

Digital filters with multi-shift sequences within a sampling period

By K. M. Wong (*Plessey*) and R. A. King (*Imperial College*)

Wednesday, 6th November

COMPONENTS AND CIRCUITS GROUP

Colloquium on BATTERIES AND POWER SOURCES

IERE Lecture Room, 10 a.m.

Advance registration necessary. For further details and registration forms, apply to Meetings Secretary, IERE

Tuesday, 12th November

JOINT IERE/IEE COMPUTER GROUP

Colloquium on 25th ANNIVERSARY OF STORED PROGRAM COMPUTERS

The Royal Society, 10 a.m.

Advance registration necessary. For further details and registration forms, apply to Meetings Secretary, IERE.

Thursday, 14th November

COMMUNICATIONS GROUP

Recent Progress in Millimetric Waveguide Systems

By R. W. White (*Post Office*)

IERE Lecture Room, 6 p.m. (Tea 5.30 p.m.)

Wednesday, 27th November

AEROSPACE, MARITIME AND MILITARY SYSTEMS GROUP

The US Navy Navigation Satellite System

By W. F. Blanchard (*Redifon Telecommunications*)

IERE Lecture Room, 6 p.m. (Tea 5.30 p.m.)

Thursday, 28th November

AUTOMATION AND CONTROL SYSTEMS GROUP

CAD of Type 2 Phase Lock Loops

By P. Atkinson and A. J. Allen (University of Reading)

IERE Lecture Room, 6 p.m. (Tea 5.30 p.m.)

Wednesday, 11th December

EDUCATION AND TRAINING GROUP

Colloquium on the THE GRADUATE ELECTRONIC ENGINEER IN BRITAIN AND EUROPE

IERE Lecture Room, 10 a.m.

Advance registration necessary. For further details and registration forms, apply to Meetings Secretary, IERE.

Wednesday, 18th December

AEROSPACE, MARITIME AND MILITARY SYSTEMS GROUP

Colloquium on ELECTRONICS AND THE MOTOR VEHICLE

IERE Lecture Room, 10 a.m.

Advance registration necessary. For further details and registration forms, apply to Meetings Secretary, IERE.

Kent Section

Wednesday, 27th November

Problem Solving and Decision Making in Management

By P. J. Curra

Lecture Theatre 18, Medway and Maidstone College of Technology, Maidstone Road, Chatham, at 7 p.m.

Thames Valley Section

Thursday, 14th November

Hybrid Computers and their Applications

By Dr. R. L. Davey (*Imperial College*)

J. J. Thomson Physical Laboratory, University of Reading, Whiteknights Park, Reading, 7.30 p.m.

Thursday, 5th December

JOINT MEETING WITH IEE

The Application of Electronics in Telephone Exchange Switching

By F. W. Croft (*Post Office*)

J. J. Thomson Physical Laboratory, University of Reading, Whiteknights Park, Reading, 7.30 p.m.

The lecture will give an outline of the Post Office electronic telephone exchange widely used in public service, and touch briefly on a new system for large electronic exchanges. Electronic equipment systems used to steer calls over the electro-mechanically stored program control processors will also be covered.

East Anglian Section

Thursday, 24th October

JOINT MEETING WITH IEE

The Electronic Organ—the Organ of the Future?

By C. C. H. Washtell

Swaffham Prior Church, Swaffham Prior, Nr. Cambridge, 6 p.m. (Tea 5.30 p.m.)

The electrophonic organ was designed and built by the lecturer and is installed in the church at Swaffham Prior, near Cambridge. It can produce results which, in many respects, are indistinguishable from the traditional North European organ of the late XVII century. In other respects it exploits the foibles of electronic sound generation. Particular features include the ability to produce 'chiff' and the 'breathing' of each sound. The lecture will include a practical demonstration of the organ.

Thursday, 24th October

Recent Advances in Display Techniques

By D. W. G. Byatt (*Marconi Research Laboratories*)

The Civic Centre, Chelmsford, 6.30 p.m. (Tea 6 p.m.)

Current display techniques applied to data handling displays such as radar and computer control systems are described together with the application of new materials. In particular the use of light-emitting semiconductors and electro-optic materials will be discussed.

Thursday, 21st November

JOINT MEETING WITH IEE

Digital Adaptive Electronic Circuits

By Professor I. Aleksander (*Brunel University*)

University Engineering Laboratories, Trumpington Street, Cambridge, at 6.30 p.m. (Tea 6 p.m.)

Southern Section

Thursday, 24th October

JOINT MEETING WITH IEE

Automatic Weather Stations

By H. R. S. Page (*Plessey Radar*)

Farnborough Technical College, 7 p.m.
(Coffee and biscuits available in Refectory from 6.30 p.m.)

Meteorological records have been kept since the 17th Century. Until recently, most of the useful weather information was gathered from manned sites on land or sea. The advent of improved sensors to withstand long periods of unattended operation in harsh environmental conditions and reliable solid state electronics, enables this to be realized economically with the use of remote, automatic monitoring stations. The paper will cover the following topics: network and systems concepts; new sensors and sensing techniques; outstation philosophy, design and construction; transmission and recording media; control receiving station configurations; data presentation and display; and other applications.

Wednesday, 30th October

AUTONULL—The Suppression of Large Interfering Signals in Single and Multi Equipment Installations

By M. M. Zepler (*Plessey*)

H.M.S. *Collingwood*, Fareham, 6.30 p.m.
(Tea 6 p.m.)

In radio receiving systems large unwanted signals often cause severe interference to the reception of small signals. These large interfering signals can originate from a variety of sources, and can be at frequencies both in and out of the receiving band. Methods are described of suppressing the unwanted signal in both co-sited installations where the large signal may be at or near the frequency to which the receiver is tuned.

Wednesday, 6th November

Why 110° Colour?

By A. W. Lee

Lecture Theatre F, University of Surrey, Guildford, 7 p.m.

The paper deals with the background and the reasons for the change to wide-angle television tubes. It compares the advantages and disadvantages of toroidal and saddle type deflexion units. The author explains how a line time-base works with particular reference to thyristors, oscillations and the manner in which the circuit controls the energy it contains. A forecast is given of probable future developments.

Friday, 15th November

Automatic Weather Stations

By H. R. S. Page (*Plessey Radar*)

Newport (IoW) Technical College, 7 p.m.
(See Farnborough meeting on 24th October)

Wednesday, 4th December

JOINT MEETING WITH IEE

Application of New Bipolar Integrated Circuits

By P. Krebs (*Ferranti*)

Lanchester Theatre, Southampton University, 6.30 p.m.

Wednesday, 11th December

Recent Advances in Digital Circuit Fault Diagnosis

By Dr. R. G. Bennetts (*Southampton University*)

Southampton College of Technology, East Park Terrace, 7.30 p.m.

South Western Section

Wednesday, 23rd October

JOINT MEETING WITH IEE

The Digital Data Network

By M. Foulkes (*P.O. Telecommunications*)

Westinghouse Canteen, Chippenham, 6 p.m.
(Tea 5.30 p.m.)

Tuesday, 12th November

JOINT MEETING WITH IEE

Colour Television

By D. Barnes

The College, Regent Circus, Swindon, 6.15 p.m. (Tea 5.45 p.m.)

Wednesday, 13th November

CEI MEETING

Off-Shore Energy in British Waters

By D. E. Rouke (*Deputy Chairman, British Gas Council*)

No. 1 Lecture Theatre, School of Chemistry, University of Bristol, 7 p.m. (Tea 6.30 p.m.)

Wednesday, 13th November

JOINT MEETING WITH IEE

The Life and Work of a Sound Recording Engineer

By R. Auger

The Main Lecture Theatre, Plymouth Polytechnic, 7 p.m. (Tea 6.30 p.m.)

Wednesday, 11th December

JOINT MEETING WITH IEE

Computation of Courses for Sailing Yachts

By J. Elliot (*EMI Electronics*)

No. 4 Lecture Theatre, School of Chemistry, University of Bristol, 7 p.m. (Tea 6.30 p.m.)

This presentation will be based on the paper published in the December 1973 Journal which gained the author the Institution's Wheatstone Premium.

Yorkshire Section

Thursday, 14th November

Development of Digital Transmission Systems

By G. H. Bennett (*P.O. Telecommunications*)

York College of Further Education, 6.30 p.m. (Tea 6 p.m.)

Wednesday, 4th December

Electronics Instrumentation for Respiratory Monitoring

By C. L. Smith (*Glamorgan Polytechnic*)

Barnsley College of Further Education, 6.30 p.m. (Tea 6 p.m.)

Merseyside Section

Wednesday, 13th November

Satellite Earth Stations 1962-1974

By D. I. Dalgleish (*P.O. Telecommunications*)

Department of Electrical Engineering and Electronics, University of Liverpool, 7 p.m.
(Tea 6.30 p.m.)

The basic requirements of Earth stations will be examined. Developments at the P.O. Earth Station, at Goonhilly from 1962 to 1974 will be surveyed and a brief look at the future will be taken.

Wednesday, 11th December

Electronics in Motor Vehicles

By L. Phoenix (*Lucas Electrical*)

Department of Electrical Engineering and Electronics, University of Liverpool, 7 p.m.
(Tea 6.30 p.m.)

Electronics may replace existing vehicle equipment but perform with greater reliability and longer life or may make possible completely new functions

West Midland Section

Thursday, 7th November

JOINT MEETING WITH IEE

The 25 metre Steerable Aerial at the Radio and Space Research Field Station

By J. A. McGivney (*Science Research Council*)

Lanchester Polytechnic, Coventry, 6.30 p.m.
(Tea 6 p.m.)

Wednesday, 13th November

Using Digital Integrated Circuits

By J. A. Scarlett (*Exacta Circuits*)

City of Birmingham Polytechnic, 7.15 p.m.
(Tea 6.30 p.m.)

Monday, 2nd December

JOINT MEETING WITH IEE

Sonar and Underwater Acoustic Communications

By V. G. Welsby (*University of Birmingham*)

PO Training Centre, Duncan Hall, Stone, 7 p.m.

A review of modern techniques based on the use of sound waves in the sea and in lakes, rivers, etc. is given and systems for diver communication and navigation are described. High resolution sonars, sometimes using focused acoustic arrays, have uses which range from the study of the behaviour of fish shoals to aiding police searches in muddy canals. Acoustic telemetry is used to control submersible vehicles and to channel collected information back to the surface. Acoustic waves are used to count migrating fish in rivers.

East Midland Section

Tuesday, 12th November

JOINT MEETING WITH IEE

Stereophonic and Ambisonic Reproduction of Sound

By Professor P. B. Fellgett (*University of Reading*)

Room J002, Edward Herbert Building, Loughborough University, 7 p.m. (Tea 6.30 p.m.)

Wednesday, 4th December

Computer Recognition of Handwritten Numbers

By Dr. D. J. Quarmby (*Loughborough University*)

Lecture Theatre 'A', Physics Block, Leicester University, 7 p.m. (Tea 6.30 p.m.)

South Midland Section

Tuesday, 29th October

Developments in Digital Transmission Systems

By G. H. Bennett (*P.O. Telecommunications*)

Gloucester College of Technology, Gloucester, 7.30 p.m.

Tuesday, 12th November

JOINT MEETING WITH IEE

Radar Approach to Weather Forecasting

By Professor E. D. R. Shearman (*University of Birmingham*)

G. C. Club, Benhall, Cheltenham, 7.30 p.m.

Thursday, 5th December

High Fidelity Sound Reproduction

By R. L. West (*Polytechnic of North London*)
The Foley Arms, Malvern, 7.30 p.m.

This meeting will be a lecture/demonstration and will trace the development of the subject from early beginnings, highlighting important landmarks en route. It will finish with demonstrations of some of the most recent equipment and techniques.

North Eastern Section

Monday, 4th November

JOINT MEETING WITH IEE

Computer Control System for Electrical Distribution

By D. H. Jones (*Midland Electricity Board*) and R. J. Scott-Kerr (*Consultant*)

University of Newcastle upon Tyne, Merz Court, 6.15 p.m. (Tea 5.45 p.m.)

Tuesday, 17th December

Noise: Some Problems Solved and Unsolved

By Professor D. A. Bell (*University of Hull*)

Main Lecture Theatre, Ellison Building, Newcastle Upon Tyne Polytechnic, Ellison Place, 6 p.m. (Tea 5.30 p.m.)

North Western Section

Thursday, 14th November

Medical Electronics

By E. T. Powner (*UMIST*)

Lecture Theatre R/H10, UMIST, 6.15 p.m. (Tea 5.45 p.m.)

Thursday, 12th December

JOINT MEETING WITH IEE

The Development of Radio

By D. E. Waddington (*Marconi Instruments*)

Lecture Theatre R/H10, UMIST, 6.15 p.m. (Tea 5.45 p.m.)

Northern Ireland Section

Tuesday, 12th November

JOINT MEETING WITH IEE

50th Anniversary of Broadcasting in Northern Ireland

The Ulster College, Jordanstown, 7 p.m.

Friday, 13th December

Dinner Dance

For information, phone Mr. A. D. Patterson, Belfast 658333

Scottish Section

Wednesday, 6th November

Napier College, Edinburgh, 7 p.m.

and

Thursday, 7th November

Glasgow College of Technology, 7 p.m.

Calculator Technology

By R. Bilton (*Hewlett-Packard*)

South Wales Section

Wednesday, 23rd October

JOINT MEETING WITH IEE

What are the Wild Waves Saying?—An Early History of Radio Detection

By Dr. V. J. Phillips (*University College of Swansea*)

University College of Swansea, 6.30 p.m. (Tea 5.30 p.m.)

Wednesday, 13th November

JOINT MEETING WITH IEE

Mobile Radio in the Era of Spectrum Congestion

By Professor W. Gosling (*University of Bath*)

Department of Applied Physics and Electronics, UWIST, Cardiff, 6.30 p.m. (Tea 5.30 p.m.)

Wednesday, 11th December

Reed Relay Telephone Exchanges

By A. N. Harris (*Wales Telecommunications Board*)

Department of Applied Physics and Electronics, UWIST, Cardiff, 6.30 p.m. (Tea 5.30 p.m.)

INSTITUTION OF ELECTRONIC AND RADIO ENGINEERS

Applicants for Election and Transfer

THE MEMBERSHIP COMMITTEE at its meetings on 28th December 1973, 7th August and 3rd September 1974 recommended to the Council the election and transfer of 32 candidates to Corporate Membership of the Institution and the election and transfer of 18 candidates to Graduateship and Associateship. In accordance with Bye-law 23, the Council has directed that the names of the following candidates shall be published under the grade of membership to which election or transfer is proposed by the Council. Any communications from Corporate Members concerning those proposed elections must be addressed by letter to the Secretary within twenty-eight days after the publication of these details.

Meeting: 28th December 1973 (Membership Approval List No. 192)

GREAT BRITAIN AND IRELAND

CORPORATE MEMBERS

Transfer from Student to Member

GRINDLEY, Richard John. *Edinburgh.*

Transfer from Graduate to Member

BALMOND, Philip Allan. *Thatcham, Berks.*

BUTLER, Edwin Lesue. *Southampton.*

CAMPBELL, Ian David. *Stevenage, Herts.*

EMERSON, Roger Whyndham. *High Ongar, Essex.*

FROST, Robert John. *Wolverhampton, Staffs.*

HAWTHORNE, Robert John Cecil. *Co. Antrim.*

HOLMES, Allan John. *Broadstairs, Kent.*

MINTO, Neil Vickers. *Darlington, Co. Durham.*

PATRICK, Colin Michael. *Broxburn, W. Lothian.*

PIXTON, John. *Blackpool, Lancashire.*

REVELL, John Alfred. *Southampton.*

RICHARDS, Paul. *South Croydon, Surrey.*

ROBINSON, Robert. *Broom, Bedfordshire.*

ROSE, Roy Thomas. *Penn, Buckinghamshire.*

SMITH, John Edward. *Uxbridge, Middlesex.*

VINCENT, Richard Ainsley Dixon. *London, W.4.*

3SS.

WARD, David Charles. *Near Royston, Herts.*

WHITESIDE, John Stephen Richmond. *Belfast*

BT4 2PH.

Direct Election to Member

AZIZ, Mohammed Abdul. *Luton, Bedfordshire.*

BOTTOMLEY, George Bede. *Malvern, Worcester.*

MORGAN, William Gerwyn. *Walsall, Stafford.*

JONES, John Albert. *Stokenchurch, Bucks.*

OWNSWORTH, Anthony Aloysius. *Glasgow.*

SMITH, Roger Barrington Baster. *St. Albans, Herts.*

TIJOU, James Arthur. *Carshalton, Surrey.*

OVERSEAS

CORPORATE MEMBERS

Transfer from Graduate to Member

IHONOR, Boniface Anthony. *Port Harcourt, Nigeria.*

MOORHOUSE, Michael John. *Ontario, Canada.*

OVERSEAS

NON-CORPORATE MEMBERS

Direct Election to Associate Member

LEE HONG-YING, John. *Western District, Hong Kong.*

Students Registered

ALEBIOSU, Christopher Abiodun. *Via Ilesha, Nigeria.*

CHEUNG CHEE HSUN. *North Point, Hong Kong.*

CHOI HON CHOY. *Hong Kong.*

KEUNG WAI SUN. *Kowloon, Hong Kong.*

LOW LYE YING. *Singapore 7.*

TAN KOK LENG. *Jalan Tiga, Singapore.*

Direct Election to Associate Member

LO, Pin Yin. *East Malaysia.*

Direct Election to Graduate

FERNANDO, Hettiakandage Michael Sunil. *Moratuwa, Sri-Lanka.*

Students Registered

CHAN, King Bor. *Hong Kong.*

CHOW, Yee Hoong. *Singapore 12.*

KOW, Chuong Chuan. *Penang, Malaysia.*

SIVAKUMARU, Thirunavukkarasu. *Colombo Ceylon.*

TEO, Koon Hoo. *Singapore 15.*

TAN, Hock Seng. *Singapore 2.*

WONG, Shu Man. *Kowloon, Hong Kong.*

Meeting: 7th August 1974 (Membership Approval List No. 193)

GREAT BRITAIN AND IRELAND

CORPORATE MEMBERS

Direct Election to Fellow

STEELE, Francis Howard. *Crawley, Sussex.*

Transfer from Student to Member

BAILLOT, John Henry. *Tillicoultry, Clackmannanshire.*

Direct Election to Member

HACKWOOD, Peter. *Erith, Kent.*

HEBBARD, John Ellesworth. *Saltash, Cornwall.*

NON-CORPORATE MEMBERS

Transfer from Graduate to Associate Member

HUDSON, David. *Hillingdon, Middlesex.*

Transfer from Associate to Associate Member

WATSON, Samuel. *Gillingham, Kent.*

Direct Election to Associate Member

OBINKWO, Michael. *London, N.16 OPR.*

RUSSELL, Christopher Henry. *Reading, Berkshire.*

Students Registered

DALY, Brendon John. *Dublin 3.*

HANDLEY, Richard Anthony. *Chesterfield, Derbyshire.*

Meeting: 3rd September 1974 (Membership Approval List No. 194)

GREAT BRITAIN AND IRELAND

NON-CORPORATE MEMBERS

Transfer from Graduate to Associate Member

BEECHING, Stephen Richard. *Newark, Notts.*

Transfer from Associate to Associate Member

OBERSBY, Derek. *Hillcroft Park, Stafford.*

Direct Election to Associate Member

HULSO, Philip John. *Malvern, Worcs.*

Transfer from Associate to Graduate

HALL, David William. *Marlow, Bucks.*

Direct Election to Graduate

JOHNSON, Howard Albert. *Morrison Swansea.*

POON, Kwok Leung. *Birmingham.*

LEGGETT, James Gerard. *Sleaford, Lincs.*

OVERSEAS

NON-CORPORATE MEMBERS

Transfer from Graduate to Associate Member

DASGUPTA, Shubhashish. *Calcutta 20, W. Bengal.*

Transfer from Student to Associate Member

WONG, Chor Shoon. *Kuala Lumpur, Malaysia.*